CANADIAN THESES ON MICROFICHE

I.S.B.N.

THESES CANADIENNES SUR MICROFICHE

National Library of Canada
Collections Development Branch

Canadian Theses on
Microfiche Service

Ottawa, Canada
K1A 0N4

Bibliothèque nationale du Canada
Direction du développement des collections

Service des thèses canadiennes
sur microfiche

NOTICE

The quality of this microfiche is heavily dependent upon the quality of the original thesis submitted for microfilming. Every effort has been made to ensure the highest quality of reproduction possible.

If pages are missing, contact the university which granted the degree.

Some pages may have indistinct print especially if the original pages were typed with a poor typewriter ribbon or if the university sent us a poor photocopy.

Previously copyrighted materials (journal articles, published tests, etc.) are not filmed.

Reproduction in full or in part of this film is governed by the Canadian Copyright Act, R.S.C. 1970, c. C-30. Please read the authorization forms which accompany this thesis.

THIS DISSERTATION
HAS BEEN MICROFILMED
EXACTLY AS RECEIVED

AVIS

La qualité de cette microfiche dépend grandement de la qualité de la thèse soumise au microfilmage. Nous avons tout fait pour assurer une qualité supérieure de reproduction.

S'il manque des pages, veuillez communiquer avec l'université qui a conféré le grade.

La qualité d'impression de certaines pages peut laisser à désirer, surtout si les pages originales ont été dactylographiées à l'aide d'un ruban usé ou si l'université nous a fait parvenir une photocopie de mauvaise qualité.

Les documents qui font déjà l'objet d'un droit d'auteur (articles de revue, examens publiés, etc.) ne sont pas microfilmés.

La reproduction, même partielle, de ce microfilm est soumise à la Loi canadienne sur le droit d'auteur, SRC 1970, c. C-30. Veuillez prendre connaissance des formules d'autorisation qui accompagnent cette thèse.

LA THÈSE A ÉTÉ
MICROFILMÉE TELLE QUE
NOUS L'AVONS REÇUE

NL-339 (r. 82/08)

Canada

117

0-315-16026-8

National Library of Canada | Bibliothèque nationale du Canada

Canadian Theses Division | Division des thèses canadiennes

Ottawa, Canada
K1A 0N4

63935

PERMISSION TO MICROFILM — AUTORISATION DE MICROFILMER

• Please print or type — Écrire en lettres moulées ou dactylographier

Full Name of Author — Nom complet de l'auteur

Béla P. Ruzsicska

Date of Birth — Date de naissance	Country of Birth — Lieu de naissance
March 23, 1954	HUNGARY

Permanent Address — Résidence fixe

c/o Prof. O.P. STRAUSZ
DEPT. of CHEMISTRY
UNIVERSITY OF ALBERTA
EDMONTON, ALBERTA, CANADA, T6G 2G2

Title of Thesis — Titre de la thèse

REACTIONS OF HALOMETHYLIDYNE RADICALS AND OBSERVATION OF DIHALOSILYLENE SPECTRA

University — Université

ALBERTA

Degree for which thesis was presented — Grade pour lequel cette thèse fut présentée

Ph. D.

Year this degree conferred — Année d'obtention de ce grade	Name of Supervisor — Nom du directeur de thèse
1983	Prof. O.P. STRAUSZ

Permission is hereby granted to the NATIONAL LIBRARY OF CANADA to microfilm this thesis and to lend or sell copies of the film.

The author reserves other publication rights, and neither the thesis nor extensive extracts from it may be printed or otherwise reproduced without the author's written permission.

L'autorisation est, par la présente, accordée à la BIBLIOTHÈQUE NATIONALE DU CANADA de microfilmer cette thèse et de prêter ou de vendre des exemplaires du film.

L'auteur se réserve les autres droits de publication; ni la thèse ni de longs extraits de celle-ci ne doivent être imprimés ou autrement reproduits sans l'autorisation écrite de l'auteur.

Date	Signature
Nov. 17, 1982	B.P. Ruzsicska

NL-91 (4/77)

THE UNIVERSITY OF ALBERTA

REACTIONS OF HALOMETHYLIDYNE RADICALS AND OBSERVATION OF DIHALOSILYLENE SPECTRA

by

Béla P. Ruzsicska

A THESIS

SUBMITTED TO THE FACULTY OF GRADUATE STUDIES AND RESEARCH

IN PARTIAL FULFILMENT OF THE REQUIREMENTS FOR THE DEGREE

OF DOCTOR OF PHILOSOPHY

DEPARTMENT OF CHEMISTRY

EDMONTON, ALBERTA

SPRING 1983

MICRO

THE UNIVERSITY OF ALBERTA

RELEASE FORM

NAME OF AUTHOR Béla P. Ruzsicska

TITLE OF THESIS Reactions of Halomethylidyne Radicals and Observation of Dihalosilylene Spectra

DEGREE FOR WHICH THESIS WAS PRESENTED Doctor of Philosophy

YEAR THIS DEGREE GRANTED 1983

Permission is hereby granted to THE UNIVERSITY OF ALBERTA LIBRARY to reproduce single copies of this thesis and to lend or sell such copies for private, scholarly or scientific research purposes only.

The author reserves other publication rights, and neither the thesis nor extensive extracts from it may be printed or otherwise reproduced without the author's written permission.

(SIGNED) .....B.P. Ruzsicska.....

PERMANENT ADDRESS

c/o Prof. O.P. Strausz

Dept. of Chemistry

University of Alberta

Edmonton, Alberta, CANADA T6G 2G2

DATED November 15, 1982

THE UNIVERSITY OF ALBERTA

FACULTY OF GRADUATE STUDIES AND RESEARCH

The undersigned certify that they have read, and recommend to the Faculty of Graduate Studies and Research, for acceptance, a thesis entitled:

REACTIONS OF HALOMETHYLIDYNE RADICALS AND OBSERVATION OF DIHALOSILYLENE SPECTRA

submitted by

BELA P. RUZSICSKA

in partial fulfilment of the requirements for the degree of Doctor of Philosophy in Physical Chemistry

.....
O. P. Strausz - Supervisor

.....
J. E. Bertie

.....
H. B. Dunford

.....
J. Hooz

.....
J. Gray - Physics

.....
P. P. Gaspar - External Examiner

Date November 8, 1982

ABSTRACT

The technique of flash photolysis - kinetic absorption spectroscopy has been used to determine the absolute rate constants for the reactions of halomethylidyne radicals, CF, CCl, CBr, with hydrocarbon substrates.

$CF(X^2\Pi)$, $CCl(X^2\Pi)$ and $CBr(X^2\Pi)$ were produced by flash photolysis of substituted dibromomethanes, $CHXBr_2$ (X = F, Cl, Br, respectively). The rate constant for the reaction of halomethylidyne with a substrate was derived from the increase in the observed decay rate of halomethylidyne relative to the background decay rate.

The rate constant for CBr reaction with isobutane was determined to be $k = 2 \times 10^9 \exp(-3.9/RT)\ M^{-1}sec^{-1}$. The reaction is concluded to be insertion into the tertiary carbon - hydrogen bond.

CF, CCl and CBr are less reactive than CH due to the back donation of electrons from the halogen and consequently display more selectivity in their reactions. The reactivity with alkenes is found to be CF < CCl < CBr and demonstrates the electrophilic nature of halomethylidyne radicals. The observation that the rate constants increase with increasing alkylation of alkenes and the linear correlation between log k_2 and ionization potential of alkenes also demonstrate this electrophilic character of halomethylidynes. The reaction with alkenes is concluded to be cycloaddition to yield the cyclopropyl radical.

Arrhenius parameters for the reaction of CBr with alkenes were determined. Activation energies are negative and decrease with increasing alkyl subsitution. The Arrhenius plot for the reaction with 2,3-dimethyl-2-butene was found to be curved.

The reactions of CBr with alkynes have the same features as for alkenes and the reaction is concluded to be cycloaddition to form the cyclopropenyl radical.

The silicon radicals, SiCl and $SiCl_2$, were observed in the flash photolysis of Si_2Cl_6. The spectrum of $SiCl_2$ was due to the transition, $^1B_1 - {}^1A_1$, with a vibrational progression involving the bending frequency of the upper state, $\nu_2' = 148\ cm^{-1}$. The electronic energy of the $^1B_1$ state was estimated to be $30295\ cm^{-1}$.

In the flash photolysis of $SiBr_4$, the silicon radicals, SiBr and $SiBr_2$, are observed. The previously unreported electronic absorption spectrum of $SiBr_2$ is assigned to the transition $^1B_1 - {}^1A_1$ and the electronic energy of the upper state is estimated to be $27600\ cm^{-1}$.

ACKNOWLEDGEMENTS

The author wishes to express his sincere appreciation to Prof. O.P. Strausz for his constant support and for providing the invaluable experience of doing research under his supervision.

Special thanks go to all members of the photochemistry group, especially Dr. F.C. James for constant, helpful advice, Mr. A. Jodhan for his technical wizardry and Drs. I. Safarik and M. Torres for many thoughtful discussions.

This research project was sustained by the heroic services of the staff of the Electronics Shop and it is a pleasure to acknowledge the help of Mr. R. Kenwell and Mr. E. Feschuk.

The author also extends his thanks to Dr. E.M. Lown for assistance in the preparation of this manuscript.

Finally, the author wishes to acknowledge the assistance of Ms. S. Melnychuk and Mrs. L. Eastman in the typing of this manuscript and extends regards to all members of the Department of Chemistry who made the time spent here memorable.

TABLE OF CONTENTS

	Page
ABSTRACT	iv
ACKNOWLEDGEMENTS	vi
LIST OF TABLES	ix
LIST OF FIGURES	xi
CHAPTER I INTRODUCTION	1
A. Molecular Properties of Carbynes	2
B. Generation of Carbynes	11
C. Carbyne Reactions	20
D. Low Valent Silicon	45
E. Aim of the Present Investigation	54
CHAPTER II EXPERIMENTAL	56
A. Apparatus	56
1. The Vacuum System	56
2. The Flash Photolysis System	58
3. The Microdensitometer	66
B. Operational Procedures	66
1. Operation of the Flash Photolysis System	66
2. Preparation of Gas Mixtures	69
3. Development of Photographic Emulsions	71
C. Materials	72
CHAPTER III RESULTS	77
A. Halomethylidyne Sources	77

B. Halomethylidyne Absorption Spectra..... 77
C. Measurement of Beer Absorption Law..... 84
D. Decay of Halomethylidyne Spectra..... 89
E. Reaction of Halomethylidynes with Alkenes..... 92
F. Reactions of CBr with Alkynes..... 106
G. Temperature Dependence of the Reactions of CBr.. 114
H. Halosilylidyne Sources..... 122
I. Absorption Spectra from Photolysis of Si_2Cl_6.... 122
J. Absorption Spectra from Photolysis of $SiBr_4$..... 128
K. Decay of the SiBr Spectrum..... 131
L. Decay of SiCl and $SiCl_2$ Spectra..... 131

CHAPTER IV DISCUSSION 134
A. Photochemistry of Halogenated Methanes..... 134
B. Background Reactions and Decay of the Halomethylidynes..... 137
C. Reaction of CBr with Isobutane..... 140
D. Reactions of Halomethylidynes with Alkenes..... 142
E. Temperature Dependence of the Reactivity of CBr with Alkenes..... 156
F. Reaction of CBr with Alkynes..... 164
G. Absorption Spectra of $SiCl_2$ and $SiBr_2$..... 171
H. Photochemistry of Halogenated Silanes..... 175

CHAPTER V SUMMARY AND CONCLUSIONS 179

BIBLIOGRAPHY..... 184

APPENDIX..... 196

LIST OF TABLES

Number		Page
I-1	Molecular Constants of Halomethylidynes.....	10
I-2	Bond Lengths and Energies of the C-X Bond.....	10
I-3	Rate Constants for Reaction of CH with Inorganic Substrates.....	25
I-4	Rate Constants for Reaction of CH with Organic Substrates.....	27
I-5	Rate Constants for Reaction of CCl with Inorganic Substrates.....	34
I-6	Rate Constants for Reaction of CCl with Organic Substrates.....	36
I-7	Rate Constants for Reaction of CCl with Silanes....	40
I-8	Rate Constants for Reactions of Bromomethylidyne...	42
I-9	Ground State Properties of Si-halogen Radicals.....	48
II-1	Purification of Inorganic Substrates and Alkanes...	73
II-2	Purification of Alkenes.....	74
II-3	Purification of Alkynes.....	75
II-4	Gas Chromatography Analysis of Alkenes.....	76
III-1	Background Rate Constants, k', for Halomethylidyne Decay.....	93
III-2	Background Rate Constant, k', for CBr Decay.....	94
III-3	k"(CF) as a Function of Concentration for the Reactions of CF.....	95
III-4	Second Order Rate Constants, k_2, for the Reaction of CF with Alkenes.....	107

III-5 $\gamma k''(CCl)$ as a Function of Concentration for the Reactions of CCl..... 108

III-6 Second Order Rate Constants, k_2, for the Reaction of CCl with Alkenes..... 110

III-7 $\gamma k''(CBr)$ as a Function of Concentration for the Reactions of CBr..... 111

III-8 Second Order Rate Constants for the Reaction of CBr with Alkenes..... 113

III-9 Bimolecular Rate Constants for CBr Reactions with Alkynes..... 117

III-10 Second Order Rate Constants for the Reaction of CBr with Alkenes and 2-methylpropane as a Function of Temperature..... 118

III-11 Arrhenius Parameters for the Reactions of CBr..... 121

III-12 Assignment of SiCl Spectrum..... 125

III-13 Assignment of $SiCl_2$ Spectrum..... 127

III-14 Wavelength Calibration of the SiBr Spectrum..... 130

III-15 Decay of SiBr Absorption in Presence of Ethylene..... 133

III-16 Decay of $SiCl_2$ Absorption in Presence of Ethylene..... 133

IV-1 Rate Constants for Reactions of Methylidyne and Halomethylidynes with Alkenes..... 143

IV-2 Activation Parameters for Radical Addition to Alkenes. 157

IV-3 Rate Constants for the Reactions of Radicals with Alkynes..... 166

IV-4 Electronic Transitions and Vibrational Frequencies of Group IV A Dihalides..... 174

LIST OF FIGURES

Number		Page
I-1	Effect of Carbyne Substituents	3
I-2	Representative Electron Arrangements Corresponding to Spectroscopic States Arising from Electron Configurations of Methylidyne	5
I-3	Symmetry Correlations between CH + H and C + H_2	22
II-1	The Main Vacuum System	57
II-2	The Flash Photolysis System	59
II-3	The Reaction Vessel and Reflective Housing	61
II-4	The Spectroscopic Flash Lamp	63
II-5	The Littrow Prism and Mounting	65
II-6	Schematic Diagram of the Microdensitometer	67
II-7	The Flash Photolysis System Circuit Diagram	68
II-8	Oscilloscope Trace	70
III-1	UV Absorption Spectra of Halogenated Methanes	78
III-2	Absorption Spectrum of CF	79
III-3	Absorption Spectrum of CCl	81
III-4	Absorption Spectrum of CBr	83
III-5	Peak Height vs Path Length for CF Absorption Bands	85
III-6	Peak Height vs Path Length for CCl and CBr Absorption Bands	86
III-7	Ln(Peak Height) vs Ln Length for CF,CCl and CBr Absorption Bands	88
III-8	Ln(peak Height) vs Time for CF Absorption Bands	90
III-9	Ln(Peak Height) vs Time for CCl and CBr Absorption Bands	91
III-10	UV Absorption Spectra of Alkenes	95

III-11 Ln(P.H.) vs Time for CF(Q_1) Absorption in Presence of Ethylene..... 98

III-12 Ln(P.H.) vs Time for CF(P_2) Absorption in Presence of 1-Butene..... 99

III-13 Ln(P.H.) vs Time for CF(P_1) Absorption in Presence of t-2-Butene..... 100

III-14 Ln(P.H.) vs Time for CCl(Q_1) Absorption in Presence of Isobutene..... 101

III-15 Ln(P.H.) vs Time for CBr(Q_1) Absorption in Presence of 2-methyl-2-butene..... 102

III-16 k"(CF) vs Concentration of Alkene for Four Alkenes..... 105

III-17 γk"(CCl) vs Concentration of Alkene for Four Alkenes..... 109

III-18 γk"(CBr) vs Concentration of Alkene for Four Alkenes..... 112

III-19 Ln(P.H.) vs Time for CBr(Q_1) Absorption in Presence of 2-Butyne..... 115

III-20 k"(CBr) vs Concentration of Alkyne for Three Alkynes..... 116

III-21 Arrhenius Plots for Reactions of CBr with Ethylene and Isobutane..... 119

III-22 Arrhenius Plots for Reactions of CBr with 2,3-dimethyl-2-butene and t-2-butene..... 120

III-23 UV Absorption Spectra of Silanes..... 123

III-24 Absorption Spectrum of SiCl..... 124

III-25 Absorption Spectrum of $SiCl_2$ 126

III-26 Absorption Spectrum of SiBr..... 129

III-27 Absorption Spectrum of $SiBr_2$..... 132

IV-1 Log k_2 vs Ionization Potential of Alkene for Reaction of CF with Alkenes..... 147

IV-2 Log k_2 vs Ionization Potential of Alkene for Reaction of CCl with Alkene..... 148

IV-3 Log k_2 vs Ionization Potential of Alkene for Reaction of CBr with Alkenes..... 149

IV-4 Qualitative Depiction of Curve Crossing for Positive and Negative Temperature Dependence..... 160

IV-5 Arrhenius Plots for Reaction of CBr with t-2-butene and 2,3-dimethyl-2-butene..... 165

IV-6 Log k_2 vs Ionization Potential of Alkyne for Reaction of CBr with Alkynes..... 168

IV-7 Log k_2 vs Ionization Potential of Alkyne for Reaction of CCl with Alkynes..... 169

I. INTRODUCTION

"Carbyne" is a commonly used term referring to a monovalent carbon species which has a single, covalently bonded substituent. The chemistry of these molecules is of interest since they are part of the family of carbon radicals comprising also trivalent carbon radicals, divalent carbon species called carbenes and carbon atoms. The reactions of trivalent carbon and carbenes have been extensively studied (1,2) and those of atomic carbon are becoming known (3). Little is known about carbyne reactions because their highly electron deficient nature makes them very reactive, unstable species, difficult to generate cleanly under conditions favorable to kinetic-mechanistic studies.

To date only a few carbynes have been studied. CH, CF, CCl, CBr and CCN have been observed in spectroscopy and CCO_2Et has been postulated as an intermediate in liquid phase studies. The CH molecule, officially called methylidyne, occurs naturally in interstellar space. In the laboratory, carbynes are produced in low yield by energetic decomposition of suitable compounds, for example, in hydrocarbon flames. These decompositions, however, generally yield other reactive species making product analysis difficult and mechanistic interpretation speculative. The majority of carbyne reactivity studies have been carried out by observation of the decay of the carbyne spectra.

The reactivity of electron deficient species such as carbenes and group VI A atoms is usually dependent on their electron configurations. Carbynes have the following ground state electron configurations: methylidyne, CH, $..3\sigma^2\ 1\pi^1$; halo- and cyanomethylidynes, CF, CCl, CBr, CCN, $..w\pi^4 x\sigma^2 v\pi^1$. The carbon atom can be thought of as being in a sp hybridized state and therefore can use p orbitals to overlap

with substituent p orbitals to form π orbitals (Fig. I-1). The electron deficiency of the monovalent carbon may be compensated for by delocalization of these $p\pi$ bonding electrons onto the carbon. The amount of delocalization will be dependent on the degree of $p\pi$ orbital overlap and the electronegativity difference between the carbon and the substituent. In other terms, the electron deficiency of the carbon may be alleviated by electron donation from different substituents. For methylidyne, CH, there is no possibility of $p\pi$ overlap and this should result in an extremely high reactivity. Substituents capable of $p\pi$ overlap should greatly modify this reactivity, suggesting the following series: $CH > CCO_2Et > CCN > CBr > CCl > CF$.

The outer electron configuration of carbynes, $\ldots\sigma^2\pi^1$, gives rise to doublet spectra, hence the name doublet state carbyne. Carbenes can have electron configurations, σ^2 or σ^1p^1, giving rise to singlet and triplet states respectively, which have different reactivities. On the basis of spin and orbital considerations, doublet carbynes are expected to be similar to singlet carbenes. Studies on singlet carbene reactions have indicated that their electrophilic character is modified by electron donating substituents (4).

Therefore, we would expect electron deficient carbynes to be highly reactive electrophilic species whose chemical reactivity should be modified by $p\pi$ electron donating substituents, similarly to the case of singlet state carbenes.

A. Molecular Properties of Carbynes

1) Methylidyne, CH

From molecular orbital theory (5), CH has the electron configuration $(1s\sigma)^2(2s\sigma)^2(2p\sigma)^2(2p\pi)^1$ resulting in a $^2\Pi_r$ electronic ground

a)

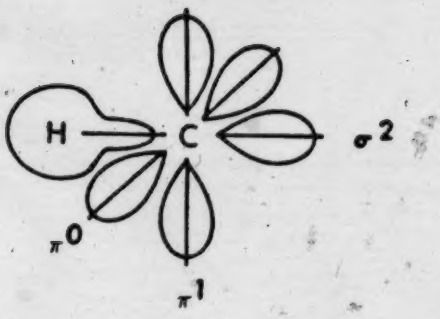

b)

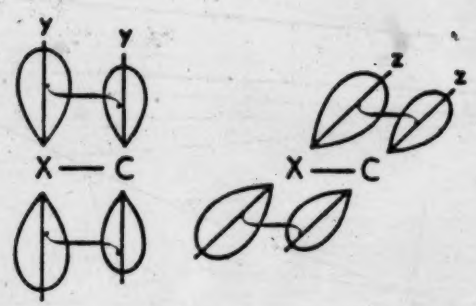

CX
(X = F, Cl, Br,

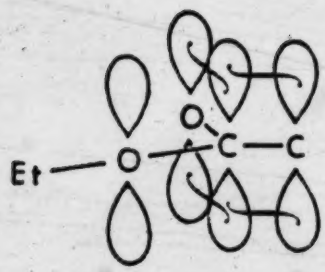

CCO_2Et

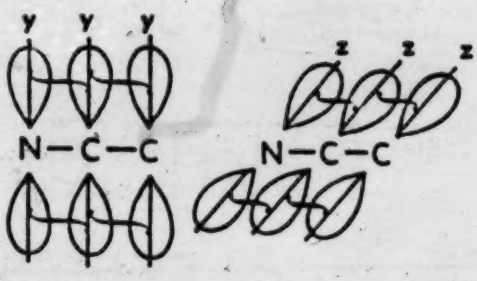

CCN

FIGURE I.1a) Orbital Occupancy of CH b) Back Donation Effect of Carbyne Substituents

state. This is in agreement with experimental observations indicating that the ground state is $^2\Pi$. Since the energy difference between $2p\sigma$ and $2p\pi$ is small, the lowest excited states are obtained, not by bringing the $2p\pi$ electron to higher orbitals, but by transferring an electron from the $2p\sigma$ to the $2p\pi$ orbital. The resulting configuration $K(2s\sigma)^2(2p\sigma)^1(2p\pi)^2$ gives rise to four electronic states, $^4\Sigma^-$, $^2\Delta$, $^2\Sigma^-$, $^2\Sigma^+$ (Fig. I-2). The transfer of $2p\pi$ electron to higher orbitals results in Rydberg transitions.

The CH molecule is of great astrophysical interest since it occurs extensively in stellar atmospheres, comets and interstellar space where its spectrum has been detected (6). The spectrum has been observed under a variety of conditions (7-10, 15) and consists of the following transitions.

Transition	Wavelength (nm)
$A^2\Delta - X^2\Pi_r$	430
$B^2\Sigma^- - X^2\Pi_r$	390
$C^2\Sigma^+ - X^2\Pi_r$	313
$D^2\Pi_i - X^2\Pi_r$	169.5
$E^2\Pi - X^2\Pi_r$	155.7
$F^2\Sigma^+ - X^2\Pi_r$	155.0
$D^2\Pi_i - B^2\Sigma^-$	300.7
Rydberg Series G - X^2	137

The $a^4\Sigma^-$ state has been detected 17 kcal $mole^{-1}$ above the ground state (16,17). The experimental spectroscopic constants for CH have been reproduced quite well by theoretical calculations (18). Recently laser techniques have been employed to monitor the CH molecules. Laser induced fluorescence of the A-X transition has been used to detect

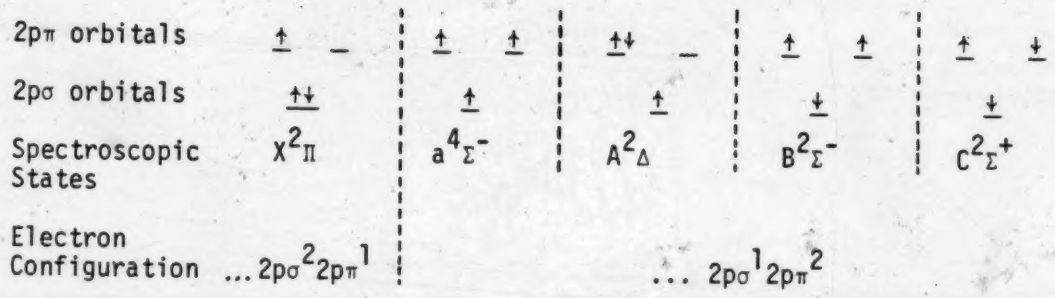

Fig. I-2 Representative Electron Arrangements corresponding to the Spectroscopic States arising from Electron Configurations of CH.

CH ($X^2\Pi$) radicals in flames (19), to measure radiative lifetimes (14) and to observe CH as a product following the multiphoton laser dissociation of several compounds (20-23).

2) Halomethylidynes, CF, CCl, CBr

The halomethylidynes have electron configurations which can be written in Mulliken notation as $...w\pi^4 x\sigma^2 v\pi^1$. Therefore they would all have $^2\Pi$ ground states. This electronic configuration is considerably different from CH. First there is the presence of filled $w\pi$ bonding orbitals and secondly the $v\pi$ orbital is a molecular antibonding orbital whereas in CH the $2p\pi$ orbital is basically the same as an atomic p-type orbital. The first excited electron configuration is expected to be $..w\pi^4 x\sigma^1 v\pi^2$ resulting in the same four electronic states as in CH.

a) Fluoromethylidyne, CF

The spectroscopy of fluoromethylidyne has been extensively studied since its electronic configuration is isoelectronic with NO. The electronic emission spectrum is observed by decomposition of CF_4 or other fluorocarbon vapors by electrical discharge (24-28) or in flames containing CF_4(29). The spectrum consists of a violet degraded band system, $A^2\Sigma^+ - X^2\Pi$, in the region 256-223 nm, and a red degraded band system, $B^2\Delta - X^2\Pi$ in the region 220-197 nm. The observation that the $A^2\Sigma^+$ state is much more strongly bonded than the $X^2\Pi$ and $B^2\Delta$ states suggests that it is the lowest Rydberg state having $...w\pi^4 x\sigma^2 \sigma 3s$ configuration (28). The $B^2\Delta$ state is assigned to the expected $...w\pi^4 x\sigma^1 v\pi^2$ configuration.

The $A^2\Sigma^+ - X^2\Pi$ transition was observed in absorption after flash discharge and flash photolysis of fluorinated hydrocarbons (30,31).

The $B^2\Delta - X^2\Pi$ absorption spectrum resulted from the vacuum ultraviolet photolysis of methyl fluoride in a low temperature matrix and also present was the CF infrared absorption at 1280 cm^{-1} (32). Recently emission from the $A^2\Sigma^+ - X^2\Pi$ and $B^2\Delta - X^2\Pi$ systems has been detected following laser decomposition of fluorinated methanes (33,34). Modern laser techniques have given precise measurements for vibrational and rotational transitions in the $X^2\Pi$ ground state (35,36). The observed esr spectrum of CF was interpreted as indicating that fluoromethylidyne has considerable double bond character (37). The electronic dipole moment of CF was found to be considerably larger (0.65 D) than that of isoelectronic NO (0.159 D) as expected on electronegativity grounds. The enthalpy of formation is fairly well agreed upon as 60 ± 2 kcal $mole^{-1}$ (38,39). This value gives a dissociation energy, D_0, of 131 ± 2 kcal $mole^{-1}$ which can be compared to the average bond energy in CF_4 of 117 kcal $mole^{-1}$. The results from multiconfiguration Hartree-Fock calculations indicated that, in the $X^2\Pi$ ground state, the fluorine $2p\pi$ orbitals have been delocalized onto the carbon and the CF σ bond is highly ionic (40).

All of the above results indicate that the fluorine substituent is acting through resonance and inductive effects to stabilize the electron deficiency of fluoromethylidyne. The electron donating resonance effect can be represented by extra canonical forms involving rearrangement of electron pairs as shown below in structures A and B. The electron attracting inductive effect is represented by structure C.

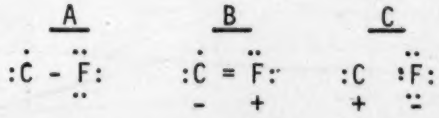

The stability and bond strength of CF compared to CH demonstrates the important contribution of these structures to the electronic distribution in fluoromethylidyne.

b) Chloromethylidyne, CCl

There is only one well documented electronic band spectrum of the chloromethylidyne molecule whose emission has been seen in electric discharges through chlorinated compounds (41-44) and in flames containing chlorinated compounds (45). This spectrum, which lies in the region 290-270 nm, has been assigned to the $A^2\Delta - X^2\Pi$ transition on the basis of rotational analysis (46-49). This transition has been observed in absorption following the flash photolysis of many chlorinated organic compounds (50-56). Tyerman observed another absorption at 230 nm which was assigned to a $B^2\Sigma - X^2\Pi$ transition (57) in agreement with the absorption spectrum of matrix isolated CCl (92). Laser techniques have been used to measure vibration-rotation spectra in the ground state (58) and to detect CCl via laser induced fluorescence of the $A^2\Delta - X^2\Pi$ transition (59).

The current value for the enthalpy of formation of CCl, 119 kcal $mole^{-1}$ (60) gives $D_0(CCl) = 81 \pm 5$ kcal $mole^{-1}$. In comparison to CF chloromethylidyne is a more weakly bonded molecule. The spectrum of CCl yields far fewer transitions than its isoelectronic counterparts, SiF, PO, NS (61, 62).

c) Bromomethylidyne, CBr

Bromomethylidyne is the poorest characterized halomethylidyne because its emission spectrum has not been observed. It was thought that the 290 nm emission band observed in flames containing brominated

hydrocarbons was due to CBr (63-65), but is was later identified as Br_2 (66,67). CBr was first seen in absorption following flash photolysis of some bromomethanes (50,51). The spectrum which occurs in the 300-306 nm region has been assigned to a $^2\Delta(a) - {}^2\Pi(a)$ transition (68). Two diffuse bands at 250 nm, which were observed once (57), have been assigned to a $B^2\Sigma^+ - X^2\Pi$ transition.

The enthalpy of formation of CBr is listed as $\Delta H^\circ_f = 123 \pm 15$ kcal $mole^{-1}$ (60) giving $D_o(CBr) = 75 \pm 15$ kcal $mole^{-1}$. These values are comparable to those of CCl. Likewise, CBr has a limited spectrum compared to its isoelectronic molecules SiCl, GeF, NSe, PS, AsO (61).

The spectroscopic molecular constants of the halomethylidynes are listed in Table I-1 and indicate certain trends. Thus the electron donating properties of the halogen substituents become evident in the bond strengths. The bond dissociation energies and bond lengths, when compared to other molecules containing the C-X bond, Table I-2, point to the bonding effect of the delocalized w_π electrons. The magnitude of the spin-orbit coupling constant (A) in the $^2\Pi_r$ ground state of halomethylidynes has been interpreted as indicating the delocalization of the $w\pi$ electrons (68). These results consistently agree with the bonding description of halomethylidynes given above.

Of the three halomethylidynes, the physical properties of CF are known the best (61). Interestingly, in contrast, the chemical properties of CF are the least known compared to the other two halomethylidynes, as will be discussed later.

3) Cyanomethylidyne , CCN

The transient absorption spectrum of CCN was observed after the flash photolysis of diazoacetonitrile (70). Rotational analysis

Table I-1 Molecular Constants of Halomethylidynes.

	CF	CCl	CBr
ΔH_f° (kcal mole^{-1})	60±2	119±5	123±15
D_o (kcal mole^{-1})	131±2	81±5	75±15
μ(D)	0.65		
r_e(Å)	1.272	1.65	1.82
A_e (cm^{-1})[a]	77	135	466
ω_e (cm^{-1})	1287	876	
Transitions[b] (nm)			
$^2\Delta - {}^2\Pi$	202.7	277.7	301.4
$^2\Sigma^+ - {}^2\Pi$	233.0	230.5	249.7

a - spin orbit coupling constant

b - wavelength of band origin

Table I-2 Bond Lengths and Energies of the C-X bond.

	F	Cl	Br
A.B.E[a] (CX_4) (kcal mole^{-1})	117	77	60
r_e(Å)(69)			
H_3C-X	1.381	1.77	1.94
$H_2C=CH$-X	1.32	1.72	1.89
$HC\equiv C$-X	1.28	1.63	1.79

a - average bond energy.

indicated that the three bands observed at 470, 446 and 375 nm belonged to the $A^2\Delta$ - $X^2\Pi$, $B^2\Sigma^-$ - $X^2\Pi$ and $C^2\Sigma^+$ - $X^2\Pi$ transitions respectively.

B. Generation of Carbynes

Due to their chemical instability, carbynes are difficult to generate in mechanistically clean, low energy processes. Several problems arise in carbyne generation. First is the choice of suitable precursors. Second is the application of appropriate high energy decomposition techniques. Last is the parallel formation of other reactive intermediates which complicate the analysis.

1) Methylidyne, CH

The most common precursor for the CH molecule is methane. The absorption spectrum of methane is continuous in the region 110-140 nm and vacuum ultraviolet photolysis in this region can result in the following primary processes.

	ΔH (kcal mole^{-1})
$CH_4 \longrightarrow CH_3 + H$	103
$\longrightarrow CH_2 + H_2$	108
$\longrightarrow CH + H_2 + H$	209
$\longrightarrow C + 2H_2$	189

The relative importance of these primary processes is still unclear because the methyl and methylene radicals are formed with excess energy and their reaction pathways are uncertain (71,72). The quantum yield of CH formation was determined to be 0.004 at 123.6 nm and 0.23 at 105-107 nm (71). In the high intensity flash photolysis of methane, the presence of CH was confirmed by its absorption spectrum (73). The

formation of CH may occur through a) the dissociation of primary products CH_3 and CH_2, b) the secondary photolysis of CH_3 and CH_2 and/or c) the direct photolytic dissociation of CH_4. $CH(A^2\Delta)$ emission has been seen following the photolysis of diazomethane and diazirine in the vacuum ultraviolet (74,75).

CH has been postulated to be formed in the vacuum ultraviolet photolysis of $CHBr_3$ ($\lambda > 165$ nm) on the basis of the detection of acetylene in the reaction products and also the presence of certain infrared emissions (76-78). Methylidyne was thought to come from the sequential three photon dissociation of $CHBr_3$. However, in other flash photolysis experiments on $CHBr_3$, only CBr has been observed in absorption and no spectrum due to CH has been seen (50,51,57). Comparing the reaction enthalpies of the two competing processes, it is not surprising that CBr is more likely to be formed:

	ΔH (kcal mole^{-1})
$CHBr_3 \longrightarrow CBr + HBr + Br$	123 ± 15
$\longrightarrow CH + Br_2 + Br$	156 ± 3

It must also be pointed out that ultraviolet multiphoton ArF (193 nm) laser photolysis of $CHBr_3$ has produced the $A^2\Delta$ and $X^2\Pi$ states of CH (79). Emission from $C(^1P_1)$ and C_2 ($d^3\Pi_g$, $C^1\Pi_g$) excited states was also detected, indicating the high energy input from multiphoton photolysis. The ArF (193 nm) and KrF (248 nm) laser photolysis of methyl halides has indicated that a two photon absorption process produces excited state CH ($A^2\Delta$, $B^2\Sigma^+$) (22). Methylidyne has been produced from the ultraviolet and infrared multiphoton photolysis of several compounds (20-23, 80, 81).

The adiabatic flash photolysis of acetylene and diacetylene

yielded the CH absorption spectrum (10,82). The extremely high temperatures resulting from the flash are responsible for the methylidyne formation, as in hydrocarbon flames.

CH is also produced from the pulse radiolysis of CH_4 (83,84). It is unclear whether it is formed by an ionic mechanism or neutral excited fragmentation. Wolfgang et al (85,86), from their studies of carbon atom reactions, postulated CH as a reactive intermediate. The presence of methylidyne was inferred by product analysis and thought to result from the decomposition of excited methylene formed from the following reaction.

$$C + H_2 \rightleftharpoons CH_2^{\dagger} \longrightarrow CH + H$$

Thrush et al. (87) thought that CH was responsible for certain reactions resulting in infrared emission and postulated that it arises from the metathetical reaction between methylene and a hydrogen atom.

$$CH_2 + H \longrightarrow CH + H_2$$

In general, it can be seen that the production of CH results from the high energy decomposition of suitable precursors or the reactions of energetic intermediates. Due to the excess energy carried by the fragments and the concomitant formation of other reactive intermediates, it is hard to identify the mechanisms of CH formation.

2) Halomethylidynes

The same general techniques and problems discussed above for the production of CH also apply to the generation of CF, CCl and CBr. These halomethylidynes are, in general, produced by decompositions of halogenated methanes. These are highly endothermic processes as shown

by the following examples.

	ΔH (kcal mole^{-1})
$CFCl_3 \longrightarrow CF + Cl_2 + Cl$	159
$CCl_4 \longrightarrow CCl + Cl_2 + Cl$	172
$CHBr_3 \longrightarrow CBr + HBr + Br$	123

a) Fluoromethylidyne, CF

CF has been the most widely observed halomethylidyne. This is understandable, since the relative stability of CF, compared to other halomethylidynes, should make it more amenable to study.

Simons and Yarwood (30,51) observed CF following the flash photolysis of di- and tribromofluoromethane and proposed that it results from the secondary unimolecular decomposition of energized radicals produced in the photolysis. This mechanism will be discussed more

$$CHFBr_2 + h\upsilon(\lambda > 165\ nm) \rightarrow CHFBr^{\dagger} + Br$$
$$CHFBr^{\dagger} \rightarrow CF + HBr$$

fully in connection with CCl.

The production of CF in the vacuum ultraviolet photolysis (λ = 147 nm) of freons ($CFCl_3$, CF_2Cl_2, $CHFCl_2$) was postulated on the basis of observed reaction products (88, 89). The quantum yield of CF from the photolysis of $CHFCl_2$ was derived to be 0.1 $\pm$ 0.002.

$$CHFCl_2 + h\upsilon(\lambda = 147\ nm) \rightarrow CF + HCl + Cl \quad \Delta H = 134\ kcal\ mole^{-1}$$

Other radicals produced in the photolysis are CHFCl, CHF and Cl. This photodissociation mechanism receives support from the observation of

the infrared and ultraviolet spectra of CF following the vacuum ultraviolet photolysis of CH_3F (32).

The focussed ArF (λ = 193 nm) laser photolysis of CF_2Cl_2 and CF_2Br_2 resulted in the formation of the $A^2\Sigma^+$, $B^2\Delta$ excited states of CF (33,34). The emission spectra from these states had a laser fluence dependence of ~3 indicating that absorption of three photons was required to produce these excited states of CF. This corresponds to an energy input of 444 kcal $mole^{-1}$ which is more than enough to produce $CF(B^2\Delta)$, indicating the partitioning of energy among the various photolytic fragments present. The excited ($^1B_1$) and ground ($^1A_1$) states of CF_2 were also produced in the photolysis of CF_2Cl_2. In the ArF photolysis of CF_2Br_2, emissions from several molecular transitions were noted: CF ($A^2\Sigma^+ - X^2\Pi$); CF ($B^2\Delta - X^2\Pi$); $CF_2(^1B_1 - {}^1A_1)$ and Br_2 ($^3\Pi_{o+u} - {}^1\Sigma_o^+$).

b) Chloromethylidyne, CCl

The most detailed studies on the generation and reactivity of a halomethylidyne have been done on CCl. Simons and Yarwood (50,57) were the first to make a systematic study on sources for chloromethylidyne by investigating the flash photolysis of a series of halogenated methanes and concluded that chloromethylidyne was generated by the decomposition of a vibrationally excited halogenomethyl radical formed in the primary photolysis:

$$CHClBr_2 + h\nu \longrightarrow CHClBr^\dagger + Br$$

$$CHClBr^\dagger \longrightarrow CCl + HBr$$

This mechanism is based upon the following observations:

- the intensity of the CCl absorption was linearly proportional to the

flash energy, which was interpreted as indicating a one photon process producing halomethylidyne.

- the energy of the absorbed light far exceeds the bond dissociation energy of the carbon-bromine bond in the halomethane, hence there is a large amount of excess energy available. Dissociation of the weakest carbon halogen bond is the general primary process in the photolysis of halomethanes (60).

- the intensity of the CCl absorption was found to be pressure dependent, indicating a quenchable precursor.

- the corresponding haloacid, HBr, was identified in product analysis as well as radical combination and disproportionation products resulting from the halogenomethyl radical.

This mechanism was supported by the results of Husain (52) who observed CCl absorption in the flash photolysis of CCl_3NO and proposed the following steps:

	ΔH (kcal mole^{-1})
$CCl_3NO + h\nu\ (\lambda > 190\ nm) \rightarrow CCl_3^{\dagger} + NO$	42
$CCl_3^{\dagger} \longrightarrow CCl + Cl_2$	101

The intensity of the CCl absorption was linearly proportional to the flash energy which was interpreted as indicating a one photon process producing CCl. The absorption spectrum of NO indicated that the nitric oxide produced by photolysis was not vibrationally excited. Therefore it was believed that the excess energy available after photodissociation was in the CCl_3 radical which decomposed to CCl and Cl_2.

Chloromethylidyne was also generated by Tyerman (55,56) in the flash photolysis of a series of 1,1 - dichloroethylenes. A mechanism was proposed whereby CCl was produced by secondary photolysis.

$$CF_2CCl_2 + h\upsilon \rightarrow CF_2 + CCl_2$$
$$CCl_2 + h\upsilon \rightarrow CCl + Cl$$

It is interesting to compare these results with those of Simons and Yarwood and Husain. Tyerman also observed that the CCl absorption intensity was proportional to the flash energy. However, he proposed a two photon process producing CCl, contrary to the one photon process suggested before. The discrepancy is believed to be caused by different spectral resolutions resulting in different relationships between absorption intensity and concentration.

CCl radicals have also been produced in the ArF (λ = 193 nm) laser photolysis of CCl_4 and $CFCl_3$ (59,90). These molecules provide good examples of the high energy reaction channels that are accessible with multiphoton laser photolysis.

The photolysis of CCl_4 yields emission from CCl ($A^2\Delta - X^2\Pi$), $CCl_2(^1B_1 - X^1A_1)$ and $Cl_2(A^3\Pi_{o+u} - X^1\Sigma_g)$ transitions. Some of the relevant reactions are listed below.

	ΔH (kcal mole^{-1})
$CCl_4 \longrightarrow CCl_3 + Cl$	71
$CCl_4 \longrightarrow CCl_2 + Cl_2$	80
$CCl_4 \longrightarrow CCl + Cl_2 + Cl$	172

The CCl_2 fluorescence at 560 nm had a laser fluence dependence of 1 while the Cl_2 fluorescence at 255 nm had a fluence dependence of 2. This result could indicate that most of the excited CCl_2 photofragments are produced in reaction channels other than the ones producing highly excited Cl_2 molecules. Two ArF photons at 193 nm provide 296 kcal mole^{-1} of energy which is sufficient to produce CCl radicals in the $A^2\Delta$ state (ΔH = 275 kcal mole^{-1}). However, if the exothermicity

of the reaction must be partitioned among different channels, then this energy requirement may not be fulfilled. In accordance with this, the CCl fluorescence at 278 nm had an average laser fluence dependence of 2.5.

In the photolysis of $CFCl_3$ similar results were obtained. Emission from CCl and Cl_2 was observed, along with the excitation spectrum of CFCl. The possible reactions are listed below.

	ΔH (kcal mole^{-1})
$CCl_3F \longrightarrow CCl_2F + Cl$	75
$CCl_3F \longrightarrow CClF + Cl_2$	90
$CCl_3F \longrightarrow CF + Cl_2 + Cl$	159
$CCl_3F \longrightarrow CCl + Cl_2 + F$	208
$CCl_3F \longrightarrow CCl + FCl + Cl$	206

The CCl fluorescence had a laser fluence dependence of 3 in agreement with the thermochemical requirement. It is interesting to note that no emission from CF was detected although this does not preclude the formation of ground state $CF(X^2\Pi)$ which may be detected by its excitation spectrum. In fact the production of CF from the 123.6 nm photolysis of $CFCl_3$ with a quantum yield of 0.04 was proposed by Rebbert (93) who also proposed the production of CCl from the 147.0 nm photolysis of CCl_4 with a quantum yield of 0.02. These results are supported by the observation of CCl from the vacuum ultraviolet photolysis of CH_3Cl in a low temperature matrix (92).

c) Bromomethylidyne, CBr

CBr has been observed only a few times. Simons and Yarwood (50,51)

obtained the CBr absorption spectrum following the flash photolysis of some brominated methanes such as $CHBr_3$ and CH_2Br_2. Their mechanism for CBr formation has been discussed above. The same absorption spectrum has been observed by other groups in the flash photolysis of the same compounds as Simons and coworkers studied (57,93,94). None of them was able to observe CH absorption in the flash photolysis of $CHBr_3$ as claimed by Lin (76-78). The ArF (193 nm) laser photolysis of CBr_4 (95) and $CHBr_3$ has not yielded any CBr emission spectra, perhaps as a result of predissociation (68).

The above discussion indicates that the known techniques for generating halomethylidynes involve high energy input and generally yield other reactive intermediates in greater abundance which will make the analysis of halomethylidynes complicated.

3) Cyanomethylidyne, CCN

The absorption spectrum of the CCN radical was obtained by the flash photolysis of diazoacetonitrile (70). Many other bands also appear. Vibrational levels of the violet system of CN, up to v" = 13, appear in absorption. The $A^2\Sigma^+ - X^2\Pi$ system of the NCO radical, the Swan bands of C_2 and the 4050 Å group of C_3 appear weakly, as does the 4315 Å band of CH. There is a strong transition beginning of 3400 Å assigned to the HCCN radical and overlapping this, intense bands due to the CNC radical appear.

4) Carbethoxymethylidyne, CCO_2Et.

In the short wavelength ($\lambda > 210$ nm) photolysis of diethylmercury-bisdiazoacetate, several different intermediates may be produced due to dissociation of the carbon-nitrogen and/or carbon-mercury bond, such as carbethoxymethylidyne and α-mercuricarbene. (95)

$$(EtO_2CCN_2)_2Hg \rightarrow Hg + 2N_2 + 2:\dot{C}CO_2Et$$
$$\rightarrow Hg + N_2 + :\dot{C}CO_2Et + N_2\dot{C}CO_2Et$$
$$\rightarrow H_2 + EtO_2CCN_2Hg\dot{C}CO_2Et$$
$$\rightarrow Hg + 2N_2\dot{C}CO_2Et$$

The mass spectrum of the parent diazomercurial compound showed a strong m/e peak of 85 which would correspond to carbethoxymethylidyne.

c) Carbyne Reactions.

Although carbynes have been characterized spectroscopically, their reactions are not well known due to two factors:

- the carbyne generating technique usually produces other reactive species, as was discussed above.

- the primary reactions of carbynes will result in excited radical intermediates which will undergo further reactions.

Strausz, Skell and coworkers (95) advanced the proposition that doublet state carbynes are analogous to singlet carbenes in their reactions while quartet carbynes should be similar to triplet carbenes. For example, the first excited state of CH, $a^4\Sigma^-$, lies only 17 kcal $mole^{-1}$ above the $X^2\Pi$ ground state compared to CH_2 where the first excited state, a^1A_1, lies ~10 kcal mole above X^3B_1(60). Thus CH shares with CH_2 and certain other radicals, the intriguing prospect of two distinct sets of chemical properties depending on the spin state. Since carbyne reactions have been studied to a limited extent, only the reactivity of doublet carbynes will be considered here and compared to singlet carbenes.

1) Methylidyne

The important factors for considering CH reactions, which will become evident, are symmetry and spin correlations and reaction enthal-

pies.

Reactions of CH with atoms have only recently been reported. This is due to the obvious difficulties of generating CH and atoms and bringing them together for reaction as discussed by Filseth et al. (96). Reaction pathways involving CH + H are given in Fig. I-3. The $CH(X^2\Pi)$ + $H(^2S)$ reaction correlates adiabatically with those of the $C(^3P)$ + $H_2(^1\Sigma_g^+)$ and $C(^1D)$ + $H_2(^1\Sigma_g^+)$ reactions through different surfaces with the assumed formation of CH_2 intermediates in C_s or C_{2v} symmetry. The $CH(X^2\Pi)$ + $H(^2S)$ reaction is then expected to yield the X^3B_1 and a^1A_1 states of CH_2 and $C(^3P)$ + $H_2(^1\Sigma_g^+)$ in exothermic, symmetry and spin allowed reactions. The reverse reaction was considered by Wolfgang et al. (85,86). In their studies ^{11}C atoms were produced by nuclear techniques in situ and were formed in ^3P, ^1D and ^1S states with high excess translational energies. In the presence of hydrogen, $CH(X^2\Pi)$ should be produced.

Recently, the reactions of CH with oxygen and nitrogen atoms have been studied by Filseth et al. (16). For the CH + O reaction the possible exothermic reactions are listed below.

	ΔH (kcal mole^{-1})
$CH(X^2\Pi) + O(^3P) \xrightarrow{1} H(^2S) + CO(d^3\Delta)$	-2
$\xrightarrow{2} HCO^+ + e^-$	-5
$\xrightarrow{3} H(^2S) + CO(a'\,^3\Sigma^+)$	-18
$\xrightarrow{4} OH(^2\Pi) + C(^3P)$	-21
$\xrightarrow{5} H(^2S) + CO(a^3\Pi)$	-37
$\xrightarrow{6} H(^2S) + CO(X^1\Sigma^+)$	-176
$\xrightarrow{7} HCO(X^2A')$	-189

The chemiionization reaction channel 2 is now generally accepted as being an important process in hydrocarbon flames (97) and interstellar

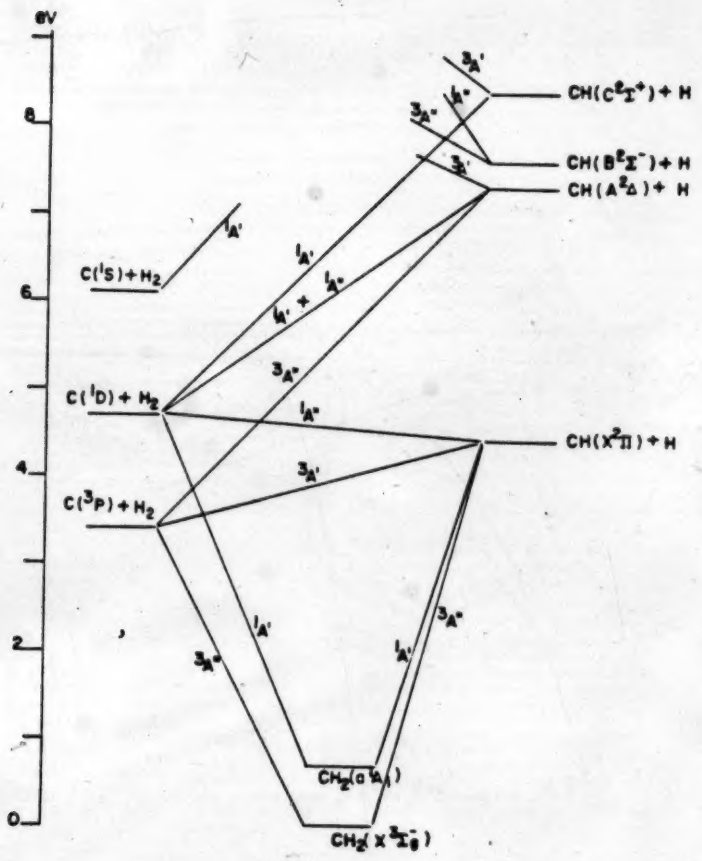

Fig. I-3 Symmetry correlations between CH + H and C + H_2 (from ref. 60)

space (98). The rate constant for this reaction has recently been measured at 295°K to be 2.4×10^{-14} $cm^3 sec^{-1}$ (99). Combining this rate with the overall reaction rate of 9.5×10^{-11} $cm^3 sec^{-1}$ measured by Filseth et al. (96) gives a branching ratio of 2.5×10^{-4}. This is to be expected as the more exothermic reaction channels should dominate. Reaction channel 6 is interesting because of its high exothermicity and the question arises as to how this excess energy is distributed. The exothermicity of atom transfer reactions often appears mainly as vibrational energy in the newly formed bond (100). Reaction channel 6 is one where much of the energy released might appear as vibrational excitation of the newly formed C-O bond. Thrush et al (87) have detected vibrationally excited ground state CO in levels up to v" = 33 (163 kcal $mole^{-1}$) which was attributed to the occurrence of reaction channel 6. Lin (76) has claimed that this reaction channel is the source of CO laser emission in flash photolysed $CHBr_3/SO_2$ mixtures with up to v" = 18 levels of CO detected.

The CH + N reaction was also studied by Filseth et al. (96). The exothermic reaction channels are listed below.

	ΔH (kcal $mole^{-1}$)
$CH(X^2\Pi) + N(^4S) \longrightarrow C(^3P) + NH(^3\Sigma^-)$	0
$\longrightarrow H(^2S) + CN(B^2\Sigma^+)$	-25
$\longrightarrow H(^2S) + CN(A^2\Pi)$	-73
$\longrightarrow H(^2S) + CN(X^2\Sigma^+)$	-99
$\longrightarrow HCN\ (X^1\Sigma^+)$	-221

The measured rate constant is high, 2.1×10^{-11} $cm^3 sec^{-1}$, which is understandable due to the presence of spin and symmetry allowed, exothermic reactions.

The reaction of CH with H_2 has been considered theoretically by Brooks and Schaefer(101). For the insertion reaction they calculated the

$CH(X^2\Pi) + H_2(X^1\Sigma_g^+) \rightarrow CH_3(^2A_2'')$ $\Delta H = -110$ kcal mole^{-1}

barrier to be ~75 kcal mole^{-1} for least motion insertion and 4 kcal mole^{-1} for non-least motion insertion.

least motion non-least motion

These results are explainable in terms of orbital interactions. In the least motion insertion, the CH $2p\sigma^2$ orbital would interact with the H_2 σ^2 orbital and there should be a repulsion barrier. However methylidyne is electron deficient in the area perpendicular to the CH bond and, in non-least motion insertion, this electron deficient orbital region interacts with the H_2 σ^2 orbital and therefore this reaction pathway should be more favorable. Due to the excess energy present in the CH_3 intermediate, the insertion reaction in the gas phase would become an overall abstraction reaction.

$CH(X^2\Pi) + H_2(X^1\Sigma_g^+) \rightarrow CH_3(^2A_2'') \rightarrow CH_2(^3B_1) + H(^2S)$ $\Delta H \cong -4$ kcal mole^{-1}

Formation of singlet methylene ($^1A_1$) is ~10 kcal mole^{-1} more endothermic. Brooks and Schaefer concluded, on a theoretical basis, that the $CH(X^2\Pi)$ reactions with molecular hydrogen were very similar to those involving $CH_2(^1A_1)$. Rate constants have been determined for the CH + H_2 reaction and are listed in Table I-3. From the above discussion, the reaction is anticipated to produce ground state CH_2 and a hydrogen atom. Thrush et al. (87) considered the reverse reaction to be the cause of formation of CH radicals.

The CH + O_2 reaction has many interesting energetically possible

Table I-3 Rate Constants for Reaction of $CH(X^2\Pi)$ with Inorganic Substrates.

Substrate	$k_2 \times 10^{-9}$ M^{-1} sec^{-1}					
	$CH(X^2\Pi)$			$CH_2(^1A_1)$[d]	$CH_2(^3B_1)$[d]	$N(^2D)$[e]
	Lin[a]	Perner[b]	Filseth[c]			
O			60±9		12	
N			12±3			
O_2	36±5	<24	20±2	18	84	3.6
N_2	0.54±0.06	0.6±0.1		3	$<6\times10^{-5}$	0.012
NO	170±40			<24	80±20	36
CO	13±2	3			$<6\times10^{-4}$	1.2
H_2	16±3	10±1		4	$<3\times10^{-3}$	1.2
CO_2	1.1±0.2				0.02	
NH_3		59±7				

a) ref. 79

b) ref. 83

c) ref. 20, 96

d) ref. 103

e) ref. 104

reaction channels and the experimentally determined rate constants are listed in Table I-3

		ΔH(kcal mole^{-1})
$CH(X^2\Pi) + O_2(X^3\Sigma_g^-)$	$\xrightarrow{1}$ $CO(a^3\Pi) + OH(X^2\Pi)$	-21
	$\xrightarrow{2}$ $CO(X^1\Sigma^+) + H(^2S) + O(^3P)$	-57
	$\xrightarrow{3}$ $CO(X^1\Sigma^+) + OH(A^2\Sigma^+)$	-68
	$\xrightarrow{4}$ $HCO(X^2A') + O(^3P)$	--77
	$\xrightarrow{5}$ $CO(X^1\Sigma^+) + OH(X^2\Pi)$	-159
	$\xrightarrow{6}$ $CO_2(X^1\Sigma_g^+) + H(^2S)$	-183

The $(A^2\Sigma^+ - X^2\Pi)OH$ emission has been observed in many hydrocarbon flames and been attributed to reaction channel 3 (102). The decay of this OH chemiluminescence was measured by Filseth et al.(20) while also measuring the CH decay kinetics. Infrared laser emissions from vibrationally excited CO and CO_2 molecules were observed by Lin (78) in flash initiated $CHBr_3/O_2$ reactions and attributed to reaction channels 5 and 6.

The CH + N_2 reaction is fairly slow compared to the other CH + diatomic molecule reactions listed in Table I-3. This is because there are no exothermic reaction channels and the reaction with the lowest reaction enthalpy does not conserve overall spin.

$$CH(X^2\Pi) + N_2(^1\Sigma_g^+) \rightarrow HCN(X^1\Sigma^+) + N(^4S) \quad \Delta H = 3 \text{ kcal mole}^{-1}$$

Lin et al. (79) found this reaction to be pressure dependent, indicating the formation of an intermediate complex, thus easing the spin conservation requirements.

Table I-3 also lists the reaction rate constants for the reaction of CH with various other inorganic substrates. The agreement between the different researchers using different systems is gratifying. The rate constants seem to agree better with those of singlet methylene

$(^1A_1)CH_2$ than with $(^3B_1)CH_2$ even though the rate constants for methylene in general are incertain (103). Rate constants for $N(^2D)$, the united atom analog of $CH(X^2\Pi)$, are also given in Table I-4. The $N(^1D) + O_2$ reaction is definitely established to be a chemical one (104).

Rate constants for the reaction of CH with a number of organic substrates have been determined and are listed in Table I-4. Reaction with alkanes may occur via two possible paths, insertion and abstraction.

$$:\dot{C}H(^2\Pi) + RH \rightarrow R\dot{C}H_2$$
$$\rightarrow :CH_2 + R\cdot$$

Both reactions are spin allowed. The insertion reaction is very exothermic whereas the abstraction reaction is nearly thermoneutral. The enthalpies of two CH + alkane reactions are shown below.

			ΔH(kcal mole^{-1})
$CH + CH_4$	$\xrightarrow{1}$	C_2H_5	-98
	$\xrightarrow{2}$	$C_2H_4 + H$	-60
	$\xrightarrow{3}$	$CH_2 + CH_3$	1
$CH + C_2H_6$	$\xrightarrow{4}$	C_3H_7	-101
	$\xrightarrow{5}$	$C_3H_6 + H$	-63
	$\xrightarrow{6}$	$C_2H_4 + CH_3$	-75
	$\xrightarrow{7}$	$CH_2 + C_2H_5$	-4

Because of the large amount of energy released in the insertion process the alkyl radicals formed are expected to undergo fragmentation reactions. For the reactions with larger alkanes, branching steps are expected to be even more complex because both insertion and abstraction processes can take place with primary, secondary or tertiary C-H bonds. Reaction

Table I-4 Rate Constants for Reaction of $CH(^2\Pi)$ with Organic Substrates

Substrate		$k_2 \times 10^{-9}$ $M^{-1}sec^{-1}$		
		$CH\ (X^2\Pi)$		$CH_2(^1A_1)^c$
		Perner[a]	Lin[b]	
Methane	CH_4	20±1	60±20	1.1
Ethane	C_2H_6		240±60	2.9
Propane	C_3H_8	82±20		3.8
n-Butane	$n\text{-}C_4H_{10}$	78±7	350±30	4.9
Cyclopropane	$c\text{-}C_3H_6$		140±40	
Cyclohexane	$c\text{-}C_6H_{12}$		280±110	
Ethylene	C_2H_4	69±6	130±50	
Acetylene	C_2H_2	45±9	130±24	
Propyne	CH_3C_2H		280±90	
Benzene	C_6H_6		50±20	

a) ref. 83

b) ref. 79

c) ref. 103

channel 2 is considered to be an important source of ethylene formation in the vacuum ultraviolet photolysis of CH_4 on the basis of the isotopic distribution of the products from labelled substrates (71, 72, 105, 106). Wolf (107) also postulated that radioactive ^{11}CH inserted into primary C-H bonds and that subsequent fragmentation produces labelled ethylene, as shown in reaction channels 2 and 6. ^{11}CH insertion into secondary and tertiary C-H bonds was believed to initiate further fragmentation reactions, as mentioned above.

The rate constants determined for the reactions of methylidyne with organic substrates do not agree as well as those for inorganic substrates and therefore only general trends can be discerned. Thus the rate of CH reactions with alkanes seems to increase with the number of CH bonds available and methylidyne seems to react indiscriminately with all types of C-H bonds.

For unsaturates, the question arises as to whether one can distinguish reaction of CH with the π bond. The reaction of CH with ethylene may proceed through several energetically accessible reaction channels:

	$\Delta H(\text{kcal mole}^{-1})$
$CH + C_2H_4 \longrightarrow \dot{C}H_2\text{-}CH = CH_2$	-113
$\longrightarrow H_2C\text{—}CH_2$ (C. H)	-88
$\longrightarrow C_3H_4 + H$	-57
$\longrightarrow$ $+ H$	-36
$\longrightarrow :CH_2 + \cdot C_2H_3$	0

The rate of reaction of CH with ethylene is faster than with methane. Since the number of C-H bonds in C_2H_4 and CH_4 is equal and their bond strengths comparable (D_o = 106 and 104 kcal $mole^{-1}$, respectively), the increased reactivity apparently results from the presence of the π bond. The rate of reaction with acetylene is approximately the same. The reaction of CH with the π bond is believed to occur *via* addition, similar to the well documented cycloaddition of $CH_2(^1A_1)$ (2). For the reaction with ethylene, it seems likely that addition and insertion reactions will occur with equal ease and that subsequent fragmentation will take place. Wolfgang *et al* (85,86) suggested that the reaction to form allyl radicals was important in their gas phase system. Recent *ab initio* molecular orbital calculations on the addition of methylidyne to ethylene suggested that asymmetric addition proceeds without an activation energy (179). This agrees with the high reaction rate constant and is also in agreement with the calculated reaction path for the addition of $CH_2(^1A_1)$ to ethylene (106).

The overall reactivity of CH can now be assessed. The highly unstable electron deficient structure of methylidyne, as was shown in molecular orbital diagrams, results in a high enthalpy of formation. This large ΔH_f° means that most methylidyne reactions with substrates will have several exothermic reaction channels resulting in the high reaction rate constants shown in Tables I-3 and I-4. These reactions should result in products which are electronically and/or vibrationally excited and mostly radicals. The secondary reactions which will then occur make conventional mechanistic interpretation difficult. The primary reactions of CH will probably have to be monitored by transient detection techniques where both reactants and products are observed.

Kinetically, the $CH(X^2\Pi)$ reactivity is difficult to compare with that of $CH_2(^1A_1)$ and $(^3B_1)$ because of limited data.

2) Halomethylidynes

a) Fluoromethylidyne, CF.

CF exhibits a marked difference in ΔH_f compared to CH. The possible reaction channels for the CF + O_2 reaction are listed below as an example in order to assess whether this change of ΔH_f will affect the reaction enthalpies.

		ΔH(kcal mole^{-1})
$CF(X^2\Pi) + O_2(X^3\Sigma_g^-)$	$\rightarrow CO(X^1\Sigma^+) + F(^2P) + O(^3P)$	-10
	$\rightarrow FCO(^2A) + O(^3P)$	-42
	$\rightarrow CO(X^1\Sigma^+) + FO(X^2\Pi)$	-65
	$\rightarrow CO_2(X^1\Sigma_g^+) + F(^2P)$	-136

In comparison to CH + O_2, the reaction of fluoromethylidyne with oxygen has fewer and less exothermic reaction channels and one might expect this reaction to be slower. However, other effects such as polarity and steric hindrance might influence the reaction. To date no kinetic measurements have been reported for CF and almost nothing has been published on its chemistry.

The possible reaction of CF with atomic oxygen can be considered first. Reaction channel 1 was used to explain $CO(a^3\Pi\text{-}X^1\Sigma^+)$ chemiluminescence (118). Reaction channel 2 was believed to be responsible for

		ΔH(kcal mole^{-1})
$CF(X^2\Pi) + O(^3P) \xrightarrow{1}$	$CO(a^3\Pi) + F(^2P)$	+11
$\xrightarrow{2}$	$CO(X^1\Sigma^+) + F(^2P)$	-128
$\xrightarrow{3}$	$FCO(^2A)$	-159

the infrared CO laser emission observed in the flash photolysis of $CFBr_3/SO_2$ mixtures (108). The third order reaction rate constant for reaction of fluoromethylidyne with atomic fluorine was deduced to be $6.6 \times 10^{20}\ T^{-2.85}\ M^{-2} sec^{-1}$ from shock tube studies (109). The possible reaction of CF with nitric oxide can proceed through some exothermic

	ΔH(kcal mole^{-1})
$CF(^2\Pi) + NO(^2\Pi) \xrightarrow{1} FCO(^2A) + N(^4S)$	-9
$\xrightarrow{2} FCN(X^1\Sigma^+) + O(^3P)$	-24
$\xrightarrow{3} CO(X^1\Sigma^+) + NF(X^3\Sigma^-)$	-48

channels. Reaction channel 3 was postulated as the source of infrared CO laser emission from flash photolysed $CFBr_3/NO$ mixtures (110).

The following reactions were used to explain the formation of certain products in the vacuum ultraviolet photolysis of $CHFCl_2$ or $CFCl_3$ (88, 89, 111)

	ΔH(kcal mole^{-1})
$CF + CH_3 \longrightarrow C_2H_2 + HF$	-104
$\longrightarrow C_2H_3F$	-125
$CF + C_2D_5 \longrightarrow C_3D_4 + DF$	-105
$CF + Br_2 \longrightarrow CFBr_2$	?

In comparison, the reactions of $CF_2(^1A_1)$ are better known. Reaction with inorganic substrates such as oxygen and hydrogen halides is slow (119). $CF_2(^1A_1)$ reacts with olefins via stereospecific addition and follows an electrophilic trend. Measurements of relative activation parameters seem to indicate that CF_2 is guided in its selectivity by both preexponential and activation energy parameters (120).

b) Chloromethylidyne, CCl

The enthalpy of formation of CCl is 119 ± 5 kcal $mole^{-1}$. This decrease in stability compared to CF should make CCl more reactive than CF since the reaction enthalpies will be more exothermic. Kinetic measurements have been made on several CCl reactions and the rate constants with inorganic substrates are listed in Table I-5. The values for the oxygen reaction rate are in good agreement and those for H_2 essentially show a very slow reaction. When these rate constants for CCl reaction are compared to those determined for CH reaction with the same substrates, the results show that the CCl reaction is roughly one order of magnitude slower than the corresponding CH reaction. The possible reaction channels for the reactions of CCl with O_2 and H_2 are listed below.

		ΔH(kcal $mole^{-1}$)
$CCl(X^2\Pi) + H_2(^1\Sigma_g)$	$\rightarrow CHCl(^1A_1) + H(^2S)$	+13
	$\rightarrow CH(X^2\Pi) + HCl(X^1\Sigma^+)$	+ 1
	$\rightarrow CH_2(^3B_1) + Cl(^2P)$	- 2
	$\rightarrow CH_2Cl$	-90
$CCl(X^2\Pi) + O_2(X^3\Sigma_g^-)$	$\rightarrow CO(X^1\Sigma^+) + ClO(A^2\Pi)$	-34
	$\rightarrow CO(X^1\Sigma^+) + Cl(^2P) + O(^3P)$	-58
	$\rightarrow ClCO + O(^3P)$	-63
	$\rightarrow CO(X^1\Sigma^+) + ClO(X^2\Pi)$	-122
	$\rightarrow CO_2(X^1\Sigma_g^+) + Cl(^2P)$	-184

Comparison between the possible reaction channels of CCl and those of CH shows that they are nearly identical in terms of exothermicity. If the measured rate constants are assumed to be correct, an intriguing

Table I-5 Rate Constants for Reaction of CCl ($X^2\Pi$) with Inorganic Substrates.

Substrate	$k_2 \times 10^{-9}$ M^{-1} sec^{-1}	
	Tyerman[a]	Wampler[b]
H_2	0.03±0.01	-
	N.R.[c]	
O_2	2.5±0.3	1.7
N_2	<0.0015	-
NO	-	22
SF_6	-	0.014

a) ref. 55

b) ref. 121

c) ref. 54 N.R. = no reaction

question arises as to why the CCl reactions are slower than the corresponding CH reactions. A qualitative explanation can be given in terms of the thermodynamic transition state formulation of the reaction rate constant.

$$k_{AB} = \frac{kT}{h} \exp(\Delta S^{\ddagger}_{AB}/R) \exp(-\Delta H^{\ddagger}_{AB}/RT)$$

The question arises as to whether a change in the entropy of activation, $\Delta S^{\ddagger}_{AB}$ and/or a change in the enthalpy of activation, $\Delta H^{\ddagger}_{AB}$, is responsible for the rate constant difference between CCl and CH. The reaction paths considered by Brooks and Schaefer (101) can serve as useful pictorial guides here. For the non-least motion insertion of CH, they calculated a barrier of 4 kcal $mole^{-1}$. For the non least motion insertion of CCl into H_2, a much larger barrier is to be expected due to two factors. The first is the steric hindrance of the bulky chlorine substituent which would affect $\Delta S^{\ddagger}_{AB}$. The second is the $p\pi$ orbital

overlap of chlorine reducing the electron deficiency around the carbon which would affect the $H^{\ddagger}_{AB}$ of the reaction. Thus the chlorine substituent acts in two ways to cause the reactivity difference.

Rate constants have been determined for the reaction of CCl with a variety of organic substrates and are listed in Table I-6. Very few substrates have been studied by more than one investigator and, for those which have been, the agreement ranges from good to bad. The agreement is reasonable for the unsaturated substrates; ethylene, acetylene and propyne. However for the reactions with alkanes, serious differences

Table I-6 Reaction of CCl with Organic Substrates

Substrates	$k_2 \times 10^{-9}$ $M^{-1}sec^{-1}$		
	Choi et al.[a]	Tyerman[b]	Wampler[c]
CH_4			N.R.
C_3H_8	<0.004	0.10±0.02	<0.002
i-C_4H_{10}	0.0045±0.0004		<0.002
c-C_6H_{12}	N.R.	0.23±0.03	
CCl_4			0.2±0.02
CH_3Cl	N.R.	0.22±0.01	
C_2H_5Cl		0.22±0.02	
CF_3Cl		0.075±0.008	
C_2H_4		0.33±0.04	0.13±0.01
C_3H_6		2.5±0.25	
t-2-C_4H_8		9.6±0.8	
i-C_4H_8		15±1	
cyclohexene	3.1±0.2		
1,3-cyclohexadiene	1.4±0.2		
1,4-cyclohexadiene	3.7±0.2		
CF_2CCl_2		1.9±0.2	
$CFClCCl_2$		8±4	
$CHClCCl_2$		4±2	
C_2Cl_4		10±5	

Table I-6 Reaction of CCl with Organic Substrates (cont'd)

Substrates	$k_2 \times 10^{-9}$ $M^{-1}sec^{-1}$		
	Choi et al[a]	Tyerman[b]	Wampler[c]
C_2H_2	0.025 ± 0.004	0.11 ± 0.01	
CH_3CCH	2.2 ± 0.2	2.4 ± 0.2	
CH_3CH_2CCH	3.7 ± 0.5		
$CH_3CH_2CH_2CCH$	4.3 ± 0.7		
CH_3CCCH_3	18 ± 3		
$(CH_3)_3CCCH$	2.4 ± 0.3		
$(CH_3)_3CCCC(CH_3)_3$	7.6 ± 0.7		

a) ref. 53,54

b) ref. 55

c) ref. 121

occur. Choi and Wampler's results suggest that the CCl reaction with the C-H bond is relatively slow and unimportant while Tyerman's results suggest that some reaction occurs. While the absolute values for the rate constants may be uncertain, the relative changes in the rate constants yield some information on CCl reactivity. For the reaction with alkyl substituted alkenes and alkynes, CCl exhibits an electrophilic trend, that, is the rate constants increase with the number of alkyl substituents. A comparison between the rate constants of CCl and CH with ethylene indicates the methylidyne reaction is ~ 500 times faster than that for chloromethylidyne. The possible reaction channels for the $CCl + C_2H_4$ reaction are listed below.

		$\Delta H(kcal\ mole^{-1})$
$CCl + C_2H_4$	$\longrightarrow CHCl\text{-}CH = CH_2$	?
	$\longrightarrow$	?
	$\longrightarrow C_3H_4 + Cl$	-57
	$\longrightarrow$ $+ Cl$	-90

It is interesting to note that the reactivity of $CCl(X^2\Pi)$ seems to parallel that of singlet dichlorocarbene. $CCl_2(^1A_1)$ is found to be fairly unreactive to paraffinic C-H bonds, but reacts with olefins via electrophilic, stereospecific addition (2,4). Skell and Cholod (114) measured the relative activation parameters for the addition of $:CCl_2$ to alkenes and found the reaction to be activation entropy dominated.

The rate constants and mechanism for the reaction of CCl with halogenated compounds are uncertain, since it is not clear whether the reaction of chloromethylidyne with a carbon-halogen bond is important.

In vacuum ultraviolet photolysis experiments, the following reactions were postulated to explain some products (90, 115)

$$CCl + CCl_4 \rightarrow C_2Cl_5^* \rightarrow C_2Cl_4 + Cl$$

$$CCl + Br_2 \rightarrow CClBr_2 \xrightarrow{Br_2} CClBr_3 + Br$$

Rate constants for the reaction of chloromethylidyne with a series of silanes have been determined and are listed in Table I-7. The results show that the reaction with silanes is extremely rapid. However, no measurable rate of reaction was observed with tetramethylsilane, indicating that reaction with Si-C and primary C-H bonds is unimportant relative to other reactions. Chloromethylidyne reacts with the Si-H bond and there was an observed correlation between the rate of reaction per Si-H bond and the hydridic character of the Si-H bond (54). The proposed reaction mechanism is a hydride ion transfer with more or less simultaneous back donation of the lone electron pair of the carbon to the silicon.

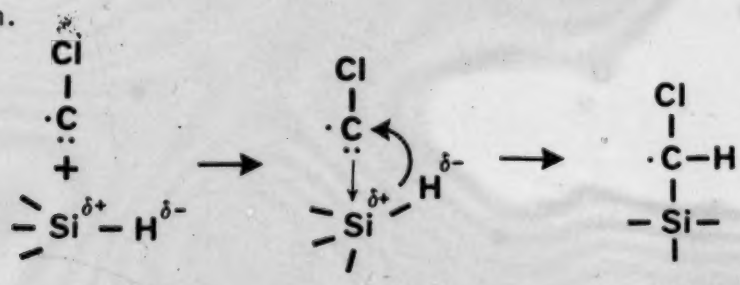

These results indicate that polar effects may have an important influence on chloromethylidyne reactions. CCl reacts with silanes at rates comparable to the insertion of CH_2 and SiH_2 into Si-H bonds. This should not be interpreted as indicating that the electrophilic character of CCl is the same as those of CH_2 and SiH_2 but merely that the Si-H bond is extremely reactive, as is well known, and unable to discriminate between the electrophilic reagents. Replacement of the methyl groups

Table I-7 Reaction of CCl with Silanes (54)

Substrate	$k_2 \times 10^{-9}\ M^{-1}sec^{-1}$
SiH_4	0.48 ± 0.05
$MeSiH_3$	1.7 ± 0.2
Me_2SiH_2	2.8 ± 0.1
Me_3SiH	2.8 ± 0.2
Et_2SiH_2	2.9 ± 0.3
Et_3SiH	4.5 ± 0.1
Me_4Si	N.R.
SiD_4	0.25 ± 0.03
$MeSiD_3$	0.98 ± 0.04
Me_2SiD_2	1.8 ± 0.1
Me_3SiD	2.8 ± 0.2
Si_2H_6	6.5 ± 0.3
Si_2D_6	5.6 ± 0.3
Me_6Si_2	0.025 ± 0.003
Cl_3SiH	$\leq$ 0.004
Cl_2MeSiH	0.029 ± 0.003
$ClMe_2SiH$	0.39 ± 0.02
Me_3SiCl	N.R.
Me_3SiF	N.R.
Cl_2Si_2	N.R.

by chlorine atoms is expected to decrease the hydridic character of the Si-H bond and causes a sharp drop in reactivity as shown by the rate constants. Chlorine deactivates the Si-H bond for electrophilic CCl insertion due to the inductive effect of the chlorine atom.

c) Bromomethylidyne, CBr

One set of reaction rate constants has been determined for CBr and the results are listed in Table I-8. The enthalpy of formation is 123 ± 15 kcal mole^{-1} (60). Therefore, the reactivity would be expected to be similar to that of chloromethylidyne. Comparing the rate constants for CBr reactions with those of CCl shows that they are very similar. The reactive channels for the reaction of CBr with O_2 and NO are outlined below.

		ΔH(kcal mole^{-1})
$CBr(X^2\Pi) + NO(X^2\Pi)$	$\xrightarrow{1}$ $CN(X^2\Sigma^+) + BrO(X^2\Pi)$	-13
	$\xrightarrow{2}$ $BrCN + O(^3P)$	-43
	$\xrightarrow{3}$ $CO(X^1\Sigma^+) + NBr(X^3\Sigma^-)$	-99
$CBr(X^2\Pi) + O_2(X^3\Sigma_g^-)$	$\xrightarrow{4}$ $CO(X^1\Sigma^+) + BrO(A^2\Pi)$	-39
	$\xrightarrow{5}$ $BrCO + O(^3P)$	?
	$\xrightarrow{6}$ $CO(X^1\Sigma^+) + Br(^2P) + O(^3P)$	-64
	$\xrightarrow{7}$ $CO(X^1\Sigma^+) + BrO(X^2\Pi)$	-119
	$\xrightarrow{8}$ $CO_2(X^1\Sigma_g^+) + Br(^2P)$	-190

Reaction channels 3,7 and 8 will definitely contribute and are probably the major source of infrared CO and CO_2 laser emissions observed in flash initiated $CHBr_3/O_2$ and $CHBr_3$/NO systems, which were attributed to CH reactions (76-78).

The reported rate constants indicate that CBr reacts slowly with tertiary C-H bonds while no measurable reactivity occurs with primary

Table I-8 Rate Constants for the Reactions of Bromomethylidyne (93)

Substrate	$k_2 \times 10^{-9}$ $M^{-1}sec^{-1}$
N_2	<0.004
H_2	<0.003
O_2	1.3 ± 0.5
NO	13 ± 2
CH_4	<0.003
iso-C_4H_{10}	0.018 ± 0.009
C_2H_4	0.46 ± 0.07
C_3H_6	5.5 ± 0.2
1-C_4H_8	9 ± 1
t-2-C_4H_8	6 ± 1
2,3-dimethyl-2-C_4H_8	12 ± 1
C_2H_3F	0.18 ± 0.01
$C_2H_2F_2$	0.12 ± 0.03

and secondary C-H bonds. These data tend to support Choi et al. and Wampler's results with regard to the reactivity of CCl towards C-H bonds. Bromomethylidyne exhibits an overall electrophilic trend in its reactions with alkenes, but there are some inconsistencies: 1-butene is expected to react more slowly than trans-2-butene and trans-2-butene should definitely react faster than propene with an electrophilic radical.

The reactivity trend for $CBr(X^2\Pi)$ appears to agree with its corresponding carbene, as was observed for the case of CCl. Dibromomethylene, $CBr_2(^1A_1)$ is unreactive towards paraffinic C-H bonds, but reacts with olefins in an electrophilic, stereospecific addition (2,4).

3) Carbethoxymethylidyne

Carbethoxymethylidyne has been reported to be a reactive intermediate in the photolysis of diethylmercurybisdiazoacetate, $(EtO_2CCN_2)_2Hg$(95). Photolysis of the parent compound in olefinic solutions results in products due to radicals which can be rationalized as arising from the addition of $:\dot{C}CO_2Et$ to the olefinic double bond to form a cyclopropyl radical and also from insertion into a C-H bond. The radicals formed undergo hydrogen abstraction to form the final products. The reaction sequence is outlined on the next page.

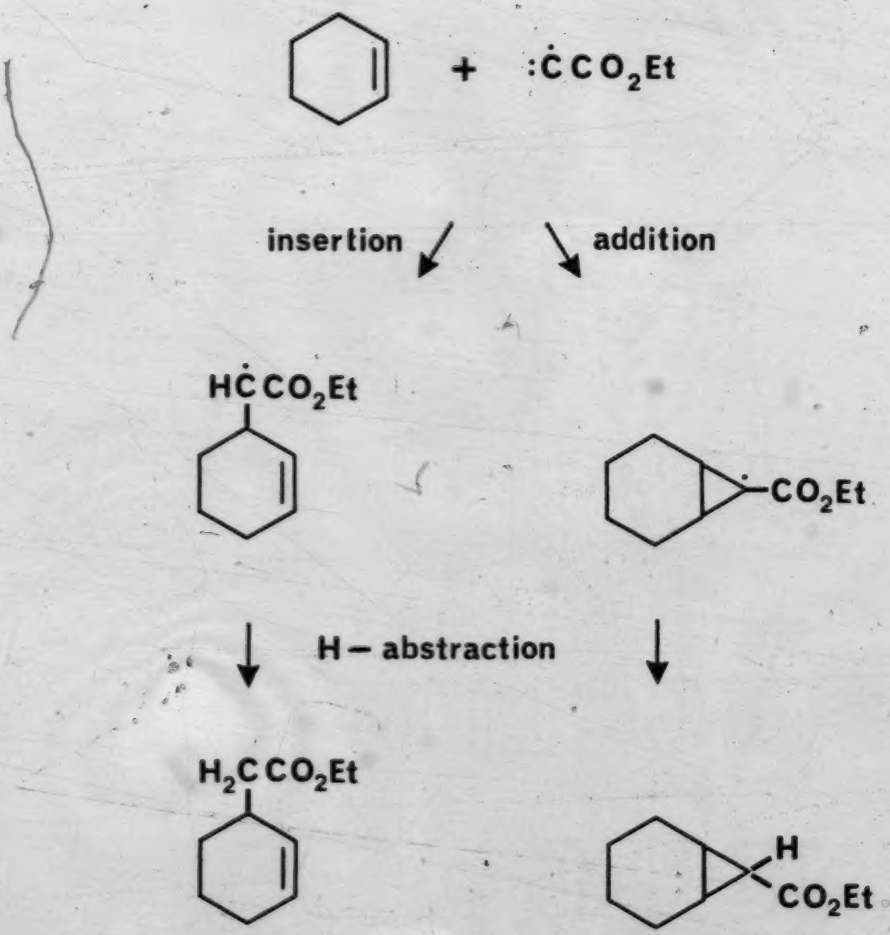
+ :ĊCO2Et
insertion
addition
HĊCO2Et
CO2Et
H – abstraction
H2CCO2Et
H
CO2Et

The presence of the carbethoxymethylidyne is supported by the fact that the primary yield of Hg in the photolysis of the parent compound is 9-18% and also by the fact that, in the mass spectrum of the parent compound, there is a strong m/e^- signal at 85 corresponding to carbethoxymethylidyne.

Photolysis of the parent compound may also yield α-mercurycarbenes which may undergo cycloaddition to olefins or insertion into C-H bonds (95, 116, 117). These compounds may undergo secondary photolysis to yield the same radicals as mentioned above.

D. Low Valent Silicon

In the previous sections, the molecular and chemical properties of carbynes were outlined. Silicon is the next member of Group IV A and it is therefore natural to examine monovalent silicon species and compare their molecular and chemical properties to monovalent carbon species. Divalent silicon species, silylenes, will also be examined. Since these fields are extensive and have been thoroughly reviewed (123-127), only a brief outline of certain silicon species, which are similar to those carbynes discussed, will be presented.

1) Molecular Properties

a) Silylidyne, SiH

The electron configuration of SiH is $...(3p\sigma)^2(3p\pi)^1$ resulting in a $^2\Pi_r$ ground state. The presence of SiH in stellar atmospheres and interstellar space has been established by observation of its spectrum (128, 129). The electronic spectrum consists of the transitions listed below.

$A^2\Delta - X^2\Pi_r$	412.8 nm
$C^2\Sigma^+ - X^2\Pi_r$	323.6 nm

$B^2\Sigma^+ - X^2\Pi_r$	323.6 nm
$D^2\Delta - X^2\Pi_r$	205.8 nm
$E^2\Sigma^+ - X^2\Pi_r$	190.6 nm

The electronic configurations of the three lower states, X,A,B are similar to those of the CH molecule. The A and B states are obtained upon exciting an electron from the bonding $3p\sigma$ to the $3p\pi$ orbital. The dissociation energy of SiH is 70.6 kcal $mole^{-1}$ (D_o(C-H) = 80 kcal $mole^{-1}$) and the $a^4\Sigma^-$ state has not been observed (130). The dipole moment of SiH has been calculated to be μ_{Si-H} = 0.302 D (μ_{C-H} = 1.57 D) with positive charge on the hydrogen (123).

b) Halosilylidynes

The electronic spectra of halosilylidynes have many more observable transitions than halomethylidynes (125).

The ground state of SiF is ... $1\pi^4 3\sigma^2 2\pi^1 - X^2\Pi_r$. Nine excited states including $a^4\Sigma^-$ have been observed and their molecular constants have been tabulated (123). The observed states may be divided into two groups: a) three non Rydberg states with ω_e < 1000 cm^{-1} and b) six Rydberg states with ω_e > 1000 cm^{-1}. The properties of the first excited state $A^2\Sigma^+$ are in accordance with the configuration ...$1\pi^4 3\sigma^2 4\sigma^1$ the 4σ orbital having strongly antibonding character. The states $C^2\Delta$ and $a^4\Sigma^-$ result from the configuration ... $1\pi^4 3\sigma^1 2\pi^2$. The very small changes in bond distance in these states are in agreement with the predicted non-bonding or slightly antibonding character of the 3σ and 2π orbitals. Therefore, in comparison to CF, the spectrum of SiF has many more transitions but there are similarities. The $B^2\Sigma^+ - X^2\Pi_r$ and $C^2\Delta - X^2\Pi_r$ transitions of SiF are the corresponding analogs of the $A^2\Sigma^+ - X^2\Pi_r$

and $B^2\Delta - X^2\Pi_r$ CF transitions but occur at lower energies. The dissociation energy of SiF is ~130 kcal $mole^{-1}$ (123) which is the same as for CF (131 kcal $mole^{-1}$)

The electronic states of SiCl, SiBr and SiI are related to SiF and show similar behaviour (123, 125). Some ground state properties are collected in Table I-9.

In summary, halosilylidynes exhibit the same bonding properties as halomethylidynes, but their spectra are much more complex and are dominated by Rydberg transitions.

c) Silylenes

Divalent silicon species, silylenes, are the homologues of carbenes and are therefore the subject of considerable attention as evidenced by several recent comprehensive reviews (124, 126, 127). Only the molecular properties of halogenated silylenes, which are similar to the dihalocarbenes discussed in the carbyne section, will be presented here.

For SiH_2 both a triplet and a singlet electronic state are

$$\ldots(1\,b_2)^2\,(3a_1)^1(1b_1)^1 - {}^3B_1$$
$$\ldots(1\,b_2)^2\,(3a_1)^2 - {}^1A_1$$

possibilities as for methylene, CH_2, where the ground state is $^3B_1$. However, $SiH_2(^3B_1)$ has not been observed and the ground state is $^1A_1$. A useful model has been provided for the effects of substituents on the singlet-triplet separations of carbenes, silylenes and isoelectronic species (131).

SiF_2 is the most thoroughly investigated silylene due to its relative stability. Molecular constants have been determined by a

Table I-9. Ground State Properties of Silicon-Halogen Radicals. (123)

	$A_e(cm^{-1})$	$\omega_e(cm^{-1})$	$\omega_e x_e(cm^{-1})$	$r_e(\mathring{A})$	D_o $(\frac{kcal}{mole})$
$SiF(X^2\Pi)$	161.9	857.2	4.7	1.60	130
$SiCl(X^2\Pi)$	207.2	535.6	2.2	2.06	92
$SiBr(X^2\Pi)$	418	424.	1.5	2.26	85
$SiI(X^2\Pi)$	700	363.8	1.3	2.45	69

variety of techniques and tabulated (123). Three electronic transitions have been observed; $a^3B_1 - X^1A_1$, 380.1 nm, $A^1B_1 - X^1A_1$, 226.6 nm and $B^1B_2 - X^1A_1$, 160.6 nm. The principal feature in the absorption spectrum due to the $A^1B_1 - X^1A_1$ transition is the presence of a long progression in the bending frequency of the upper electronic state, v_2' (132).

The electronic transitions of $SiCl_2$ have been observed in three systems. A broad absorption band with a maximum at 315 nm was observed in matrix isolation studies and in a high temperature furnace (133, 134). Asundi et al (125) detected a number of features superimposed on a continuous emission between 315 and 365 nm in the spectrum resulting from a discharge through $SiCl_4$ vapor. These features were assigned to two transitions of $SiCl_2$ one of which corresponds to the absorption at 315 nm and is assigned to $^1B_1 - {}^1A_1$ transition. The following vibrational frequencies were derived from this spectrum.

$$v_1'' = 540\ cm^{-1} \qquad v_1' = 445.3\ cm^{-1}$$

$$v_2'' = 248\ cm^{-1} \qquad v_2' = 201.1\ cm^{-1}$$

However the spectrum was poorly resolved and contained some inconsistencies in vibrational assignments and is in disagreement with recent assignments of $v_2'' = 202\ cm^{-1}$ and $v_1'' = 510\ cm^{-1}$ from the infrared spectrum of matrix isolated $SiCl_2$ (134, 135).

The infrared spectrum of $SiBr_2$ gives the following values for ground state vibrational frequencies; $v_1'' = 402.6\ cm^{-1}$, $v_2'' = 120\ cm^{-1}$ and $v_3'' = 399.5\ cm^{-1}$. No electronic transition of $SiBr_2$ has yet been detected although it has been mentioned as a possibility in emission spectra from a discharge through $SiBr_4$ (136). The spectrum, in the region 425-595 nm, showed intervals of 425, 240, 170 and 120 cm^{-1}.

The silylenes HSiCl, HSiBr and HSiI all have similar electronic transitions near 500 nm, assigned to $^1A' - {}^1A''$, exhibiting a long progression involving the bending frequency of the upper state ν_2'.

To sum up, all silylenes exhibit a singlet ground state with small bond angles at the Si atom. They may be excited throughout to a singlet upper state with considerably widened angles resulting in absorption spectra dominated by a progression involving ν_2'.

2) Generation of Silicon Radicals

The emission spectrum of halosilylidynes is usually generated by a discharge through SiX_4 (X = halogen) vapor. The absorption spectra of some silylidynes have been observed in the flash photolysis of halogenated silanes. SiBr and SiI have been seen in absorption following the flash photolysis of $SiBr_4$ and SiI_4 (137, 138). The flash photolysis of H_3SiI resulted in the absorption spectra of Si_2, SiH, SiI and HSiI (140). Hexachlorodisilane was flash photolysed to obtain the absorption spectrum of SiCl (141). It is also of interest to note the observation of SiF fluorescence from the photolysis of SiF_4 by a CO_2 laser, which led to the discovery of the phenomenon of collisionless infrared multiphoton absorption and dissociation (142).

The two most widely used methods for the generation of halogenated silylenes are: a) reduction of halosilanes and b) thermal decompositions of polysilanes.

The reduction of silicon tetrahalides by silicon resulting in the following equilibrium was used to demonstrate the existence of

$$SiX_4 + Si \rightleftharpoons 2SiX_2$$

dihalosilylenes and measure their thermodynamic functions and bonding

energies (127). These reactions take place only at temperatures above 800°C and give excellent yields of SiF_2, $SiCl_2$ and $SiBr_2$.

The thermolysis of polysilanes has been the most widely used method for generation of all types of silylenes. The thermal degradation of hexahalodisilanes, first examined 100 years ago, gives silanes and higher polysilane compounds (127). The intermediacy of silylenes was established by trapping experiments. From studies on thermal

$$Si_2X_6 \xrightarrow{\Delta} SiX_4 + :SiX_2 \longrightarrow (SiX_2)_n$$

disilane decomposition a model has been presented for the transition state for silylene extrusion, which involves a 1,2 substituent shift (124, 138). This process, also called α elimination, is postulated to occur through a pentacovalent sp^3d hybridized silicon atom, which is in accord with experimentally determined entropies of activation for silylene extrusion. For polysubstituted disilanes where different silylenes may be extruded, it is found that certain substituents have a greater facility to migrate. For example, when a chlorine atom and a hydrogen atom are in an identical environment, the hydrogen atom shift is considerably more favored (140). This is reflected in experimentally determined activation parameters (139).

Higher polysilanes can also undergo this silylene extrusion process through the migration or shift of a silyl substituent. The study of silylene reactions was greatly facilitated by the discovery a decade ago that photolysis of orgonopolysilanes also results in silylene extrusion under much milder conditions (141). Differences occur between the photolysis and thermolysis of polysilanes due to the energies and electronic state involved. In thermolysis, the lowest free energy

path tends to be the dominant reaction while in photolysis, due to the involvement of electronically excited states, more energetic decompositions became accessible and there is a competition between various substituents for migration resulting in different silylenes being generated. This behaviour is illustrated below in the photolysis of an alkoxypolysilane.

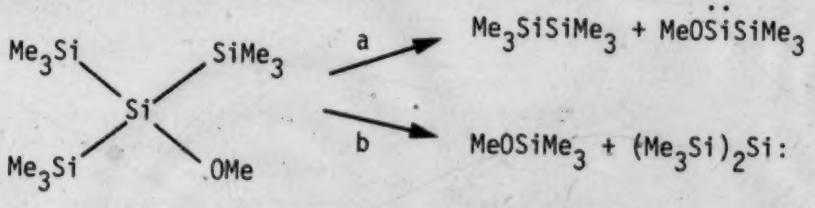

Migration of an alkoxy group, process b, is the exclusive thermolytic pathway whereas in photolysis process a, migration of a silyl group competes with process b in a statistical ratio of 2:1 respectively (124).

There are various other methods to generate silylenes which are covered in detail in the reviews (124, 126, 127, 137).

3) Reactions

Nothing is known about monovalent silicon reactions although these species occur in interstellar space (129). On the other hand, the reactions of silylenes constitute an area of great interest in chemistry because of the carbene relationship. The general reactions of silylenes will be outlined here with emphasis on dihalosilylenes.

Silylenes undergo a variety of insertion reactions: into silicon-silicon bonds; into oxygen-hydrogen and nitrogen-hydrogen bonds; into carbon-oxygen bonds of ethers and into silicon-oxygen bonds of alkoxysilanes (124). Intramolecular insertion into a C-H bond has been proposed to account for some silylene rearrangement products (124).

Dimerization of silylenes has long been proposed but only recently has been used to synthesize a room temperature-stable compound containing a silicon-silicon double bond (142).

One example of these reactions is the expansion of furans upon reaction with thermally generated dichlorosilylene, reported by Chernyshev and coworkers (143).

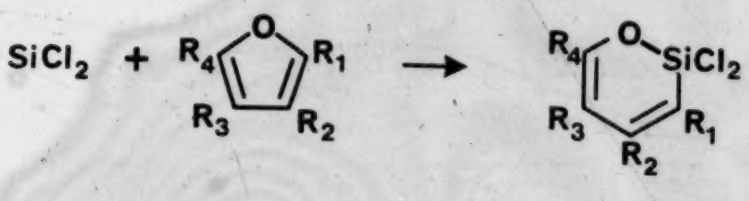

Singlet organosilylenes resemble closely their carbene counterparts in their addition to olefins, conjugated dienes and acetylenes. Concerted 1,2 cis-additions seems to be the rule and the major difference between silylene and carbene additions stems from the much lower stability of the silacyclopropane products. Thus secondary products are often isolated from silylene additions, due to rearrangement of the primary adducts under the influence of heat or light.

The addition reactions of dihalosilylenes have received less attention and the mechanism is somewhat uncertain. When SiF_2 was generated in the gas phase, reactions with various substrates were believed to be initiated by dimerization to form a diradical since all stable reaction end products contained more than one SiF_2 unit (144, 145). However, recent evidence suggests that monomeric SiF_2 reactions with substrates can take place (146,147). The observed reaction products of $SiCl_2$ with alkenes, dienes and alkynes suggest the initial addition of $SiCl_2$ to the double or triple bond (144).

E. Aim of the Present Investigation

It has been shown in the previous sections that there is a limited amount of knowledge concerning the reactions of carbynes. Most of this information has come from kinetic measurements. Rate constants have been determined for CH reactions with a variety of substrates and they are all very high, close to collision frequency, and consequently exhibit little variation with the nature of the substrates. Some rate constants for the reactions of CCl and CBr with selected alkanes, alkenes and alkynes have been reported. In general they are lower than those for the analogous CH reactions and there is a much greater discrimination amongst a variety of substrates. The pattern of reactivity towards alkyl substituted alkenes suggests electrophilic character for CCl and CBr. However, for CBr the reported data show that trans-2-butene reacts more slowly than propylene and 1-butene which is not expected of an electrophilic reagent.

Now the major aim of this investigation was to examine and compare the electrophilic reactivity of the halomethylidynes, CF, CCl and CBr. To do this it was decided to measure the rate constants of the reactions of these carbynes with a series of alkyl substituted alkenes using the flash photolysis technique for the following reasons:

1) Alkyl substituted alkenes have been used to characterize the electrophilicity of a wide variety of reagents.

2) There have been no measured rate constants for the reaction of CF with alkenes.

3) For CCl the reaction with only four alkenes had been measured. Since this investigator's results with other substrates did not agree well with other measurements (see Table I-7) it was desirable to

remeasure the rate constants and extend the series of alkenes.

4) In view of the above mentioned inconsistency for CBr reactions, it was desirable to remeasure the rate constants with alkenes and to extend the series.

5) Since CF, CCl and CBr can be generated by flash photolysis of similar precursors, the reactivities could be measured in an identical manner. This should eliminate any systematic errors and provide better comparisons of their relative reactivity.

At the time this project was initiated, there were only two reported rate constants for the reaction of CCl with alkynes, namely with acetylene and propyne. It was therefore decided to measure the rate constants for the reaction of CBr with alkyl substituted alkynes since no data were available. Later measurements of the reaction of CCl with similar substrates provided a comparison between the two halomethylidynes (54).

Since there had been no data available on the effect of temperature on any carbyne reactions, it was decided to measure the variation of rate constants with temperature for the reaction of CBr with some substituted alkenes. The determination of the activation parameters of rate constants and their variation with different substrates provide details about the mechanistic features of the reaction.

Lastly, since the halosilylidynes, SiCl and SiBr could be generated by flash photolysis and no kinetic data were available, it was decided to attempt to measure the rate constants of the reaction of SiCl and SiBr with ethylene so that comparisons of reactivity could be made.

II. EXPERIMENTAL

Since flash photolysis is a well established technique and many excellent articles have been written on the subject (153) only a brief description of a conventional system is given here.

In flash photolysis, a non-equilibrium situation is created in a short initiation time of microseconds by a flash discharge lamp which produces a high intensity light flash. This light flash photolyses suitable molecules to generate relatively large concentrations of transient intermediates which undergo reaction. The decay rate of these transient intermediates, due to reactions, is monitored by either flash spectroscopy or kinetic spectrophotometry. In the first approach, which was used in this study, the absorption spectrum is recorded at a given time. This is accomplished by a monitoring beam from the spectroscopic lamp, fired at a pre-set delay time after the photolysis flash, which essentially provides a background continuum. After passing through the reaction mixture, the beam is resolved by the spectrograph and recorded by photographic material. The procedure is repeated at various delays so as to obtain a time profile of the chosen absorption band of the transient.

A. Apparatus

1. The Vacuum System

A conventional high vacuum system constructed of Pyrex was used for the gas phase kinetic study. It was completely grease free, utilizing helium-tested Hoke values, and consisted of a distillation train and storage bulbs (Fig. II-1).

The vacuum system was evacuated to a pressure of 10^{-6} torr by

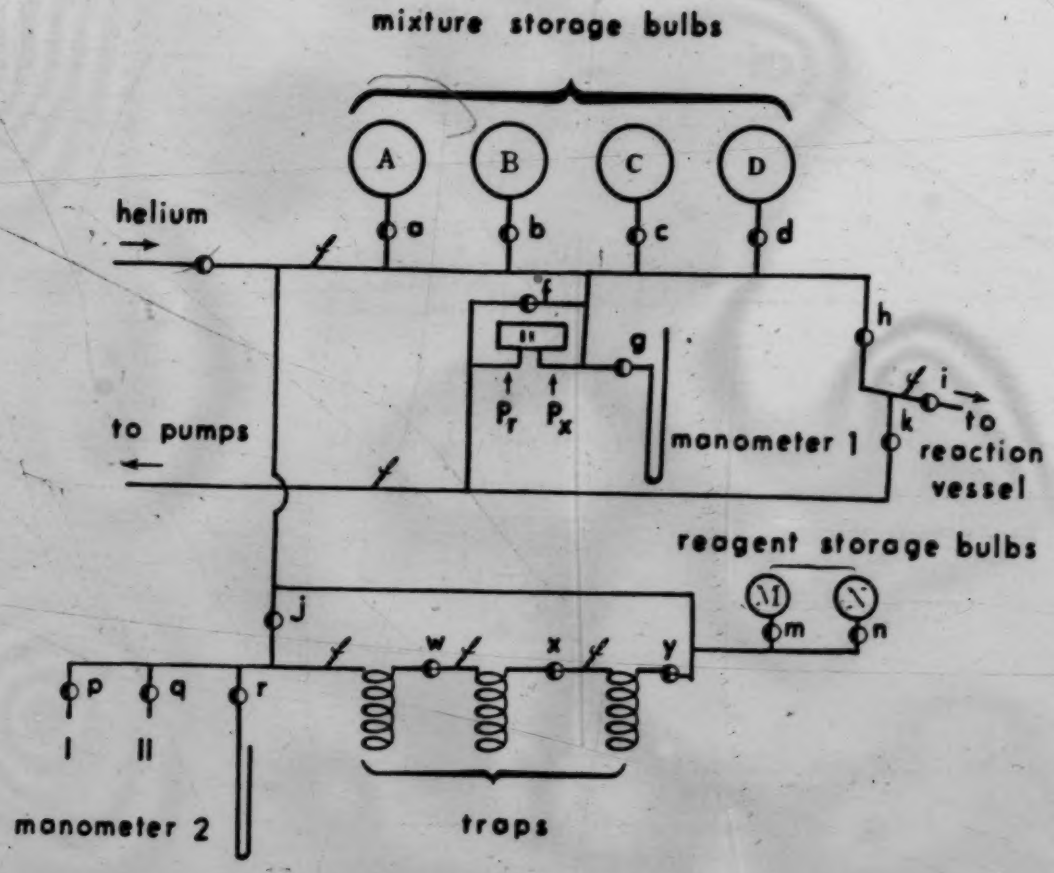

f : Pirani Vacuum Gauge Tube

" : Baratron Pressure Meter Head

◐ : Hoke Valve

⊖ : Teflon Valve

I : Inlet for the introduction of liquid reagents

II : Inlet for the introduction of gaseous reagents

FIGURE II.1 The Main Vacuum System

means of a mercury diffusion pump backed by a rotary pump (Duo-Seal Vacuum pump, Model 5KC42, JG14A, Welch Manufacturing Company). Pressures were monitored by Pirani Vacuum Gauges (type GP140), Magnevac Vacuum Gauges (type GMA140), MKS Baratron Pressure Meters (type 77 and type 170 M-6B) and mercury manometers which were capable of measuring pressures in the range 10^{3} to 10^{-3} torr.

The distillation train, consisting of a series of three traps isolated by Hoke Valves, was used for purification of reagents. The storage system consisted of several 3 or 5 litre bulbs for the temporary storage of reaction mixtures to be used in the flash photolysis.

Argon was introduced into the main vacuum system after passage through a 30 cm long column of copper turnings (heated to 350°C for the removal of oxygen) and a 30 cm long column of molecular sieve (type 5A for the removal of water vapor).

A separate mercury free line was used to fill the flash lamps. Vacuum was achieved by a Duo Seal Vacuum pump with a liquid nitrogen trap and the pressure was monitored by a Pirani Vaccum Gauge (type GP-140) and measured by Edwards CG3 gauges.

2. The Flash Photolysis System.

The major components of the flash photolysis system are illustrated in Fig. II-2.

a) The Reaction Vessel and Reflective Housing

The reaction vessels used were cylindrical tubes 73 cm long and 25 mm in inner diameter. They were made of either quartz (wavelength cutoff 195-200 nm) or suprasil (wavelength cutoff 165-170 nm). For the temperature work a special double walled reaction vessel was con-

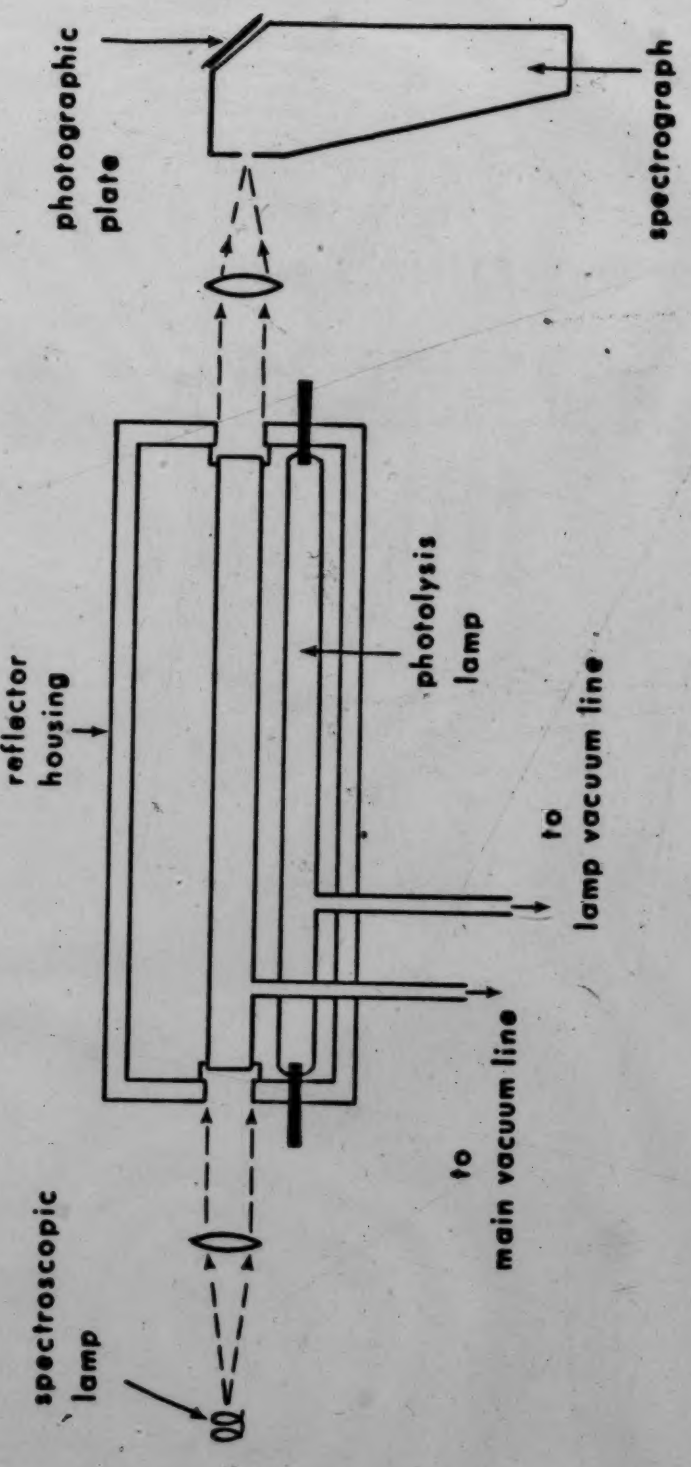

FIGURE II.2 The Flash Photolysis System

structed of quartz. The reaction vessels were equipped with flat quartz windows on both ends and a side arm for the introduction and evacuation of the reaction mixture. The side arm was connected to the main vacuum system by a Cajon valve, which facilitated the detachment of the reaction vessel from time to time for cleaning. The reaction vessel used for the temperature work had two extra outlets to the outer cavity which were connected to a Calora temperature bath for circulation and heating of a fluid for temperature maintenance of the reaction vessel. The fluid used in this study was ethylene glycol.

The reaction vessel, sitting on two end supports, was positioned at the centre of a reflective housing assembly lying horizontally along the optical path. Apertures on both ends allowed the passage of light in and out through the reaction vessel. The housing (Fig. II-3) was constructed of aluminum and was cylindrical in shape, 80 cm long and 15 cm in inner diameter. It consisted to two half cylinders joined together by hinges on one side, so that the upper half could be opened for the removal of the reaction vessel and photolysis lamp for cleaning. The lower half, upon which the ends of the reaction vessel and photolysis lamp rested, was mounted by two supports onto the optical bench. The inner surface of the housing was coated with $BaSO_4$ which is highly reflective in the ultraviolet region of the electromagnetic spectrum.

b) The Photolysis Lamp

The photolysis lamp (Fig. II-2 and II-3) was a quartz or suprasil tube 25 mm in diameter with a sidearm for filling and evacuation. Molybdenum alloy electrodes (Vitreosil Model T/E7/232) were sealed into each end by standard lead seals able to withstand high thermal and mechanical shock. The distance between the tips of the electrodes,

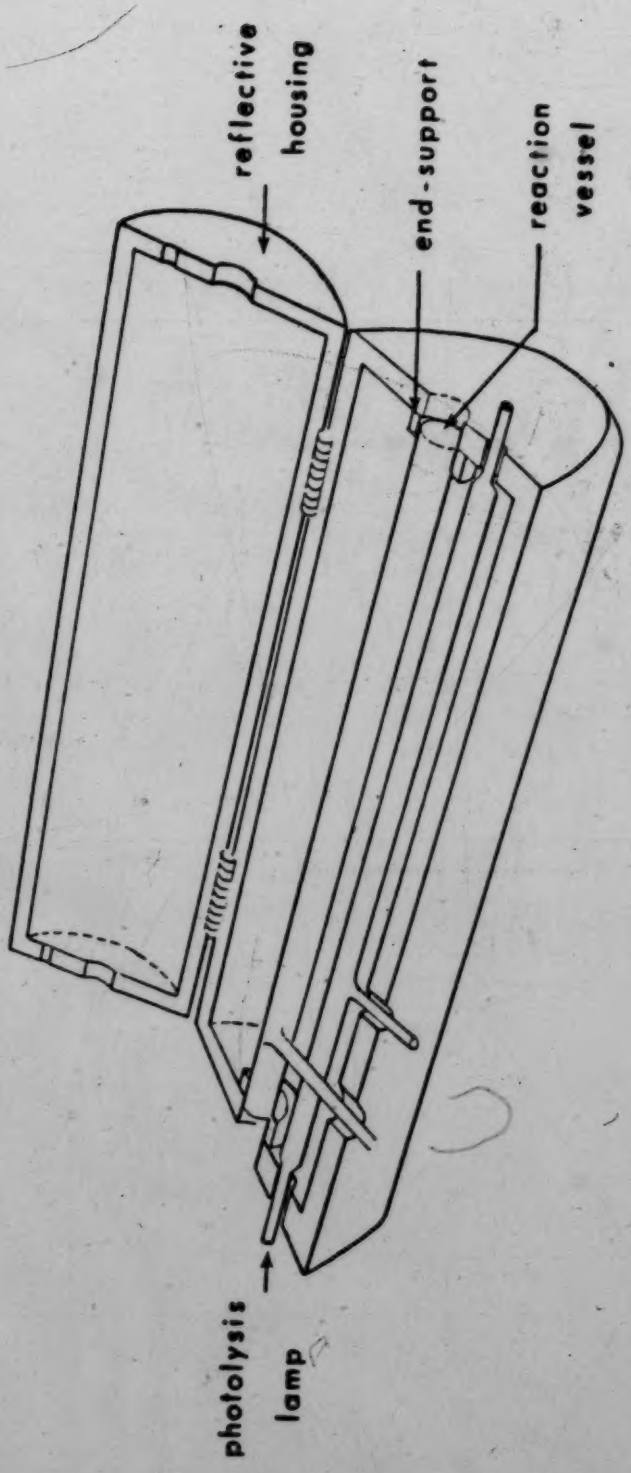

FIGURE II.3 The Reaction Vessel and the Reflective Housing

73 cm, was the same length as the reaction vessel. The side-arm was connected to the lamp vacuum line through a high vacuum stopcock (Pyrex V-4) and a detachable ball joint. The stopcock isolated the lamp from the vacuum line while the ball joint facilitated the removal of the lamp for cleaning.

The lamp was placed horizontally next to the reaction vessel with the electrodes resting on the ends of the reflector housing and protruding outside through the end apertures. When filled with 25 mbar Xenon gas, the light flash reached its maximum intensity in 10 microsec and had a half life of about 20 microsec with a long tail, as recorded by a photocell (Sylvania 90 CV) and displayed on an oscilloscope (Hewlett Packard 130C). The lamp circuit included an ignitron (Westinghouse Size A, WL 7709) and a G.E. Energy Storage Capacitor (capacitance 14.5 μF, 20 KV). The lamp circuit was discharged at either 17 or 20 KV which dissipated 2095 or 2900 Joules through the xenon gas filling, creating the plasma which generated the light output. To condition a new lamp the following method was used; the lamp circuit was discharged initially at a low voltage and the discharges were repeated with gradually increasing voltages until the desired voltage was reached. The repeated discharges condition the new lamp to the high thermal and mechanical shock of discharging at a high voltage.

c) The Spectroscopic Lamp

The spectroscopic lamp was also made of quartz, and molybdenum alloy electrodes (Vitreosil Model T/E7/232) were sealed into the side arms by standard lead seals. They were separated by a short capillary

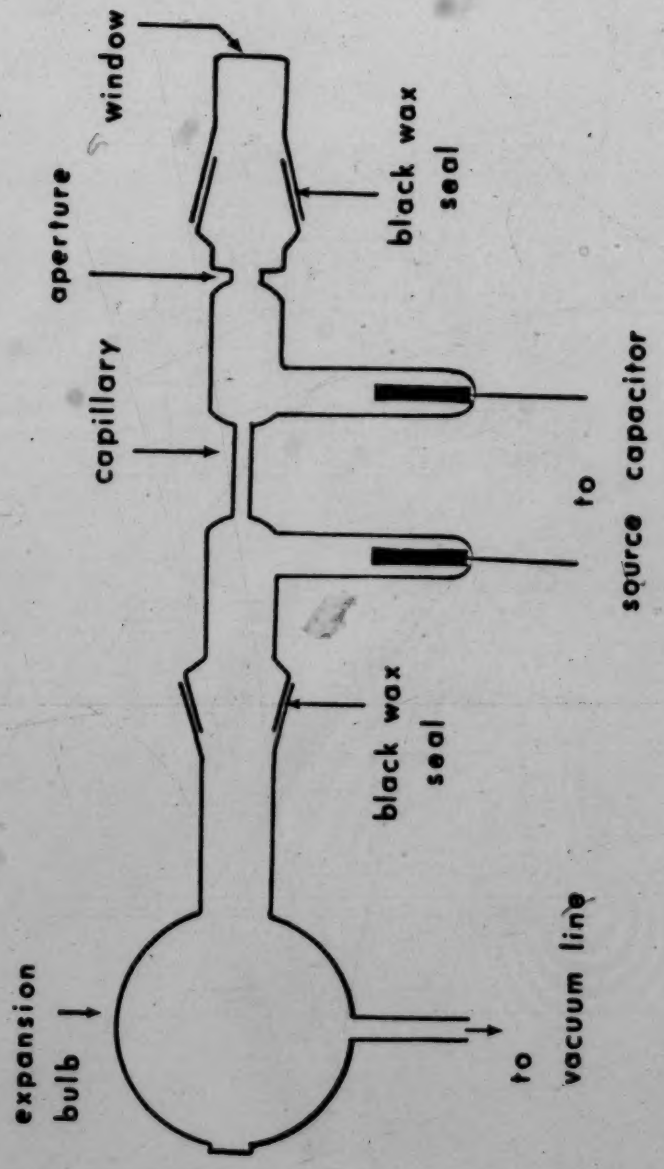

FIGURE II.4 The Spectroscopic Flash Lamp

tube, 5 cm long and 3 mm in inner diameter, to ensure high current density and intense light output. An aperture which was close to the lamp window minimized the deposit of silica on the window and an expansion bulb was used to accomodate the shock wave which accompanied the discharge. The lamp parts were sealed together by Apiezon Black Wax to facilitate frequent cleaning and the lamp was connected to the lamp vacuum line through a high vacuum stopcock (Pyrex V-4) and a detachable ball joint. The spectroscopic lamp was filled with 75 mbar Xenon to provide a background continuum. The light flash reached its maximum intensity in 5 microsec and had a half life of 10 microsec. The spectroscopic lamp circuit included an ignitron (Westinghouse Size A, WL 7709) and a SCI Energy Capacitor (Model 25 W67/TN, capacitance 1.0 μF, voltage 25 KV) which was discharged at 20 KV to provide 200 Joules per flash. The spectroscopic lamp was also conditioned by repeated discharges at lower voltages. Fused quartz lenses were used to collimate the light beam from the spectroscopic lamp through the reaction vessel and to focus it at the entrance slit of the spectrograph.

d) The Spectrograph

The spectrograph (Hilger-Watts Model 742-1) operates with a Littrow mounting system, utilizing a quartz prism as a non-linear dispersion device (Fig. II-5) and the resolved spectrum is focussed on a light sensitive photographic material. In this study Kodak Spectroscopic Plates Type 103a-O were used to observe absorption spectra at wavelengths greater than 240 nm and Kodak Special Film Type 101-01 was used for absorption spectra below 240 nm. The absorption lines

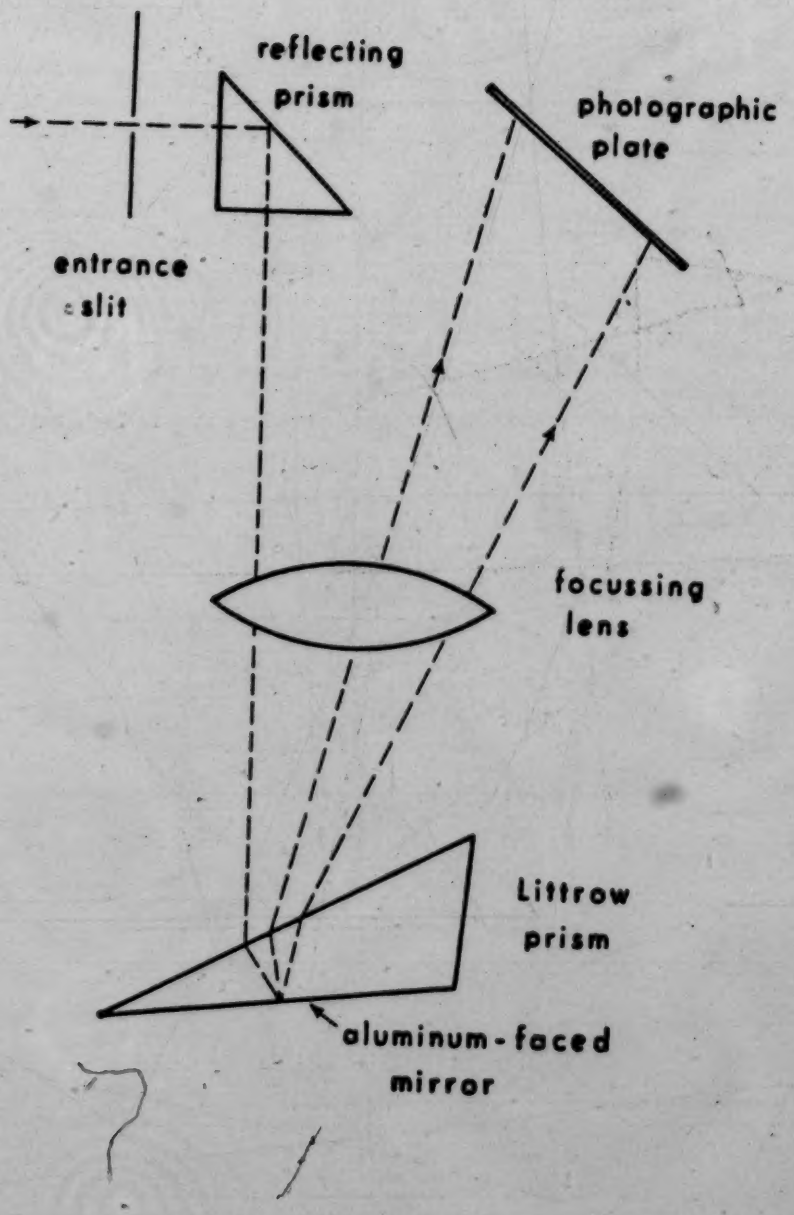

FIGURE II.5 The Littrow Prism and Mounting

in the spectrum recorded by the photographic material were traced out as absorption peaks using a microdensitometer.

3. The Microdensitometer

The microdensitometer (Joyce Loebl MK 11C, Fig. II-6) is operated on a double beam system. The analysis beam is scanned across the photographic material and the reference beam passes through an optical density wedge. As the sample spectrum is scanned, the two beams were alternately fed into a photomultiplier detector. Any difference in the intensities of the beams was amplified and the resulting signal activated a servo motor to drive the optical density wedge so as to nullify the intensity difference. A pen attached to the optical density wedge traced out the resulting spectrum. An adjustable slit in the analytical light beam path combined with the optical magnification to give an effective exit slit width which, when multiplied by the dispersion of the spectrograph, gives the spectral band width.

B. Operational Procedures

1) Operation of the Flash Photolysis System

The circuit diagram is illustrated in Fig. II-7. The two lamp capacitors were first charged up to the desired voltages. Then a pulse delay generator was activated which sent out two voltage pulses, one to the photolysis lamp ignition and the other to the spectroscopic lamp ignition. These pulses closed the lamp circuits and caused the capacitors to discharge through the lamps, producing the photolysis and spectroscopic light flashes. The delay between the two pulses could be adjusted from 25 to 9999 micro-seconds. The light pulses from the two discharges were picked up by a photocell (Sylvania 90CV), amplified and displayed on an oscilloscope screen (Hewlett-Packard 130C). The

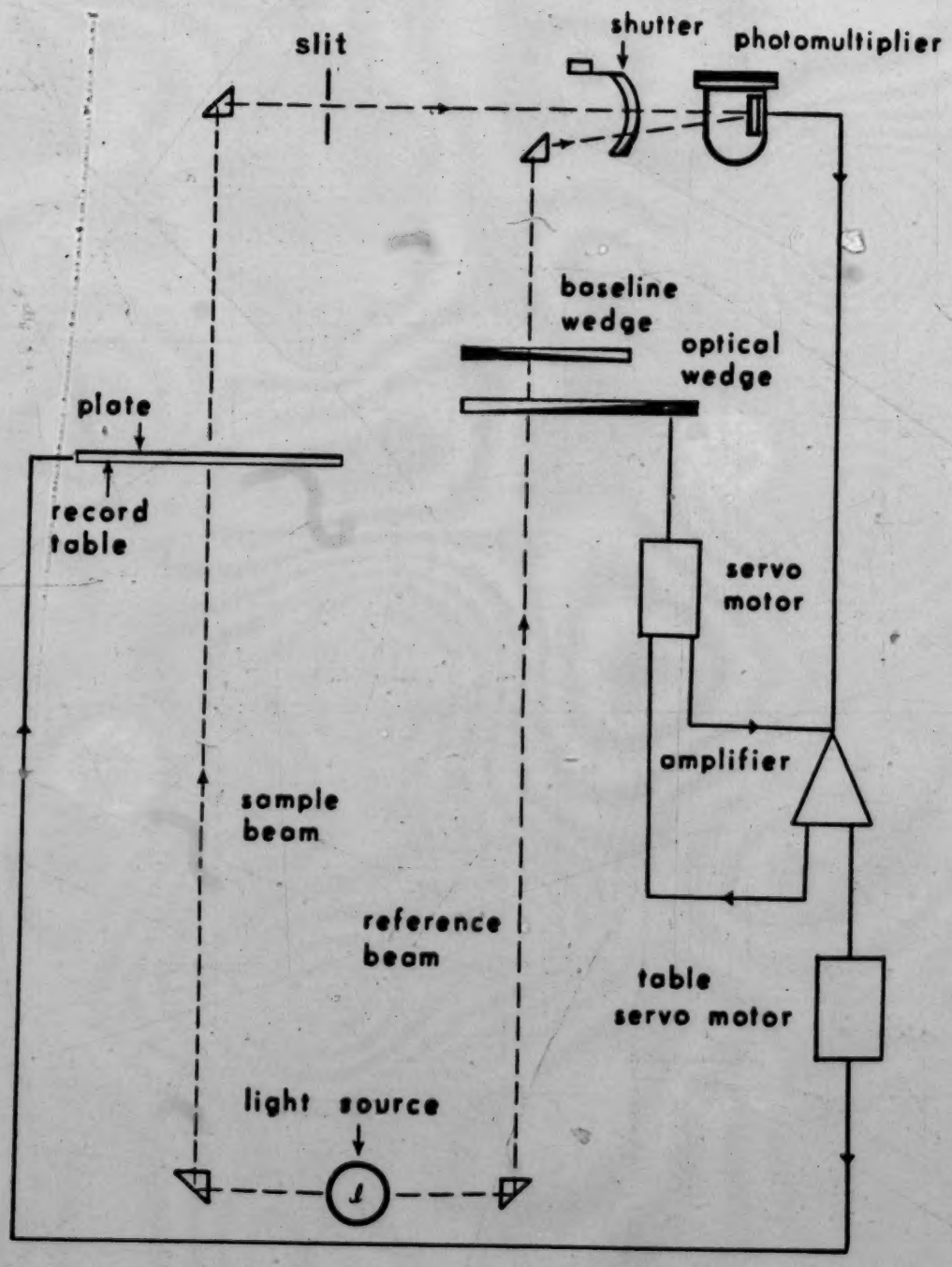

FIGURE II.6 Schematic Diagram of the Microdensitometer

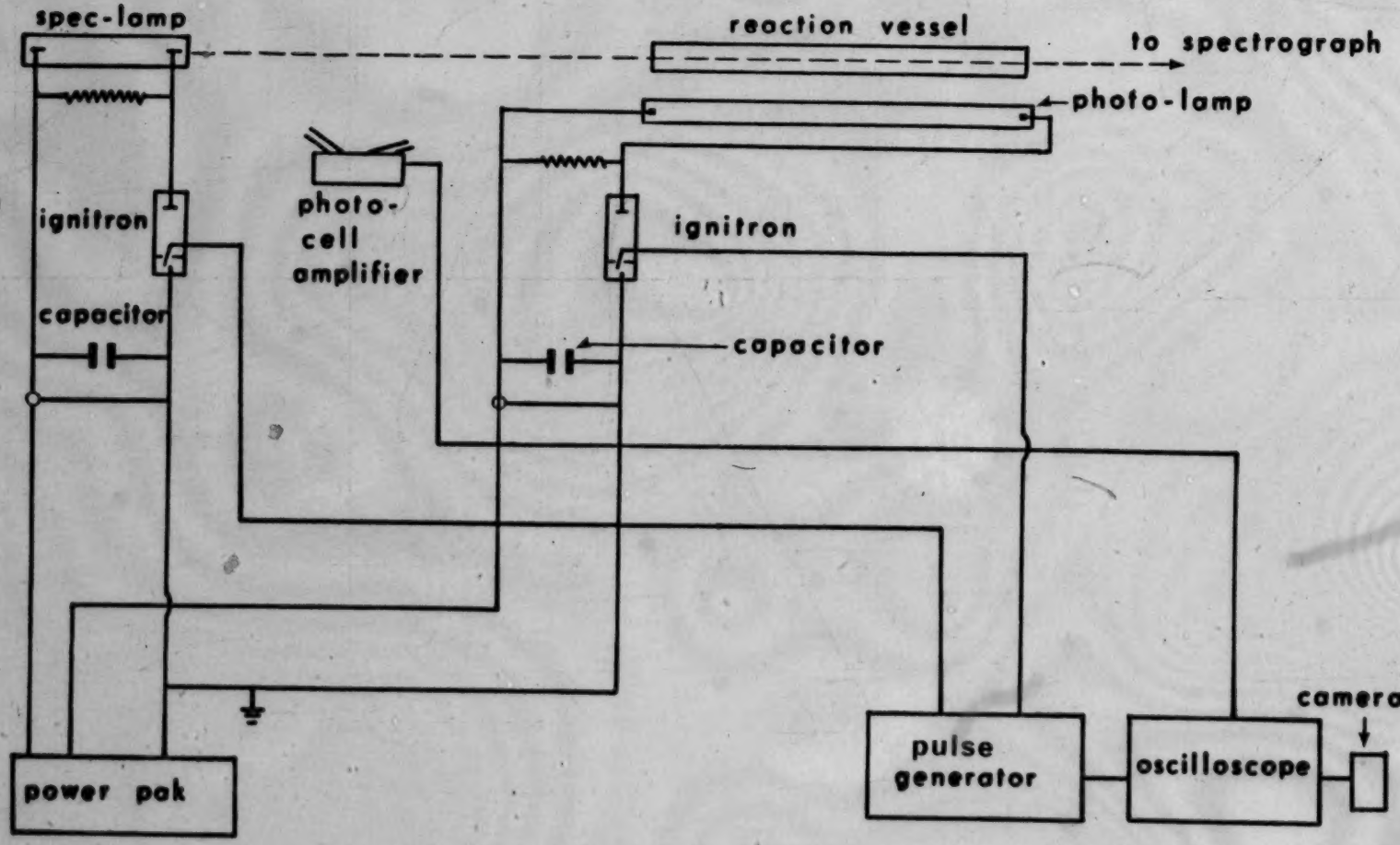

FIGURE II.7 The Flash Photolysis System: Circuit Diagram

trace was photographed (Hewlett-Packard Oscilloscope Camera Model 197A using Polaroid Type 107 Land Film) and the separation between the peak of the photolysis flash signal and that of the following spectroscopic flash signal was taken as the time delay. A typical oscilloscope trace is shown in Fig. II-8.

2) Preparation of Gas Mixtures

The gas mixtures, which contained the source of the transient intermediate and differing amounts of reactive substrate in a large excess of argon, were prepared using the 3 or 5 litre storage bulbs (Fig. II-1). Pressures were monitored by the MKS Baratron Pressure Meters for pressures below 100 torr and mercury manometers for higher pressures.

The procedure employed for preparing a mixture (consisting, for example, of 2 torr ethylene and 1 torr $CHBr_3$ in a total pressure of 500 torr argon) in a storage bulb was as follows.

First $CHBr_3$, which is stored in a reagent bulb, is introduced into the vacuum line and storage bulb until the Baratron Pressure Meters read 1 torr. This pressure is allowed to stabilize for a few minutes, then the storage bulb valve is closed and the $CHBr_3$ in the vacuum line is pumped away. With 1 torr $CHBr_3$ already in the bulb and a desired pressure of 2 torr ethylene, a total pressure of 3 torr is required in the storage bulb. The ethylene is introduced into the vacuum system until a pressure greater than 3 torr is achieved. When the storage bulb valve is opened, the ethylene will diffuse into the storage bulb until the pressure equalizes as indicated by the MKS Baratron Pressure Meters. When the pressure stabilizes the storage bulb valve is closed and the

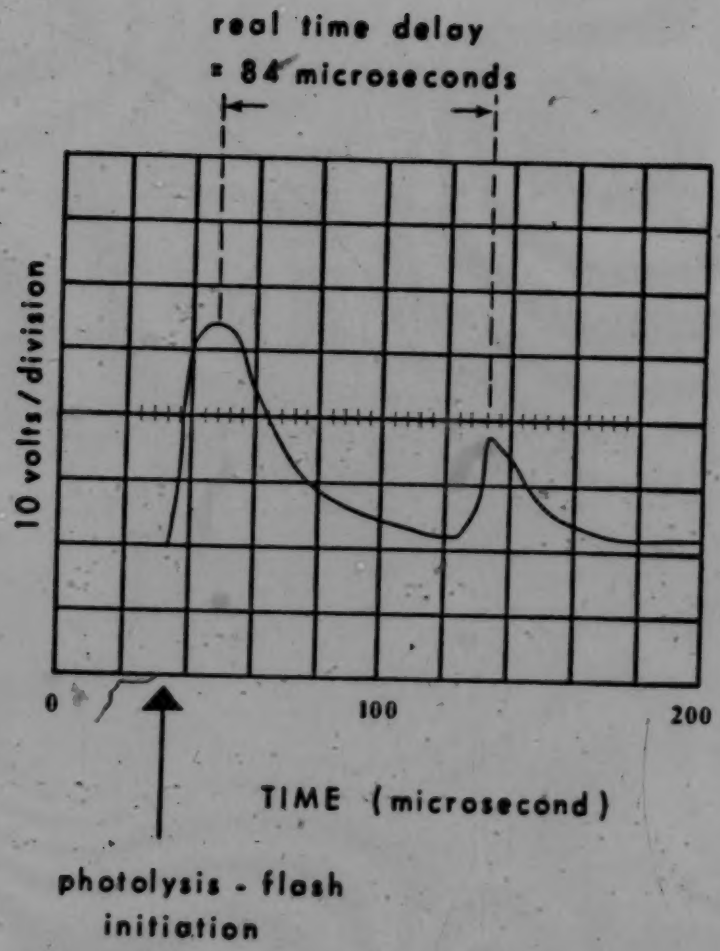

FIGURE II.8 Oscilloscope Trace

procedure is repeated until a stable pressure of 3 torr is recorded on the MKS Baratron Pressure Meters. The vacuum line is then evacuated. Argon is then introduced and the pressure monitored by the mercury manometer. After the pressure is well past 3 torr the storage bulb valve is opened and when 500 torr argon has been admitted, the storage bulb valve and the argon supply line valve were closed and the excess argon was evacuated.

The gas mixtures are usually stored overnight to achieve homogeneity. For the flash photolysis experiment, a mixture from one of the storage bulbs is introduced into the reaction vessel until a pressure of 50 torr is achieved. After flash photolysis the reaction vessel is evacuated with the pressure being monitored by the Pirani Vacuum Gauge. After proper evacuation the procedure is repeated.

Due to deposition of materials from the photolysis of the mixtures, the reaction vessel was cleaned frequently by rinsing with 10% hydrofluoric acid. The two lamps were also cleaned frequently with 10% hydrofluoric acid to remove deposits of silica and metal from the electrodes.

3) Development of Photographic Emulsions

The Kodak 103a-O spectroscopic plates were developed in Kodak D-19 Developer for 3 min @ 24°C, 4 min @ 20°C or 5 min @ 16°C. The Kodak 101-01 photographic film was pre-rinsed in distilled water for 1 min and then developed in a solution of 50% Kodak D-19 Developer and 50% distilled water for 4 min @ 20°C. Both the photographic plates and films were then rinsed successively in a stop bath (1-2% acetic acid) for 1 min, in Kodak Rapid Fixer for 4 min and running water for 20-30

min. The photographic materials were then air dried and placed on the microdensitometer for scanning.

C. Materials

The materials used in this study, their sources and source purity level and methods of purification are listed in Tables II-1-II-3. Generally, the materials were introduced into the vacuum system, degassed several times to remove air contamination, distilled from trap to trap with retention of only the middle fraction and stored in vacuum tight bulbs. The purity of some of the compounds was checked by gas chromatography. The samples were introduced onto an 8 ft. Paropak N column operating initially at 53°C with a helium flow rate of 40 ml/min. After 20 min the temperature was increased at the rate of 3 deg/min until a temperature of 165°C was reached. The samples were detected by a Gow Mac type thermal conductivity detector and analyzed on a Varian CDS 101 recorder. Table II-4 lists the retention time and purity level of the samples that were analyzed by gas chromatography. The ultraviolet absorption spectra of some compounds were recorded on Unicam SP 800 instrument using a gas phase 10 mm cell.

Table II-1

Purification of Inorganic Compounds and Alkanes.

Material	Source and Purity Level	Purification
Fluorodibromomethane	PCR chemicals 97%	Distilled at -63°C trapped at -107°C
Chlorodibromomethane	Eastman Organic Chemicals	Distilled at -23°C trapped at -78°C
Bromoform	Eastman Organic Chemicals	Distilled at 0°C trapped at -78°C
Silicon Tetrabromide	Alfa Chemicals	Distilled at 0°C trapped at -78°C
Hexachloradisilane	PCR Chemicals 97%	Distilled at 0°C trapped at -78°C
Argon	Matheson 99.95%	Passed over Cu at 350°C and then Molecular Sieve 5A
2-methylpropane	Phillips Petroleum Co. 99.8%	Distilled at -107°C trapped at -131°C

Table II-2

Purification of Alkenes.

Material	Source and Purity Level	Purification
Ethylene	Matheson Gas Products 99.98%	Distilled from -160°C trapped at -195°C
Propylene	Phillips Petroleum Co. 99.8%	Distilled from -145°C trapped at -195°C
1-Butene	Linde Gas Co. 99.8%	Distilled from -112°C trapped at -160°C
t-2-Butene	Phillips Petroleum Co. 99.8%	Distilled from -112°C trapped at -160°C
2-methyl-2-propene (iso-Butene)	Linde Gas Co. 99.8%	Distilled from -107°C trapped at -160°C
2-methyl-2-butene	Chemical Samples Co. 99%	Distilled from -78°C trapped at -112°C
2,3-dimethyl-2-butene	Chemical Procurement Labs. 99%	Distilled from -63°C trapped at -107°C

Table II-3

Purification of Alkynes.

Material	Source and Purity Level	Purification
Acetylene	Matheson Gas Products 99.6%	Distilled from -131°C trapped at -160°C
Acetylene-d_2	Merck, Sharpe and Dohme of Canada, Ltd.	Distilled from -131°C trapped at -160°C
Propyne	Matheson Gas Products 99.7%	Distilled from -107°C trapped at -139°C
1-Butyne	Chemical Procurement Labs 99%	Distilled from -84°C trapped at -131°C
2-Butyne	Farchan Research Labs	Distilled from -64°C trapped at -107°C
1-Pentyne	Chemical Procurement Labs 99%	Distilled from -64°C trapped at -107°C
2-Pentyne	Chemical Procurement Labs 99%	Distilled from -45°C trapped at -107°C
2,2,5,5- tetramethyl 3-Hexyne	Chemical Samples Co. 99%	Distilled from 0°C trapped at -64°C
Perfluoro-2-Butyne	Aldrich Chemical Co.	Distilled from -78°C trapped at -112°C

Table II-4

Gas Chromatography Analysis

Material	Retention time (min)	Purity Level
Acetylene	8.3	99.95%
Ethylene	6.7	99.9%
t-2-Butene	44.5	99.8%
2-methyl-2-propene	44.7	99.2%

III. RESULTS

A) Halomethylidyne Sources

The halogenated methanes $CHFBr_2$, $CHClBr_2$ and $CHBr_3$ were used as sources of the halomethylidynes CF, CCl and CBr, respectively in this study since it was reported that the most intense halomethylidyne spectra were obtained from these halogenated methanes (50,51) and also because of their structural similarity. The ultraviolet absorption spectra of these halogenated methanes are shown in Fig. III-1 and are in agreement with the reported UV absorption spectra of brominated methanes (154,155).

B) Halomethylidyne Absorption Spectra

1) Fluoromethylidyne, CF

The absorption spectrum shown in Fig. III-2 results from the photolysis of 0.15 torr $CHFBr_2$ with 50 torr Argon in a quartz system with 2900 J flash energy and 20 μsec time delay. Three exposures were necessary to obtain the spectrum due to the background absorption of $CHFBr_2$. As a result of this problem the CF absorption intensity as recorded is weak and the background continuum is not uniform. This imposes severe instrumental requirements on the kinetic measurements of CF reactions.

The absorption spectrum observed is due to the $A^2\Sigma^+ - X^2\Pi$ (1-0) transition of CF. Four rotational bandheads are observable; $^0P_{12}$ (224.27 nm), P_2 (224.18 nm), P_1 (223.88 nm) and Q_1 (223.79 nm) in agreement with previous observations of CF absorption spectra (30,37). A very weak absorption, having the same structure as the 1-0 band, is

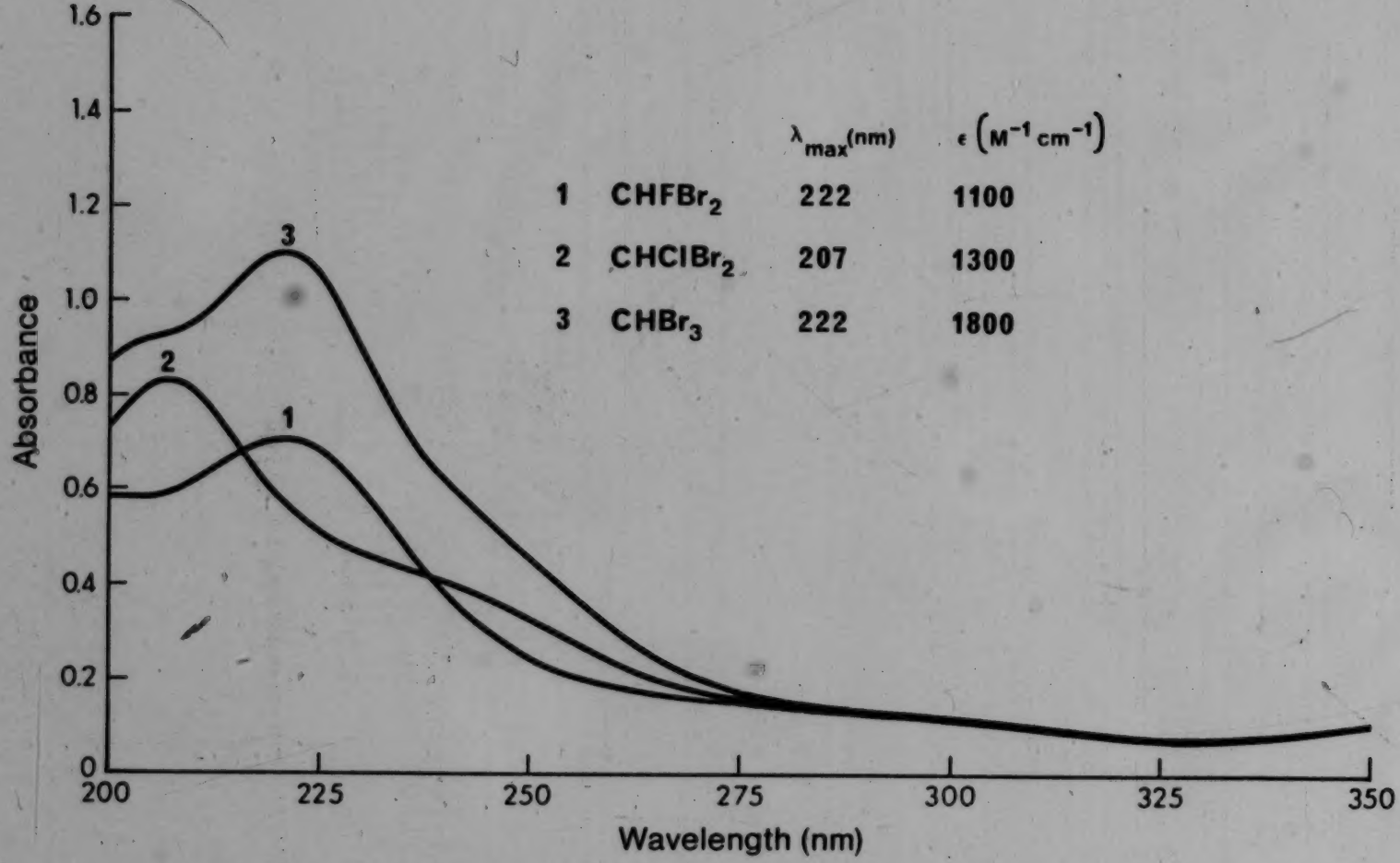

Fig.III-1. UV Absorption Spectra of Halogenated Methanes.

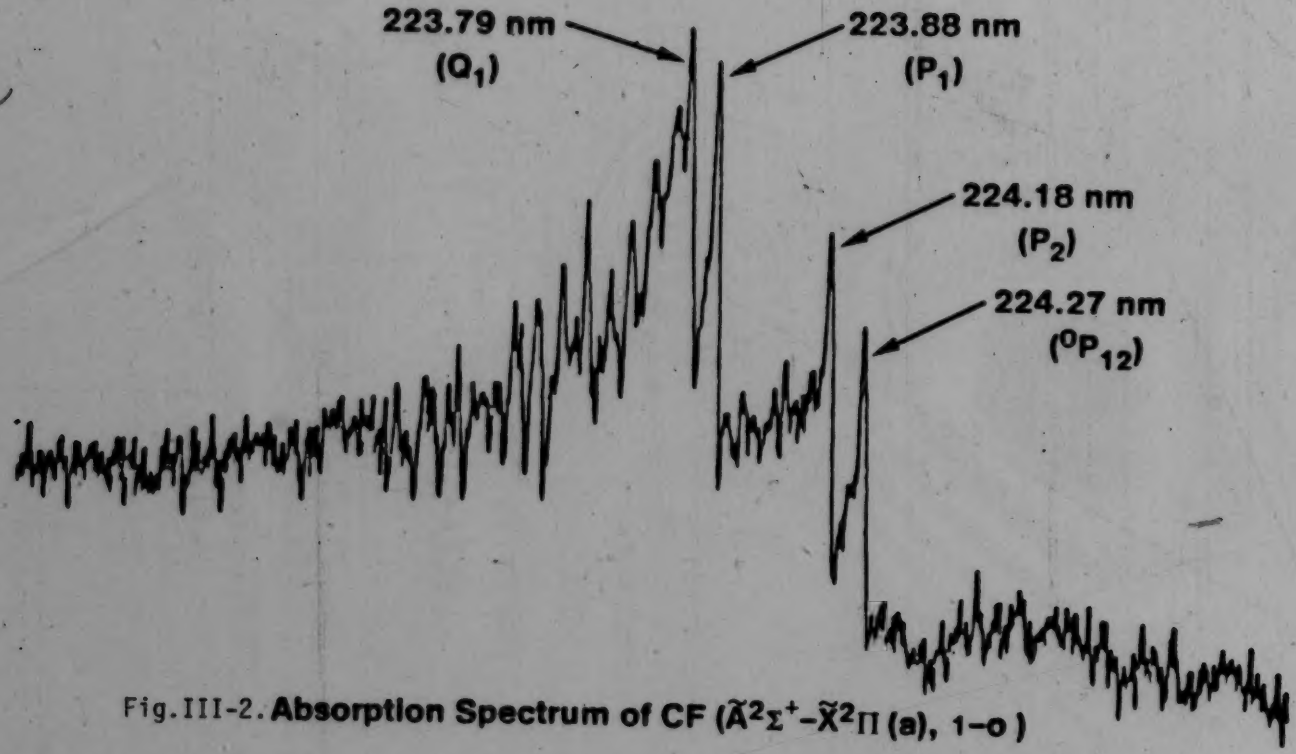

Fig. III-2. **Absorption Spectrum of CF ($\tilde{A}^2\Sigma^+$–$\tilde{X}^2\Pi$ (a), 1–o)**

seen at 233 nm after five exposures. This system is due to the (0-0) band of the $A^2\Sigma^+$-$X^2\Pi$ transition.

In earlier flash photolysis studies on $CHFBr_2$, the absorption spectra of $CBr(X^2\Pi)$ and $HCF(^1A_1)$ were observed, along with other unidentified transient spectra (122). In this study a weak absorption spectrum due to the $CBr(^2\Delta-^2\Pi)$ transition was observed, but no spectrum attributed to HCF could be seen.

For kinetic measurements, the P_2, P_1 and Q_1 absorption bands of the 1-0 transition of CF were used.

2) Chloromethylidyne, CCl

The absorption spectrum shown in Fig. III-3 results from photolysis of 0.30 torr $CHClBr_2$ with 50 torr Argon in a quartz system with 2900 J flash energy and 20 μsec delay. One exposure is sufficient to record the spectrum which is due to the $A^2\Delta(b) - X^2\Pi(a)$, 0-0 transition of CCl. The assignment of the bandpeaks was made on the basis of the rotational analysis of the spectrum by Verma and Mulliken (46). The wavelengths were determined by calibration with an iron arc spectrum and agree with the reported spectrum.

Another absorption system of CCl was observed very weakly following the flash photolysis of 0.60 torr $CHClBr_2$ with 100 torr Argon. Six exposures were necessary to obtain the spectrum, due to the background absorption of $CHClBr_2$. The spectrum consisted of two diffuse bands with peaks at 230.43 and 231.15 nm which are in agreement with previous reports (57,92). The spectrum is tentatively assigned to a $B^2\Sigma$-$X^2\Pi$ transition but no detailed spectral analysis has yet been done.

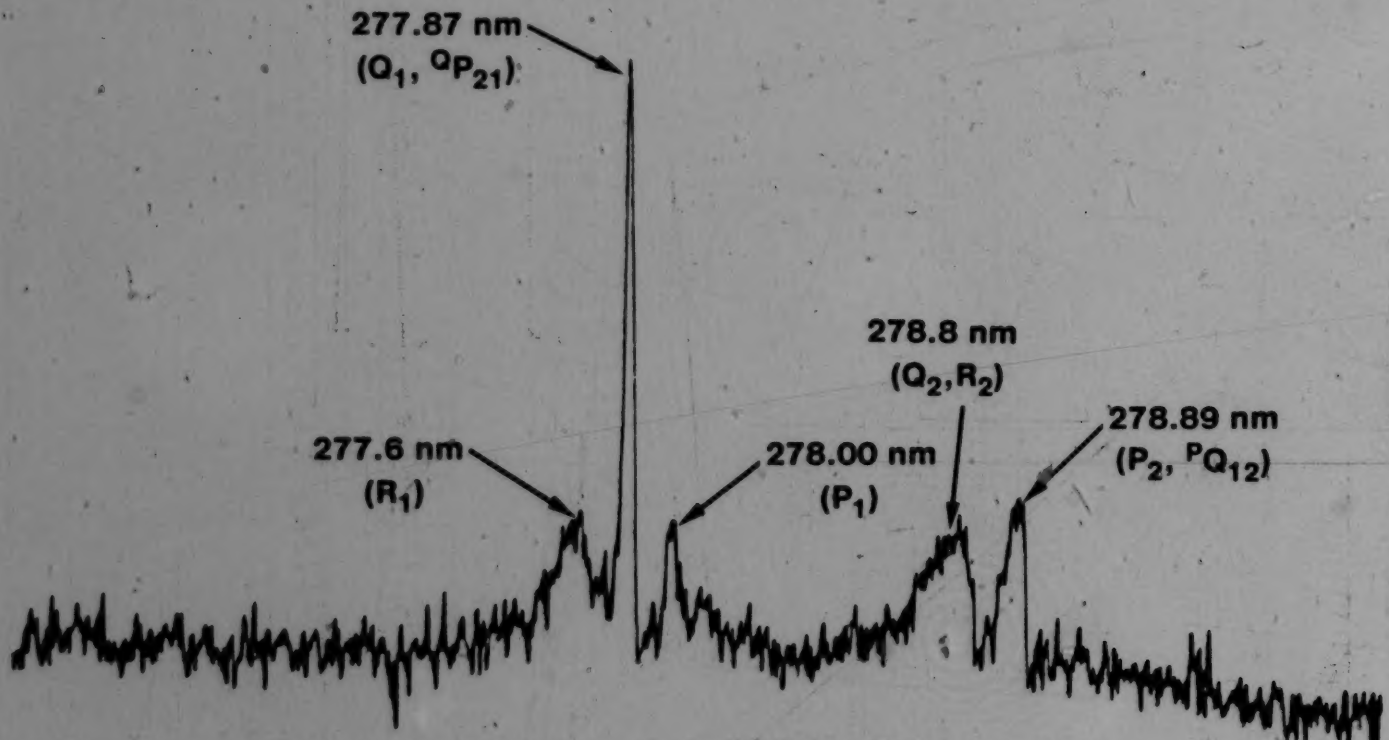

Fig.III-3. **Absorption Spectrum of CCl ($\tilde{A}\ ^2\Delta$(b)–$\tilde{X}^2\ \Pi$ (a), o–o)**

In other flash photolysis experiments on $CHClBr_2$ (94), absorptions due to $CBr(X^2\Pi)$ were also observed, along with the Swan bands of C_2 and also bands of Br_2 which were present at longer delays. Absorption due to $HCCl(^1A_1)$ was also observed. In this study, in addition to the $CCl(X^2\Pi)$, only the CBr $(X^2\Pi)$ absorption at 301 nm was observed weakly.

The intense, sharp absorption band at 277.87 nm used for kinetic analysis, which is a combination of two band heads, Q_1 and $^QP_{21}$, will be referred to as the Q_1 band.

3) Bromomethylidyne, CBr

The transient absorption spectrum shown in Fig.III-4 results from the flash photolysis of 0.10 torr $CHBr_3$ and 50 torr argon. One exposure was sufficient to record this spectrum which was taken with an accidental time delay of ∿5 μsec, not normally available. This short delay results in the observation of absorption bands due to vibrationally excited species. These absorptions are the (Q_1, 1-1) and (Q_2, 1-1) bands of the $^2\Delta(a)$-$^2\Pi(a)$ transition of CBr and were normally not observable. The assignment of the bandheads was made on the basis of the rotational analysis carried out by Dixon and Kroto (68). The wavelengths were determined by calibration with an iron arc spectrum and agree with the reported spectrum. An attempt was made to observe the second reported absorption transition of CBr at 249 and 252 nm (57). A spectrum from the flash photolysis of 0.2 torr $CHBr_3$ in 100 torr argon with a time delay of ∿15 μsec showed no observable absorption in this region although the background continuum was strong and the A-X absorption intensity high. Perhaps more exposures at shorter time delays with higher pressure of $CHBr_3$ are required to observe the absorption although

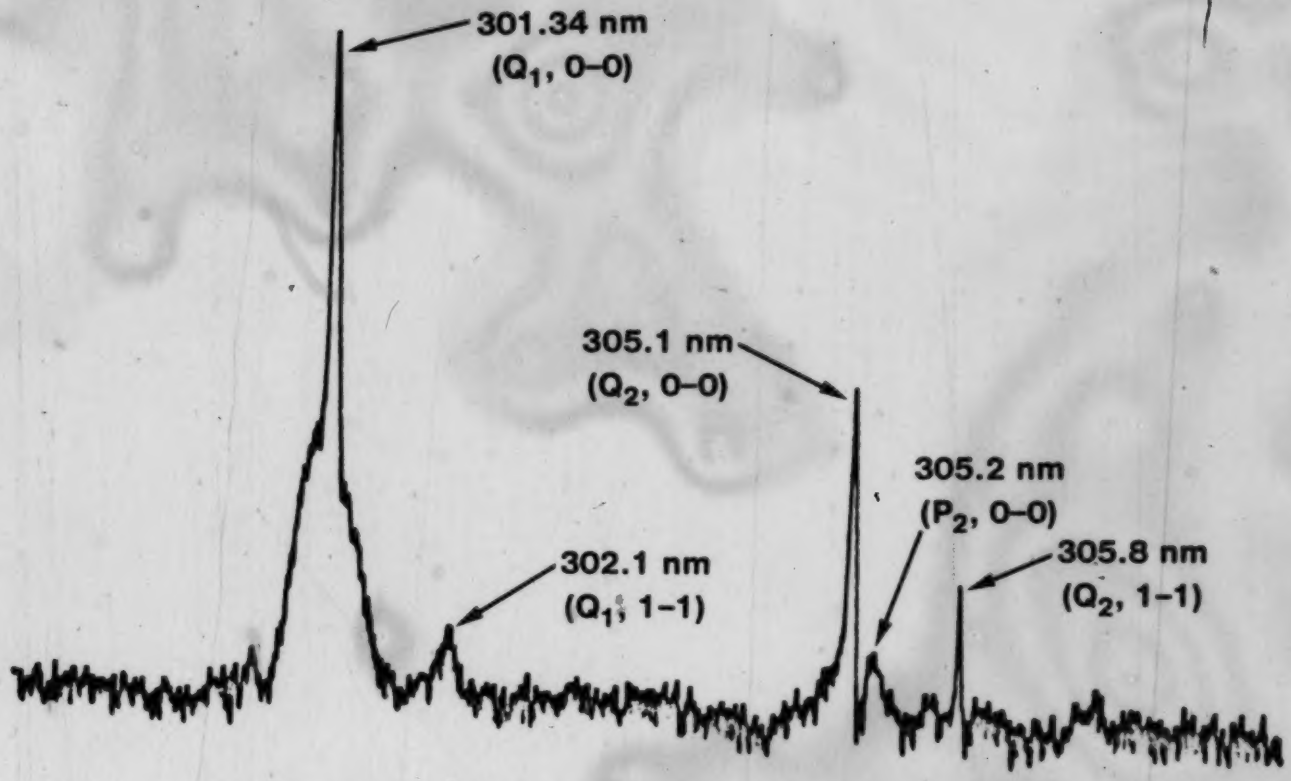

Fig. III-4. **Absorption Spectrum of CBr ($\tilde{A}^2\Delta(a) - \tilde{X}^2\Pi(a)$)**

no comparison can be made because of the lack of experimental detail in the literature report (57).

A careful check was always made for the absorption spectrum due to the $C^2\Sigma^+ - X^2\Pi$ transition of CH at 314.3 nm due to the claim to CH production from the flash photolysis of $CHBr_3$ (76-78). Flash photolysis was also carried out in a suprasil vessel but CH absorption was never detected. The Q_1, 0-0 band of CBr at 301 nm was used for kinetic measurements.

C) Measurement of Beer Absorption Law

The absorption band intensity of the halomethylidyne is transformed by the microdensitometer into the absorption peak height. The peak height as recorded is linearly proportional to the optical density on the photographic plate. Therefore the following relationship should exist

$$\text{Peak Height} \propto \text{Optical Density} = \text{Absorbance} = \varepsilon c l$$

if Beer's absorption law is followed (where ε is the molar extinction coefficient, c is the concentration of absorbing species and l is the path length). Therefore this relationship must be tested. If it holds, then a plot of absorption peak height vs path length should be linear and pass through the origin of the coordinate system. These graphs were plotted for each of the halomethylidyne absorption bands and are shown in Fig. III-5 and III-6. The data were obtained by flash photolysis of the standard mixtures of the halomethylidyne sources with various portions of the reaction vessel covered up, thereby varying the path length, l. The concentration of the halomethylidyne remains

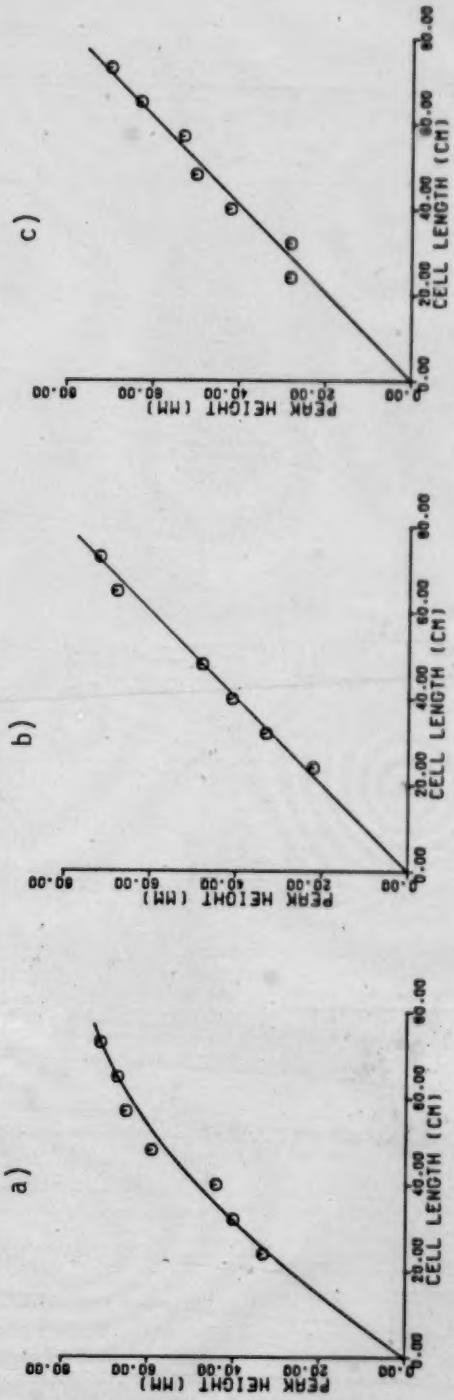

Fig.III-5. Peak Height vs Path Length for a) $CF(Q_1)$, b) $CF(P_2)$ and c) $CF(P_1)$

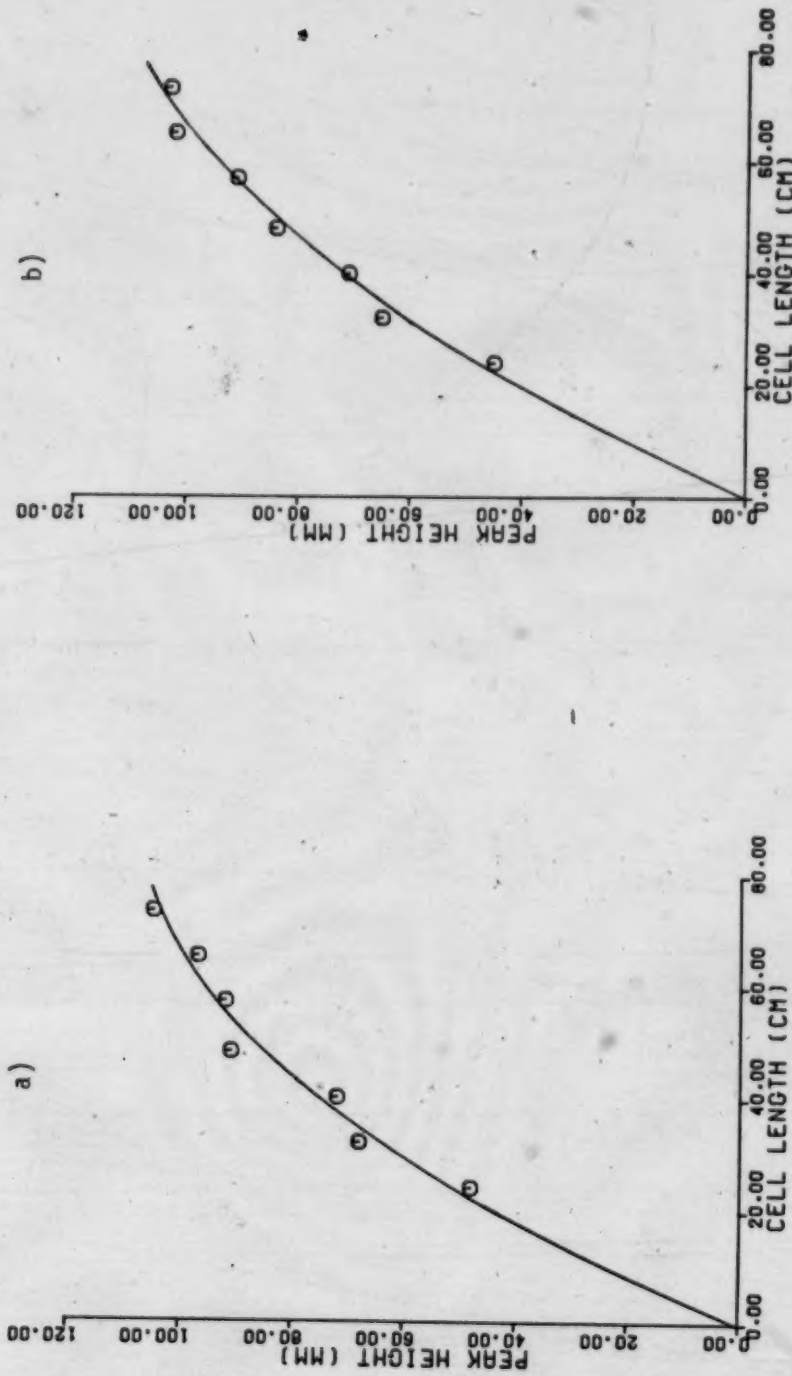

Fig.III-6. Peak Height vs Path Length for a) $CCl(Q_1)$ and b) $CBr(Q_1)$

constant at a fixed time delay. The graphs demonstrate that while the Beer absorption law holds for the P_2 and P_1 absorption bands of CF, it fails for the Q_1 absorption bands of CF, CCl and CBr as shown by the negative curvature. This negative deviation from Beer's law is caused by poor instrumental resolution and occurs when the absorption band width is of the same order as the spectral band width (60,148). In such cases, the measured absorbance is no longer directly proportional to the concentration of the absorbing species and a modified form of the above relation exists:

$$\text{Absorbance} = \varepsilon(cl)^{\gamma}$$

The Beer coefficient, γ, is an empirically determined correction factor whose value is dependent on the type of absorption system studied. The relationship between the absorption peak height and concentration becomes:

$$\text{Peak Height (P.H.)} \propto \varepsilon(cl)^{\gamma}$$

$$\ln (\text{P.H.}) = [\ln(\varepsilon c^{\gamma}) + \gamma \ln l]$$

Thus a plot of ln (P.H.) vs ln l, at a fixed time delay, gives a slope of γ. Fig. III-7 shows these plots for the Q_1 absorption bands of CF, CCl and CBr. The slope, γ, was determined by standard least squares analysis and the average values are listed below. Each experiment consisted of seven points.

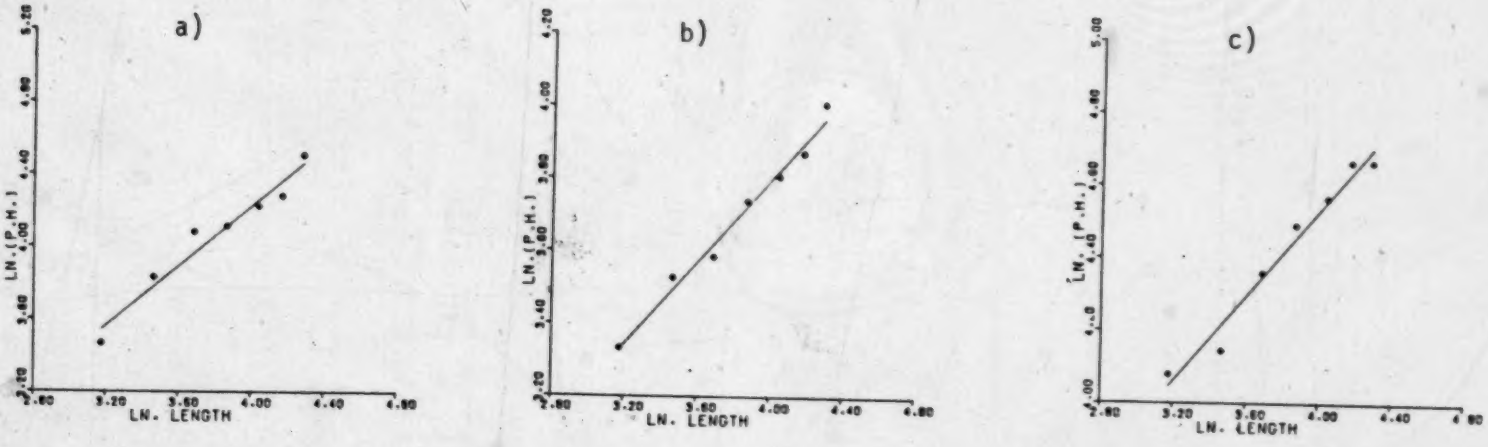

Fig.III-7. Ln (Peak Height) vs Ln Length for a) $CF(Q_1)$, b) $CCl(Q_1)$ and c) $CBr(Q_1)$

Absorption Band	γ	No. of expts.
$CF(A^2\Sigma^+-X^2\Pi)$ Q_1, 1-0	0.85 ± 0.05	5
$CCl(A^2\Delta-X^2\Pi)$ Q_1, 0-0	0.51 ± 0.04	4
$CBr(A^2\Delta-X^2\Pi)$ Q_1, 0-0	0.66 ± 0.05	4

D) Decay of the Halomethylidyne Spectra

Now that the relationship between absorption peak height and halomethylidyne concentration has been established, the disappearance of the halomethylidyne can be employed for kinetic measurements. A first order expression for the decay of halomethylidyne is as follows:

$$-\frac{d[CX]}{dt} = k'[CX]$$

which is integrated to give

$$\ln [CX] = -k't + \text{const.}$$

From the previously established relationship P.H. $\alpha[CX]^{\gamma_{CX}}$, the final form of the rate expression is derived.

$$\ln (P.H.)_{CX} = \gamma_{CX} k't + \text{const.}$$

The decay of each halomethylidyne spectrum was analyzed and the best fit to the data was given by this first order decay expression as shown by the linear proportionality of the graphs of $\ln (P.H.)_{CX}$ vs time for CF, CCl and CBr spectra (Fig. III-8, III-9). This pseudo-first order background decay is in complete agreement with other kinetic measurements involving methylidyne and halomethylidyne reactions (54,55,73,79

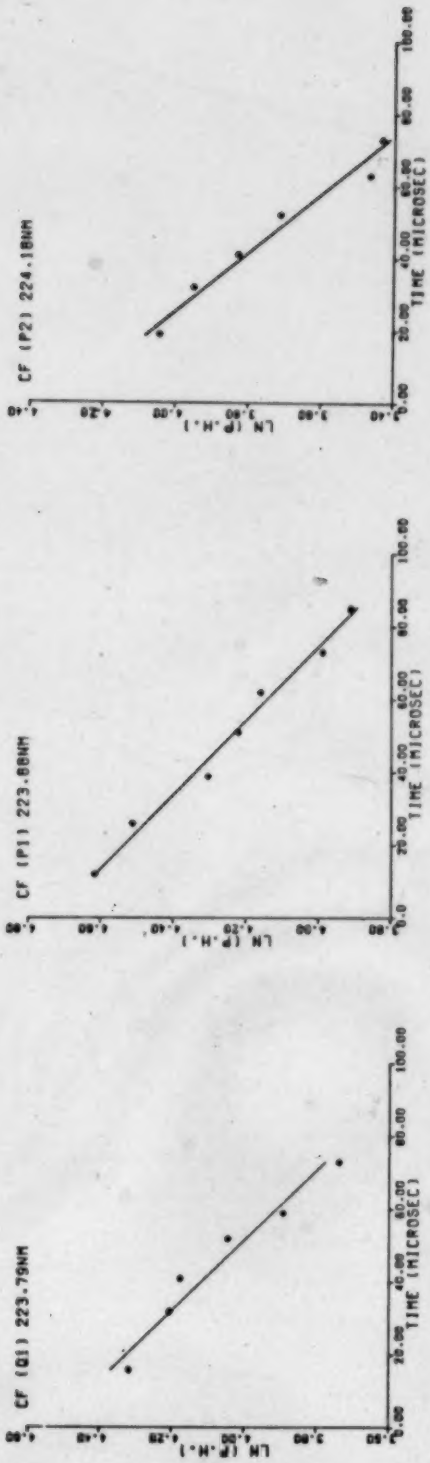

Fig.III-8. Ln (Peak Height) vs Time for CF absorption peaks.

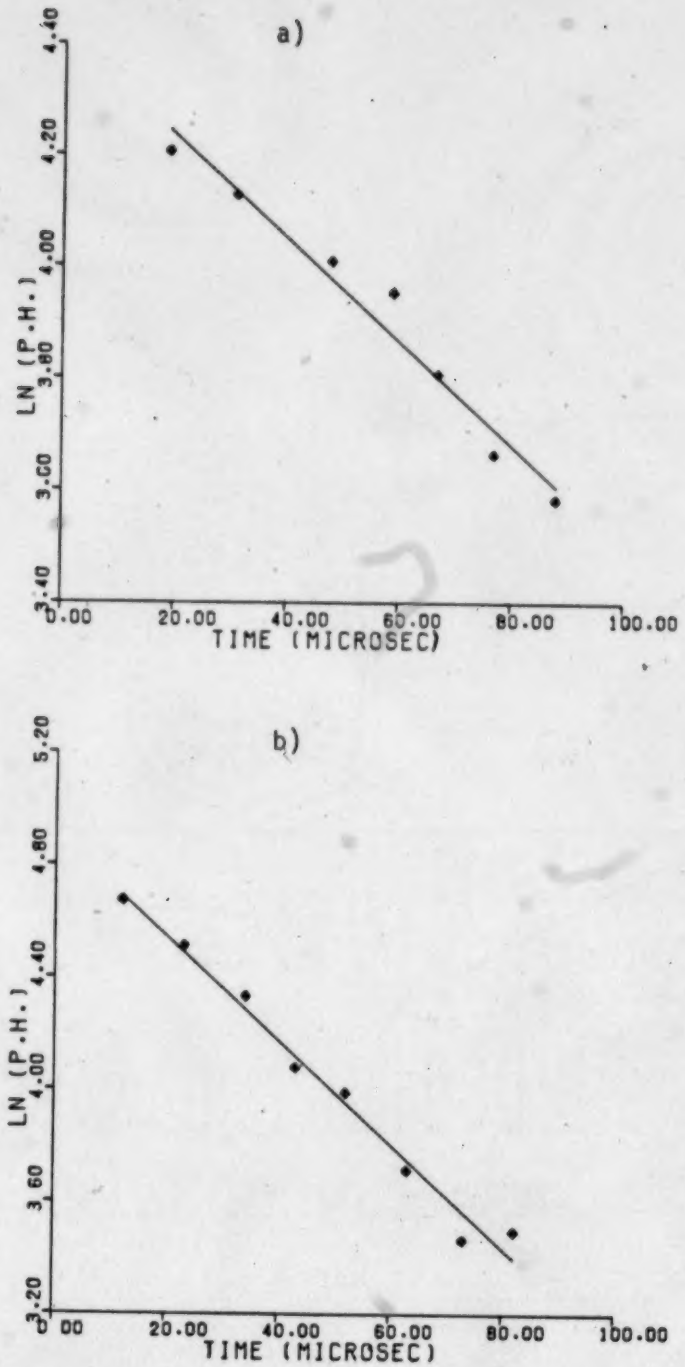

Fig.III-9. Ln(Peak Height) vs Time for a) $CCl(Q_1)$ and b) $CBr(Q_1)$

83,93,96). The slope of these plots is $-\gamma_{cx}k'$ and therefore by correcting the decay of each halomethylidyne spectra by its Beer coefficient, γ_{cx}, the background rate constant k' can be determined for each halomethylidyne. Tables III-1,2 list the average values of k' for each halomethylidyne spectrum under a variety of conditions. One of the most important factors to note is that the background rate constants are fast, almost reaching the limits of measurement of the flash photolysis technique operating on a microsecond time scale. The fastest decay rate constants that can be measured are approximately 30-40 $msec^{-1}$, depending upon the intensity of the absorption. From the limited results, the background rate constants seem to be independent of wavelength and temperature. However Choi (54) found the background pseudo first order rate constant for CCl to be dependent on flash energy and concentration of $CHClBr_2$. These results indicate that the halomethylidynes decay by radical-radical reactions with the photolytic products.

E) Reaction of Halomethylidynes with Alkenes

The following series of alkenes was investigated: ethylene, propylene, 1-butene, t-2-butene, 2-methyl-2-propene (isobutene), 2 methyl-2-butene (trimethylethylene) and 2.3-dimethyl-2-butene (tetramethylethylene). Figure III-10 shows the gas phase ultraviolet absorption spectra of three of the alkenes, which agree with the literature absorption spectra (149). The main absorption, V-N, occurs below 200 nm, but with increasing alkyl substitution, a shoulder due to the R-N absorption band extends into the far ultraviolet, which is readily apparent for tetramethylethylene (203). For trimethylethylene this absorption is much less

Table III-1 Background Rate Constants, k', for Halomethylidyne Decay[a]

Spectral Transition	k' ($msec^{-1}$)	Photolysis Wavelength (nm)	Mixtures Photolysed
$CF(P_2)$	9 ± 1	λ > 165	0.15 torr $CHFBr_2$+
	10 ± 1	λ > 200	50 torr Ar
$CF(P_1)$	9 ± 1	λ > 165	"
	11 ± 1	λ > 200	
$CF(Q_1)$	9 ± 1	λ > 165	"
	12 ± 1	λ > 200	
$CCl(Q_1)$	20 ± 1	λ > 165	0.30 torr $CHClBr_2$+
	19 ± 1	λ > 200	50 torr Ar
$CBr(Q_1)$	28 ± 1	λ > 165	0.10 torr $CHBr_3$+
	28 ± 1	λ > 200	50 torr Ar

[a]Flash energy, 2900 J; temperature, 300 ± 2 K .

Table III-2 Background Rate Constant, k', for CBr Decay[a]

k'(msec^{-1})	Temperature (deg K)
23 ± 1	298 ± 1
18 ± 1	323 ± 1
23 ± 1	348 ± 1
23 ± 1	373 ± 1
22 ± 1	398 ± 1
23 ± 1	423 ± 1

[a]Photolysis Wavelength, $\lambda > 220$ nm; flash energy, 2095 J

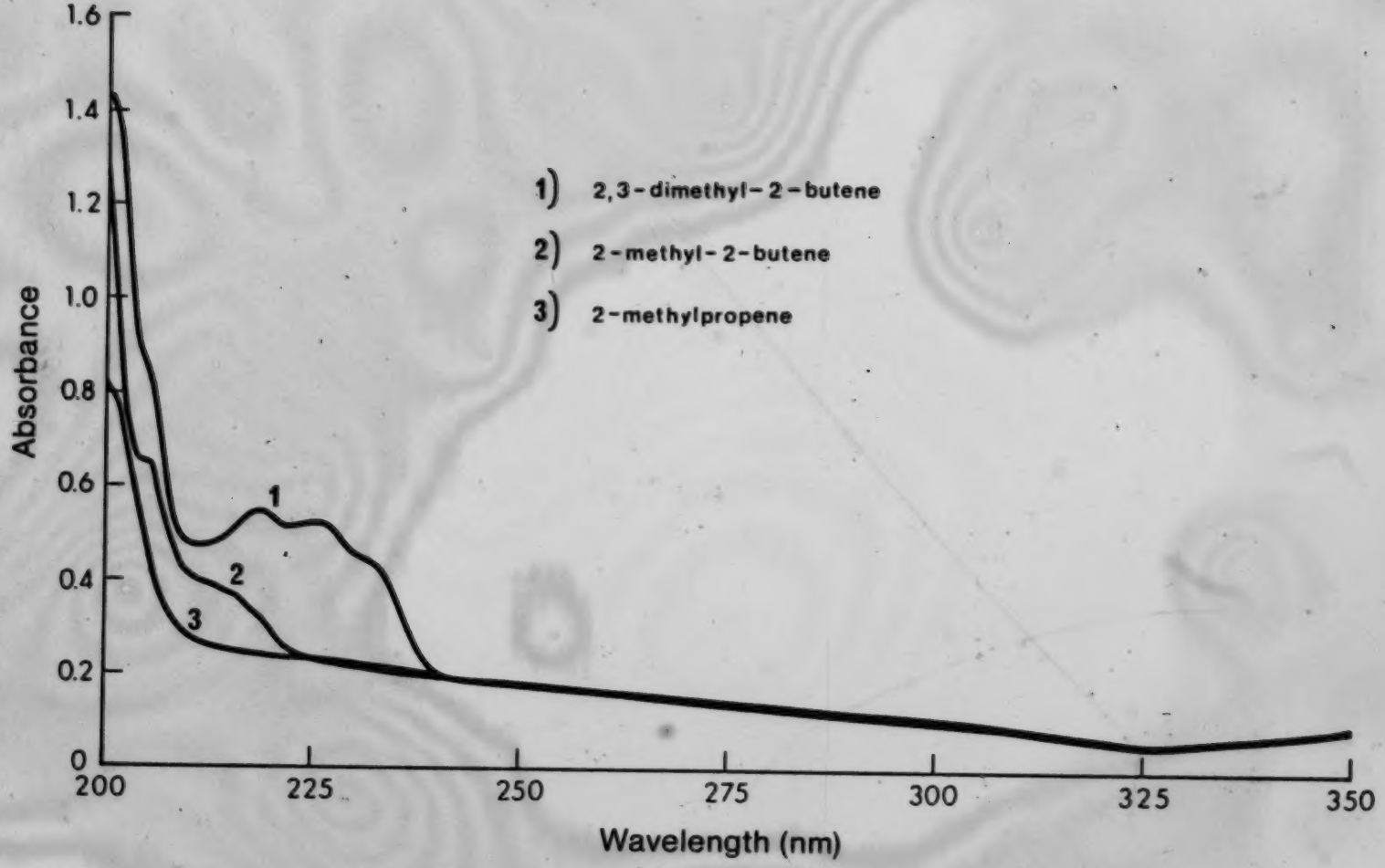

Fig.III-10. UV Absorption Spectra of Alkenes.

intense and for isobutene it is negligible, as it is for the other alkenes. The photolysis of tetramethylethylene maypresent some problems in the determination of reaction rate constants.

In the presence of a reactive substrate such as an alkene, the rate expression for the decay of halomethylidyne, CX, becomes:

$$\frac{-d[CX]}{dt} = k'[CX] + k_2[S][CX] = k''[CX],$$

where [S] = concentration of substrate

k_2 = rate constant for reaction of CX with S

$k'' = k' + k_2[S]$

This expression integrates to

$$\ln[CX] = -k''t + \text{const.}$$

and using the expression relating absorption peak height and halomethylidyne concentration gives the following kinetic expression for the decay of halomethylidyne in the presence of a substrate.

$$\ln(P.H.)_{CX} = -\gamma_{CX}k''t + \text{const.}$$

Therefore a plot of $\ln(P.H.)_{CX}$ vs. time gives $-\gamma_{CX}k''$ as the slope. The value of the slope was determined by standard least squares analysis. Figures III-11 to Figures III-15 are typical plots and show the increase in the slope, $-\gamma_{CX}k''$, (i.e. increase in the decay rate) with increasing substrate concentration, indicating reaction of CF, CCl and CBr with the substrate. The pressure of a substrate was converted into concentration using the Ideal Gas Equation $PV = nRT$.

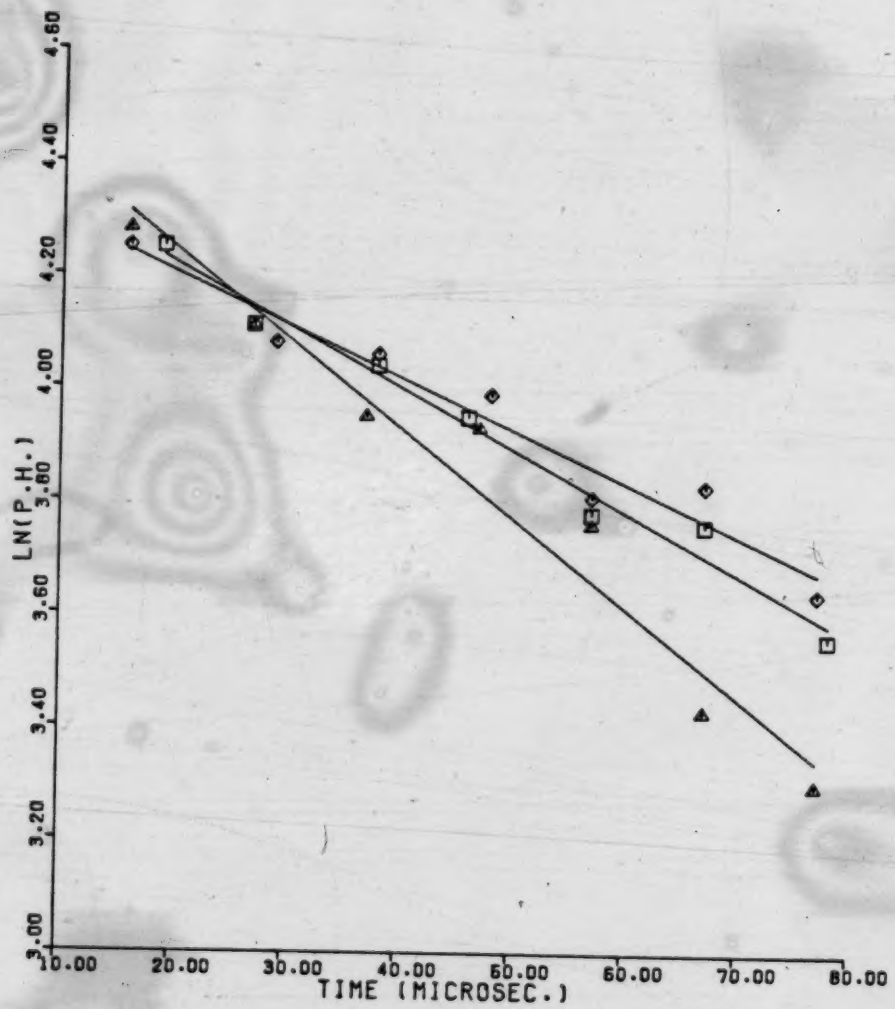

Fig.III-11. Ln (P.H.)vs Time for CF(Q_1) absorption peak in presence of Ethylene; ◇ - 0.0 micromolar, □ -32.6 micromolar and △ - 62.5 micromolar.

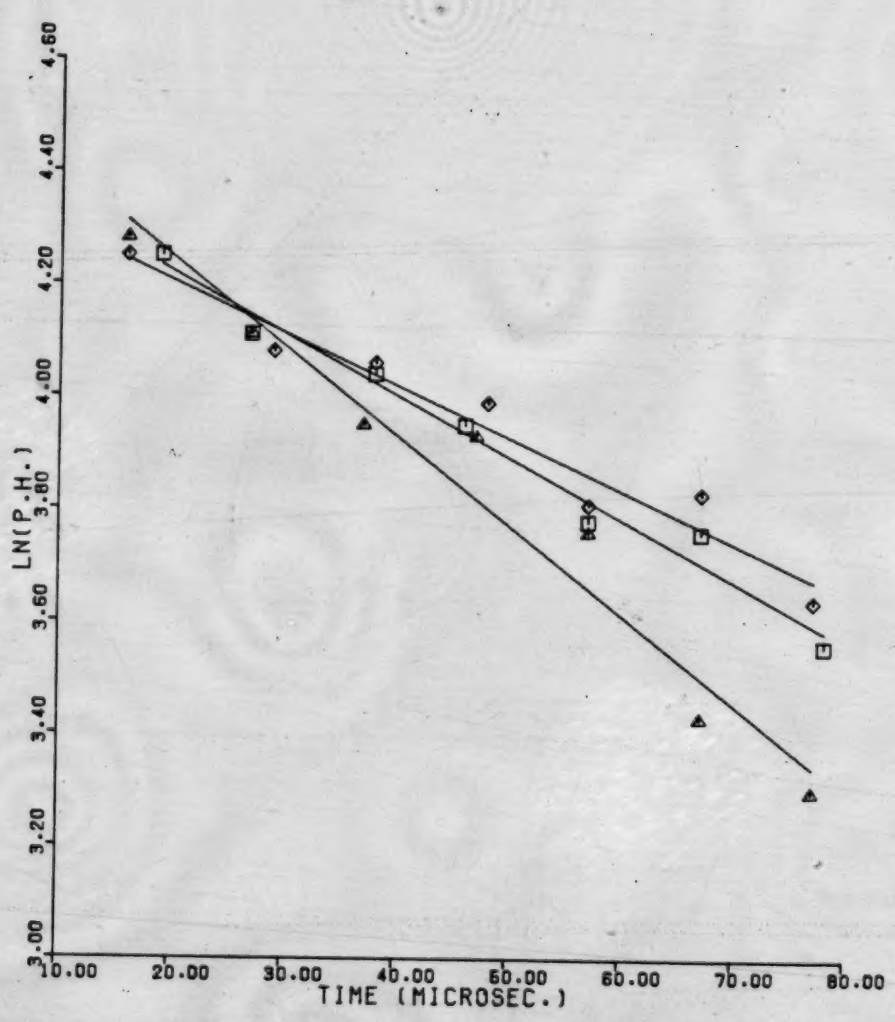

Fig.III-11. Ln (P.H.)vs Time for CF(Q_1) absorption peak in presence of Ethylene; ◇ - 0.0 micromolar, □ -32.6 micromolar and △ - 62.5 micromolar.

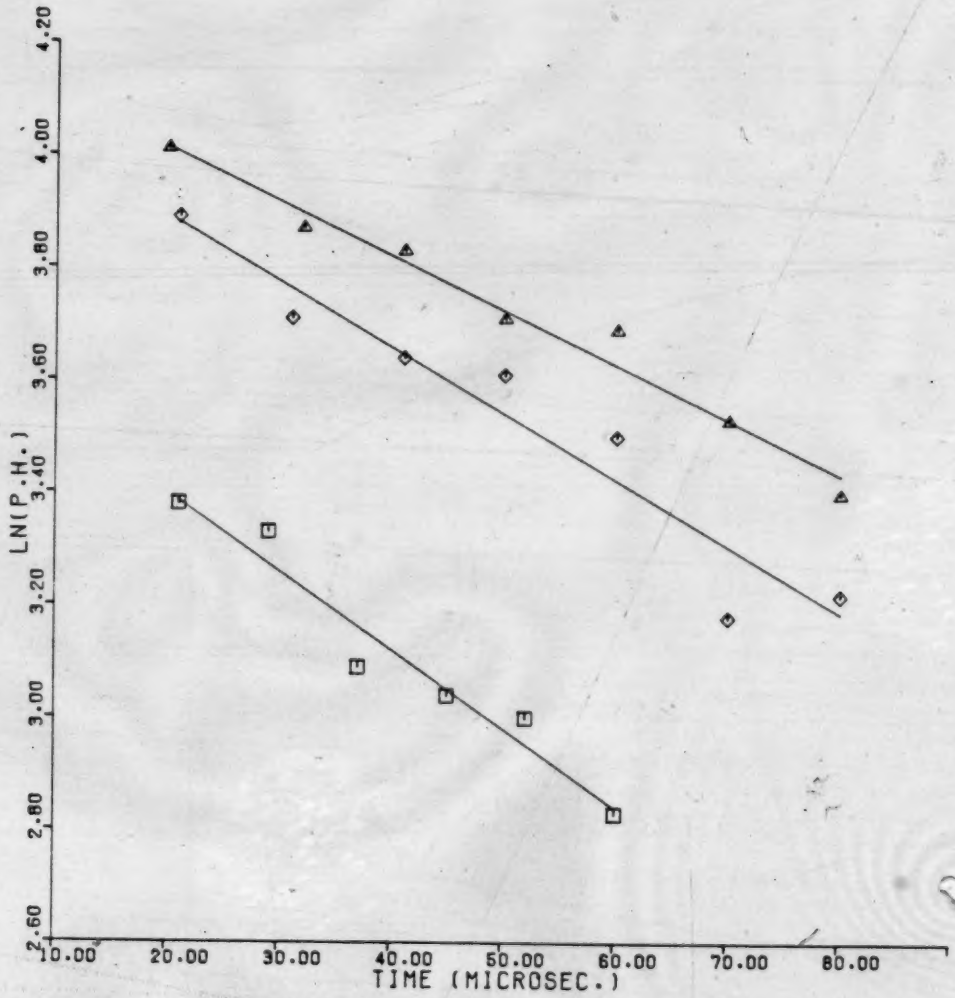

Fig.III-12. Ln (P.H.) vs Time for CF(P_2) absorption peak in presence of 1-Butene; △ - 0.0 micromolar, ◇ - 5.13 micromolar and □ - 15.9 micromolar.

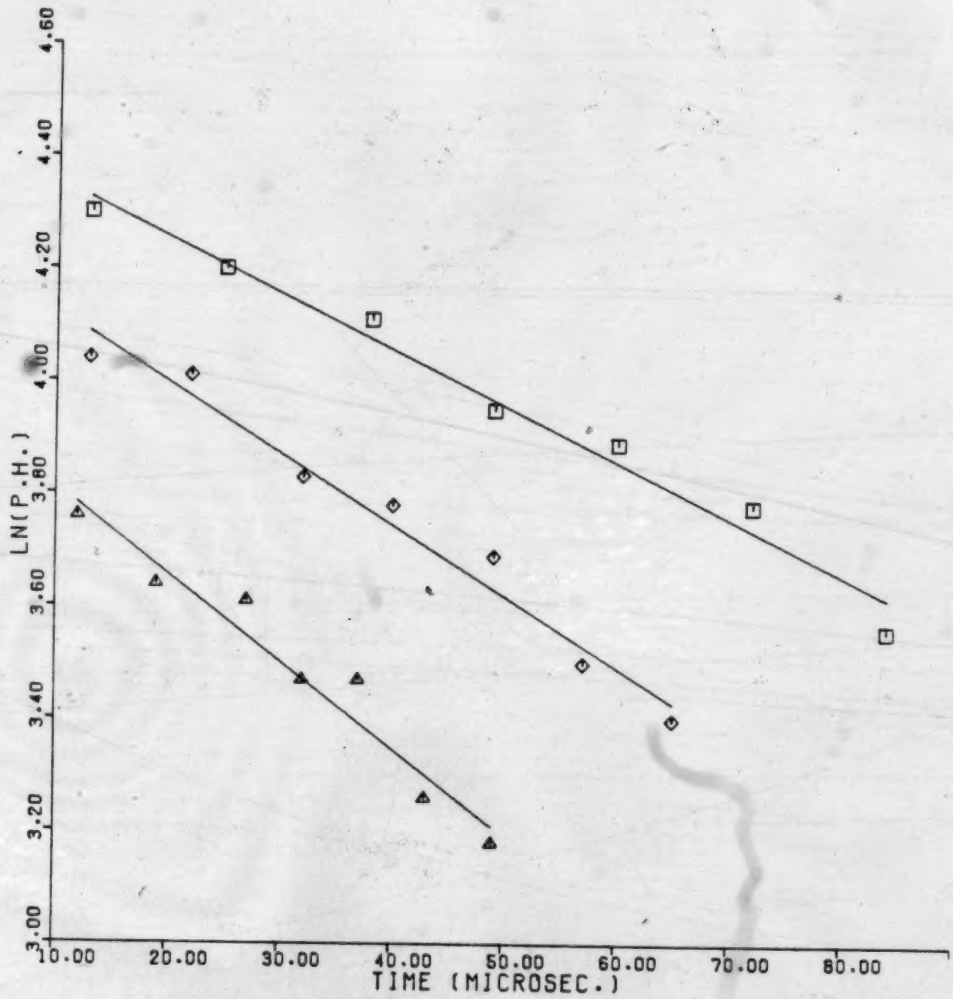

Fig.III-13. Ln (P.H.) vs Time for CF(P_1) absorption peak in presence of t-2-Butene; □ - 0.0 micromolar, ◇ - 2.57 micromolar and △ - 8.02 micromolar.

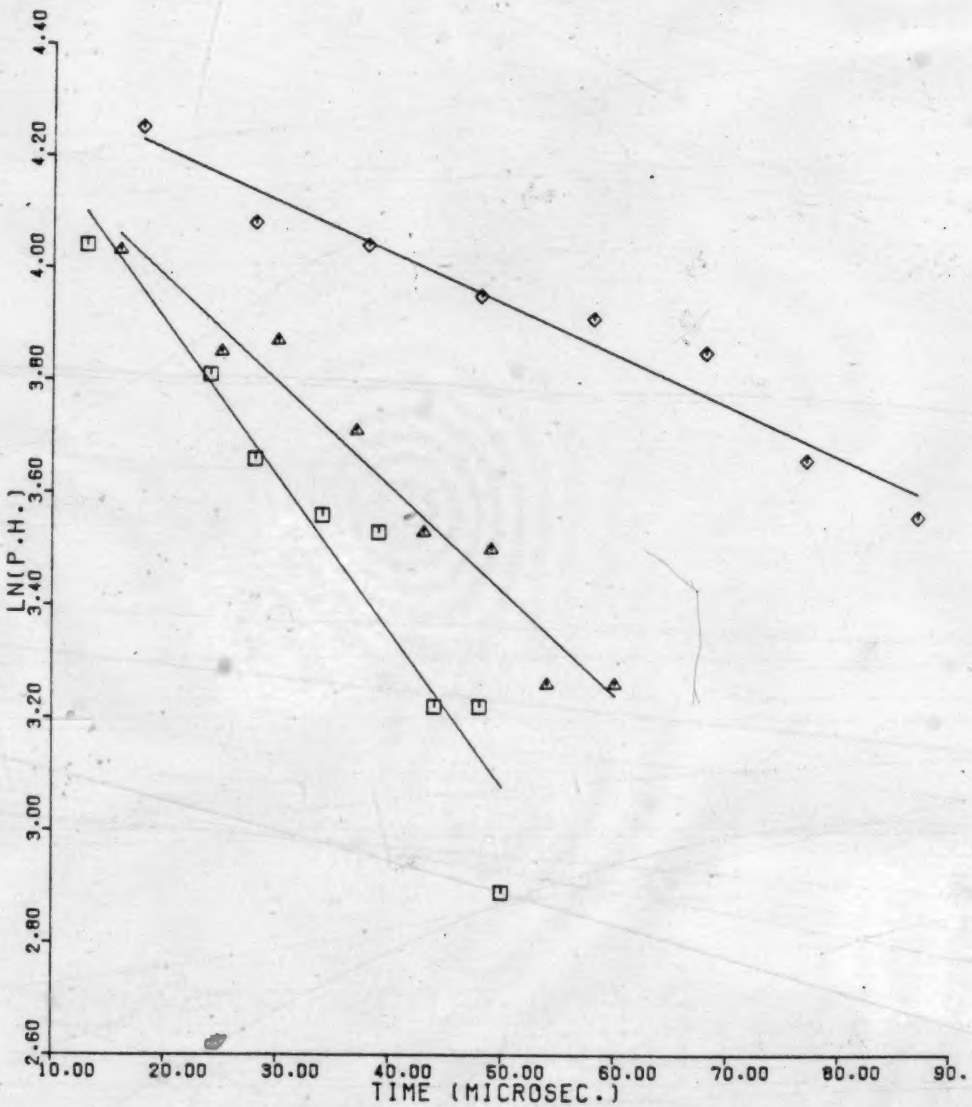

Fig.III-14. Ln (P.H.) vs Time for CCl(Q_1) absorption in presence of Isobutene; ◇-0.0 micromolar, △-6.15 micromolar, □-8.98 micromolar.

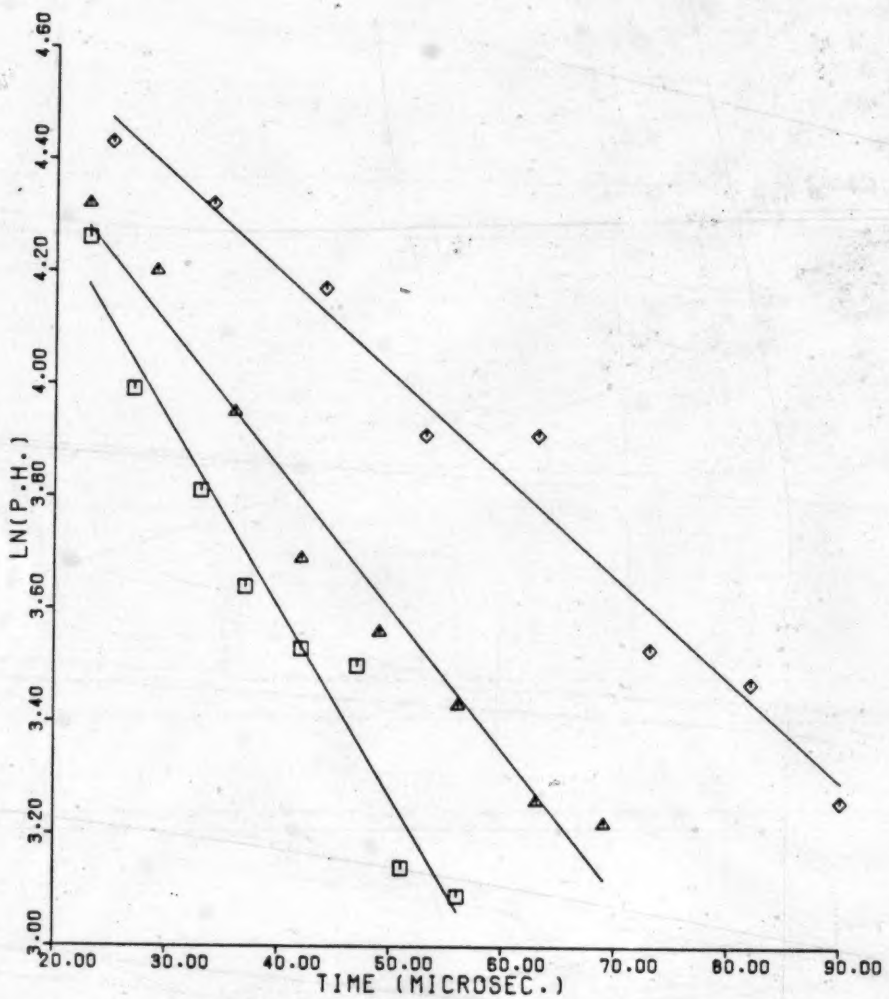

Fig.III-15. Ln (P.H.) vs Time $CBr(Q_1)$ absorption peak in presence of 2-methyl-2-butene; ◇-0.0 micromolar, △-0.64 micromolar, □-1.23 micromolar.

1) Reaction of CF with alkenes.

It was mentioned above that at least 3 exposures have been necessary to obtain the CF absorption spectrum. This requires that the flash photolysis apparatus fire off three times in succession with exactly the same time delay. This requirement for reliable and reproducible time delays was a major instrumental problem which took considerable effort and time to resolve.

For CF on the average, three decays of the absorption spectrum were analysed for each concentration of substrate. Due to the weak absorption signal obtained, the results are scattered. Therefore for each absorption peak an average value of $\gamma_{cx}k''$ was determined. From the kinetic expression derived above, $k'' = k' + k_2[S]$, the second order plot of k" versus [S] gives k_2 as the slope and k' as the intercept.

For the reaction of CF with ethylene, a value of k_2 was determined separately for each of the three CF absorption bands, P_2, P_1 and Q_1. Within the rough precision of the experiment, no difference was found between the values of k_2, as expected. Therefore the decays of the CF absorption bands were averaged together as follows. For each absorption band an average value of $\gamma_{cx}k''$ was determined from three decays of the spectrum. The Q_1 absorption band was corrected for its Beer coefficient, $\gamma = 0.85$, while for the P_1 and P_2 absorption bands this was unnecessary since $\gamma = 1$. The values of k" were averaged together to give an overall value for the CF absorption spectrum k"(CF). The values of k"(CF) as a function of alkene concentration are listed in Table III-3. Fig. III-16 shows the corresponding plots of k"(CF) versus [S], concentration of alkene. The slope of these plots, which is k_2, the reaction rate constant for CF + alkene, was determined by standard least squares

Table III-3 k"(CF) as a Function of Concentration for the Reaction of CF with a) ethylene b) propylene c) t-2-butene and d) isobutene.

a) Ethylene

conc. (micromolar)	k"($msec^{-1}$)
0.0	10.4 ± 0.7
23.8	10.9 ± 0.7
32.3	10.7 ± 0.8
48.6	13.2 ± 0.7
62.5	13.9 ± 0.8
81.2	13.8 ± 0.9
97.8	13.8 ± 0.6
113.8	15.4 ± 1.0

b) Propylene

conc. (micromolar)	k"($msec^{-1}$)
0.0	10.6 ± 0.9
2.9	10.4 ± 0.7
6.4	12.9 ± 0.6
8.9	10.8 ± 0.6
11.7	11.2 ± 0.8
15.7	15.5 ± 0.8
17.9	15.1 ± 0.8
21.5	16.9 ± 0.8

c) trans-2-butene

conc. (micromolar)	k"($msec^{-1}$)
0.0	10.3 ± 0.4
1.98	12.5 ± 0.6
2.55	13.7 ± 0.5
3.63	12.4 ± 0.8
5.24	14.9 ± 0.9
6.57	16.2 ± 1.0
8.02	17.3 ± 0.9
8.77	21.8 ± 1.2

d) Isobutene

conc. (micromolar)	k"($msec^{-1}$)
0.0	11.5 ± 0.6
1.45	13.8 ± 0.6
2.67	12.0 ± 0.8
3.96	10.7 ± 0.7
5.29	15.4 ± 0.8
6.84	19.0 ± 1.1
7.80	20.0 ± 1.6
8.50	20.0 ± 1.4

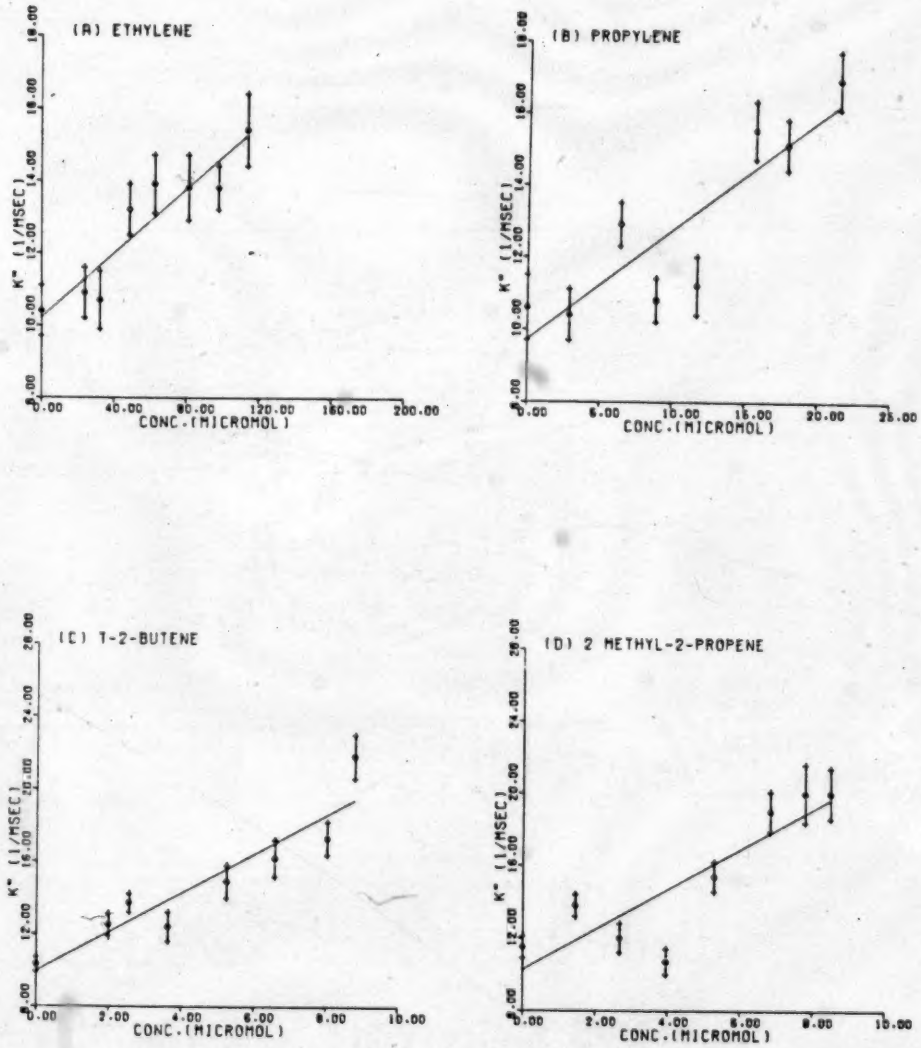

Fig.III-16. k"(CF) vs [S],concentration of alkene, for four alkenes.

analysis. Since we have an average value of k" with its standard deviation which is shown as error bars in Fig. III-16, a weighted least squares analysis can also be performed. No significant difference was observed between the standard and weighted least mean squares analysis results. The rate constants determined for the reaction of CF with alkenes are listed in Table III-4.

2) Reaction of CCl with Alkenes

For the reaction of CCl with alkenes, four decays of the CCl(Q_1) absorption peak were analysed for each concentration of the substrate. Therefore an average value of $\gamma_{CCl}k"$ was obtained and Table III-5 lists average values of $\gamma_{CCl}k"$ for the reaction of CCl with some alkenes. Fig. III-17 shows the plots of $\gamma k"$ versus concentration. The slope of these plots, which is $\gamma_{CCl}k_2$ was determined by standard and weighted least squares analysis and no significant difference was found. These values were corrected for the CCl Beer coefficient ($\gamma = 0.51 \pm 0.04$) to give the second order reaction rate constants, k_2, for the reaction of CCl with alkenes, which are listed in Table III-6.

3) Reaction of CBr with Alkenes

The second order rate constants for the reaction of CBr with alkenes were determined using the CBr(Q_1) absorption band in exactly the same method as determined for the CCl reactions described above. The results are shown in Tables III-7 and III-8 and Fig. III-18.

F) Reactions of CBr with Alkynes

The reactions of CBr with a series of alkynes were also studied. The alkynes studied were: acetylene, acetylene-d_2, propyne, 1-butyne,

Table III-4 Second Order Rate Constants,

k_2 for the Reaction of CF with Alkenes

Substrate	$k_2 \times 10^{-9}$ M^{-1}sec^{-1}	No. of Decays*	Pressure Range of Substrate (torr)
Ethylene	0.04 ± 0.01	65	0 - 2.13
Propylene	0.3 ± 0.1	65	0 - 0.40
1-Butene	0.4 ± 0.1	71	0 - 0.30
trans-2-Butene	1.1 ± 0.2	69	0 - 0.16
iso-butene	1.1 ± 0.3	68	0 - 0.16

*The average number of points on each decay plot was 6.

Table III-5 $\gamma k''(CCl)$ as a Function of Concentration for the Reaction of CCl with a) ethylene, b) 1-butene, c) iso-butene, d) 2-methyl-2-butene

a) ethylene

conc. (micromolar)	$\gamma k''(msec^{-1})$
0.0	9.9 ± 0.5
14.0	10.1 ± 0.4
26.7	11.4 ± 0.5
39.9	12.5 ± 0.7
53.0	13.2 ± 0.6
66.0	14.7 ± 0.4
79.4	16.3 ± 0.7
94.0	17.1 ± 0.8

b) 1-butene

conc. (micromolar)	$\gamma k''(msec^{-1})$
0.0	9.3 ± 0.6
3.8	12.8 ± 0.6
5.5	15.1 ± 0.8
7.9	16.9 ± 0.8
11.2	19.9 ± 1.0
13.3	22.2 ± 1.2
16.5	23.3 ± 1.3
18.8	27.3 ± 1.2

c) isobutene

conc. (micromolar)	$\gamma k''(msec^{-1})$
0.0	9.8 ± 0.5
1.60	13.8 ± 0.8
3.05	15.1 ± 0.7
4.49	19.0 ± 0.9
6.15	19.9 ± 1.2
6.89	23.2 ± 1.3
8.12	24.4 ± 1.3
8.98	25.4 ± 2.4

d) 2-methyl-2-butene

conc. (micromolar)	$\gamma k''(msec^{-1})$
0.0	9.0 ± 0.6
0.64	12.9 ± 0.6
1.32	16.4 ± 1.0
2.30	19.9 ± 1.0
2.81	22.1 ± 1.1
3.90	25.8 ± 1.4
4.50	25.7 ± 1.6

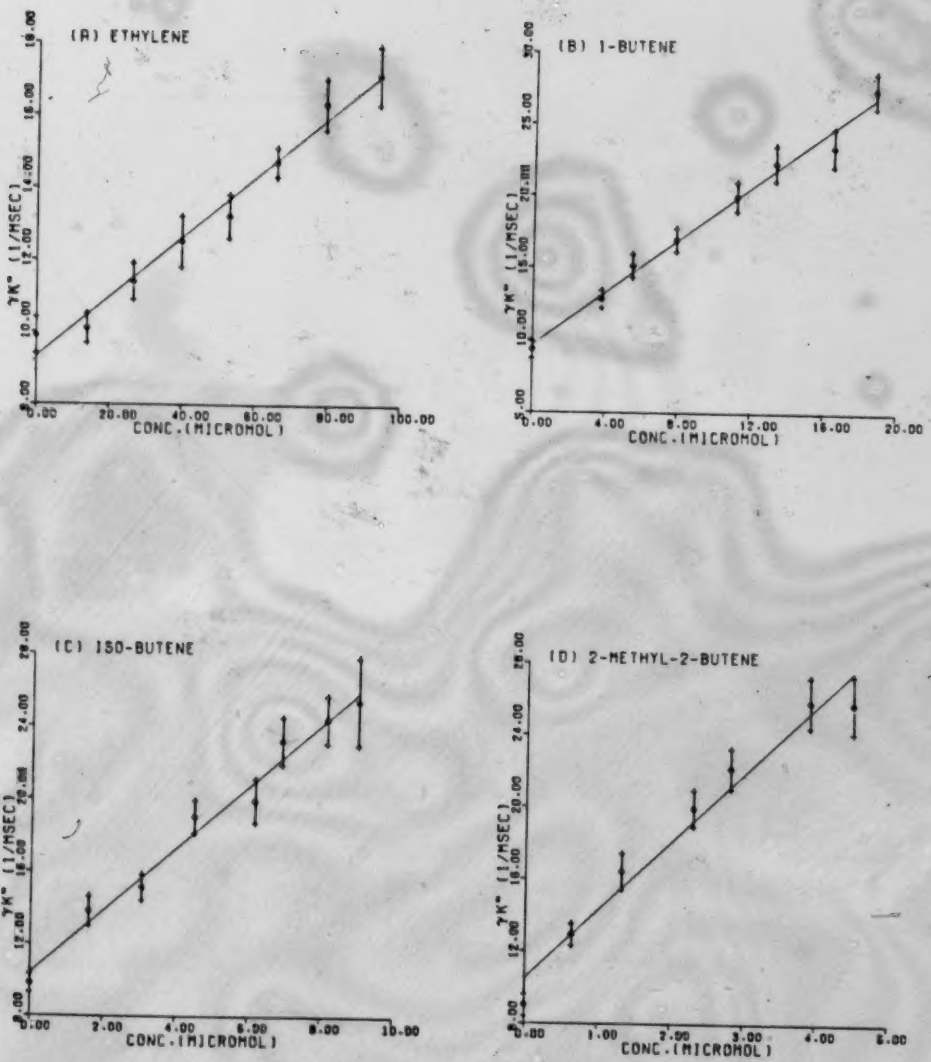

Fig.III-17. γk"(CCl) vs [S],concentration of alkene,for four alkenes.

Table III-6 Second Order Rate Constants, k_2, for the Reaction of CCl with Alkenes*

Substrate	$k_2 \times 10^{-9}$ M^{-1} sec^{-1}	No. of Decays	Pressure Range of Substrate (torr)
Ethylene	0.16 ± 0.01	32	0 - 1.75
Propylene	1.0 ± 0.1	32	0 - 0.56
1-butene	1.7 ± 0.2	30	0 - 0.35
trans-2-butene	2.6 ± 0.2	38	0 - 0.17
iso-butene	3.5 ± 0.3	32	0 - 0.17
2-methyl-2-butene	8 ± 1	31	0 - 0.084
2.3-dimethyl-2-butene	14 ± 2	28	0 - 0.044

* The average number of points in each decay plot was 7.

Table III-7 $\gamma k''(CBr)$ as a Function of Concentration for the Reaction of CBr with a) ethylene, b) propylene, c) trans-2-butene and d) 2,3- dimethyl-2-butene

a) Ethylene

conc. (micromolar)	$\gamma k''(msec^{-1})$
0.0	17.1 ± 0.4
5.4	18.0 ± 0.5
10.7	20.8 ± 0.3
16.2	22.0 ± 0.4
21.3	23.4 ± 0.6
26.9	26.4 ± 0.7
31.6	27.3 ± 0.6
37.0	29.6 ± 1.1

b) Propylene

conc. (micromolar)	$\gamma k''(msec^{-1})$
0.0	18.0 ± 0.4
1.98	24.0 ± 1.0
3.37	22.8 ± 0.6
5.13	27.7 ± 1.2
6.89	32.8 ± 1.0
8.50	35.7 ± 1.7
10.48	37.5 ± 1.7
15.71	44.4 ± 2.4

c) trans-2-butene

conc. (micromolar)	$\gamma k''(msec^{-1})$
0.0	18.7 ± 0.5
0.42	21.8 ± 0.5
1.12	25.2 ± 0.7
1.33	23.5 ± 0.8
1.66	27.2 ± 1.2
2.30	30.3 ± 0.9
2.89	33.0 ± 0.9

d) 2,3 dimethyl-2-butene

conc. (micromolar)	$\gamma k''(msec^{-1})$
0.0	18.0 ± 0.5
0.0	22.4 ± 0.6
0.10	16.3 ± 1.3
0.11	28.2 ± 0.8
0.22	26.9 ± 1.7
0.37	25.8 ± 0.9
0.37	31.1 ± 1.2
0.53	22.5 ± 0.9
0.69	28.0 ± 1.0
0.69	37.5 ± 1.2
0.86	30.8 ± 1.6
1.10	39.4 ± 1.9

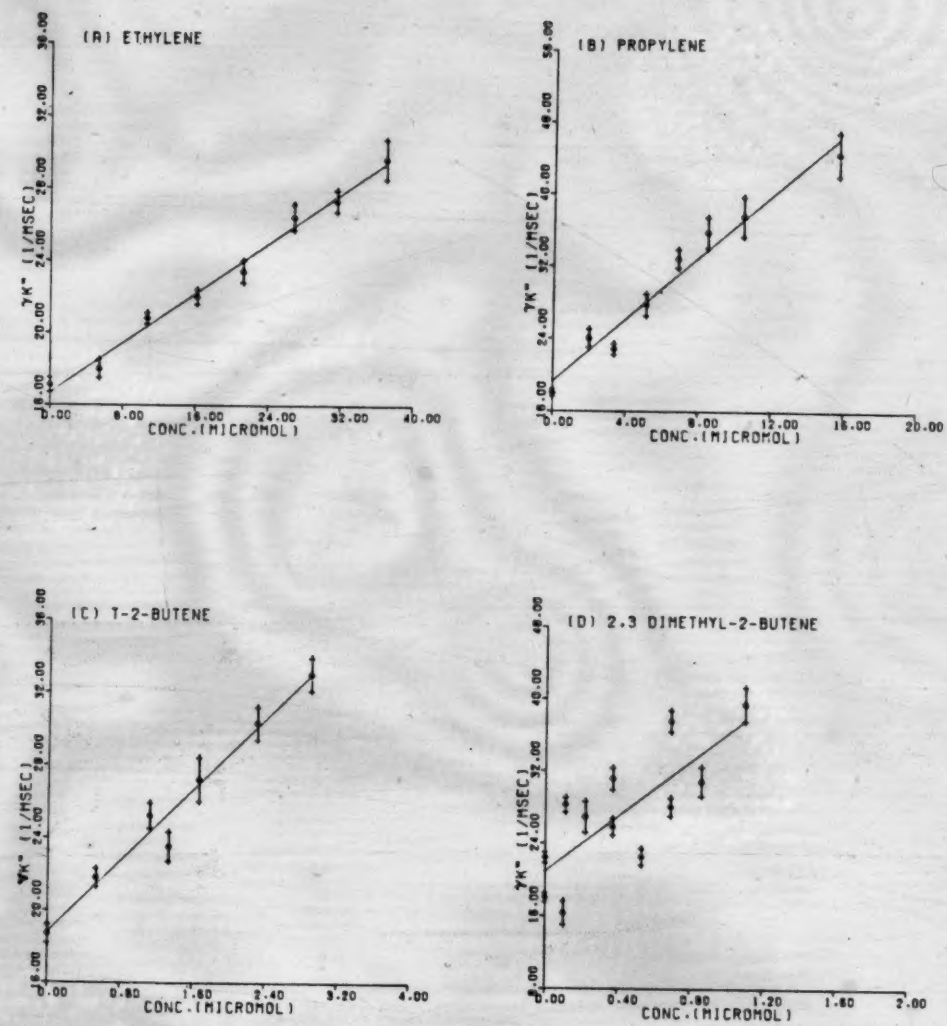

Fig.III-18. γk"(CBr) vs [S],concentration of alkene,for four alkenes.

Table III-8 Second Order Rate Constants for the Reaction of CBr with Alkenes*

Substrate	$k_2 \times 10^{-9}$ M^{-1} sec^{-1}	No. of Decays	Pressure Range of Substrate (torr)
Ethylene	0.52 ± 0.2	32	0 - 0.69
Propylene	3.0 ± 0.2	30	0 - 0.29
1-Butene	3.5 ± 0.3	30	0 - 0.14
trans-2-Butene	7.4 ± 0.8	32	0 - 0.076
iso-butene	8 ± 1	31	0 - 0.061
2-methyl-2-butene	17 ± 2	32	0 - 0.023
2,3-dimethyl-2-butene	23 ± 6	45	0 - 0.020

* The average number of points in each decay plot was 8.

2-butyne, 1-pentyne, 2-pentyne, 2,2,5,5- tetramethyl-3-hexyne and perfluoro-2-butyne. The reactions were analyzed in exactly the same manner as before although fewer decays were taken. Fig. III-19 shows the change in the decay rate of CBr as a function of 2-butyne pressure. Fig. III-20 illustrates the reaction of CBr with 3 different alkynes. Table III-9 lists the second order rate constants for the reactions with alkynes.

G) Temperature Dependence of the Reactions of CBr with Alkenes

To check the effect of temperature on the reactions of CBr with alkenes, a double walled quartz reaction vessel was used. This reaction vessel was connected to a Calora temperature bath and ethylene glycol was circulated through the outer wall of the reaction cell to regulate the temperature which was varied from 25 - 150°C. The ethylene glycol had an absorption beginning at ~ 220 nm, so this was the effective wavelength cutoff. Whenever the ethylene glycol became colored by decomposition, it was replaced with a freshly distilled sample. The mixtures were photolyzed with 2095 J of flash energy. The bromoform pressure was varied so that the concentration remained constant with temperature. The total pressure of the mixtures was 75 torr. The decays were analyzed in exactly the same manner as described before for CBr reactions. The temperature dependence of the second order rate constants for the reaction of CBr with ethylene, trans-2-butene, 2,3 dimethyl-2-butene and iso-butane is presented in Table III-10. The Arrhenius plots of these data are shown in Figs. III-21, 22. Standard least mean squares analysis of these Arrhenius plots yielded the Arrhenius parameters listed in Table-III-11.

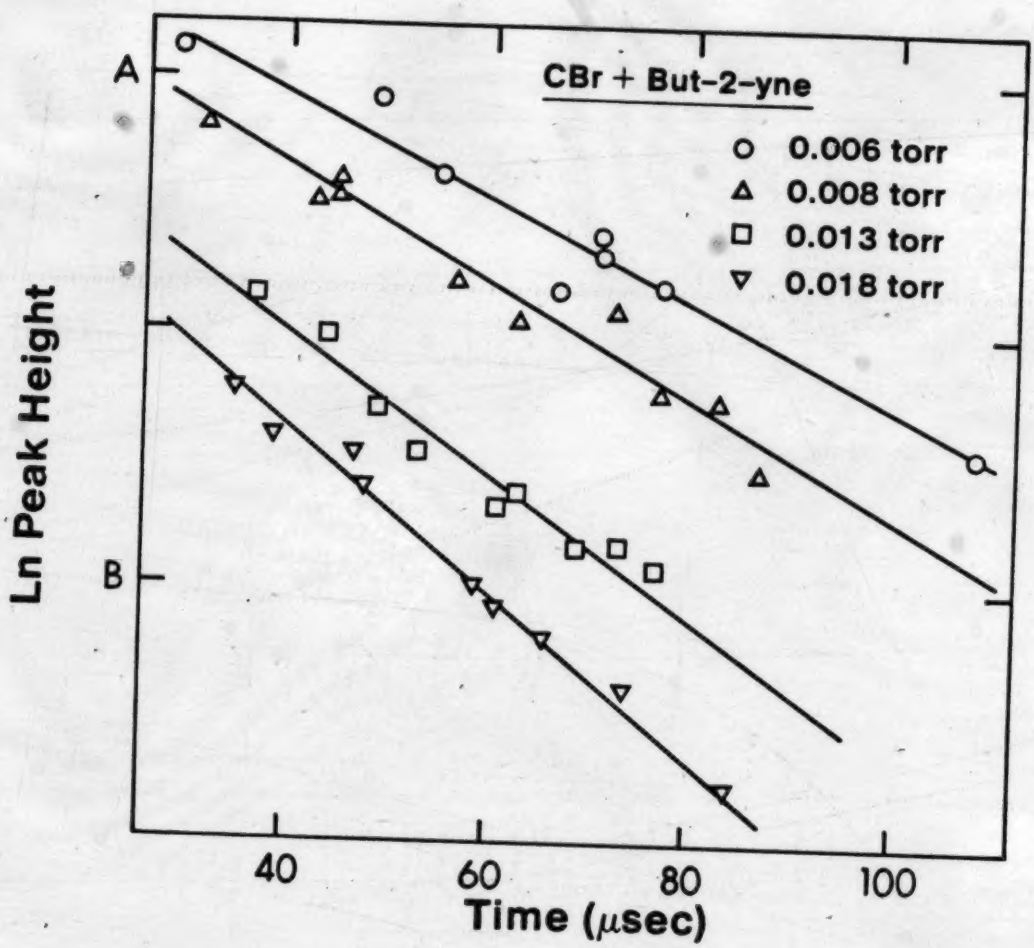

Fig.III-19. Ln (P.H.) vs Time for CBr(0_1) absorption peak in presence of 2-Butyne.

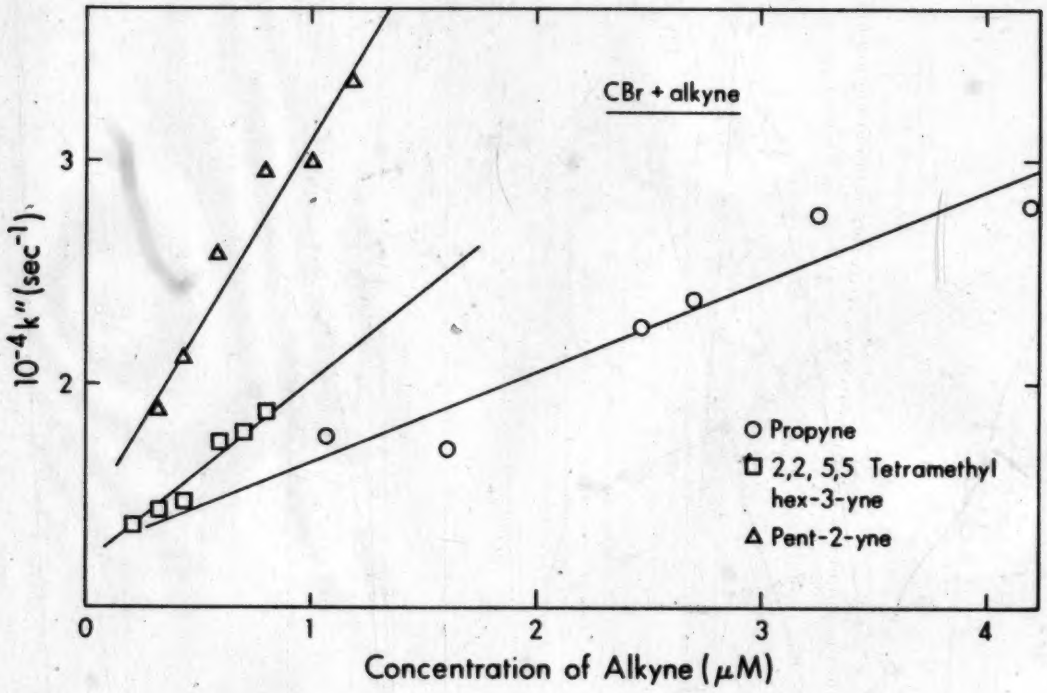

Fig.III-20. k"(CBr) vs [S],concentration of alkyne, for three alkynes.

TABLE III-9

Bimolecular Rate Constants for CBr Reaction with Alkynes

Substrate	$k_2 \times 10^{-9} M^{-1} s^{-1}$ (298°K)
C_2H_2	0.081 ± 0.007
C_2D_2	0.072 ± 0.017
C_3H_4	4.8 ± 0.6
1 - C_4H_6	6.2 ± 1.1
1 - C_5H_8	3.6 ± 0.8
2 - C_4H_6	24 ± 5
2 - C_5H_8	20 ± 3
$(CH_3)_3C\text{-}C\equiv C\text{-}C\text{-}(CH_3)_3$	9.7 ± 1.6
2 - C_4F_6	0.020 ± 0.002

Table III-10. Second Order Rate Constants, k_2, for Reaction of CBr with Alkenes and 2-methylpropane as a Function of Temperature

Substrate	Temperature(deg K)	$k_2 \times 10^{-9}$ $M^{-1}sec^{-1}$	No. of Decays*
Ethylene	278	0.58 ± 0.04	31
	338	0.54 ± 0.06	16
	379	0.46 ± 0.06	16
	423	0.44 ± 0.06	16
t-2-Butene	298	14 ± 1	24
	323	11 ± 1	16
	348	11 ± 1	16
	373	11 ± 1	16
	398	9 ± 1	16
	423	8 ± 1	16
2,3-dimethyl-	273	32 ± 3	14
2-butene	298	32 ± 3	32
	313	31 ± 3	16
	328	31 ± 3	16
	358	25 ± 3	16
	383	20 ± 3	16
	403	20 ± 3	16
	413	18 ± 3	16
	423	15 ± 2	16
2-methylpropane	298	0.0016 ± 0.0005	20
	323	0.0042 ± 0.0006	8
	348	0.0066 ± 0.0007	8
	373	0.0072 ± 0.0008	8
	398	0.0089 ± 0.0009	8
	423	0.014 ± 0.001	12

* The average number of points in each decay plot was 8

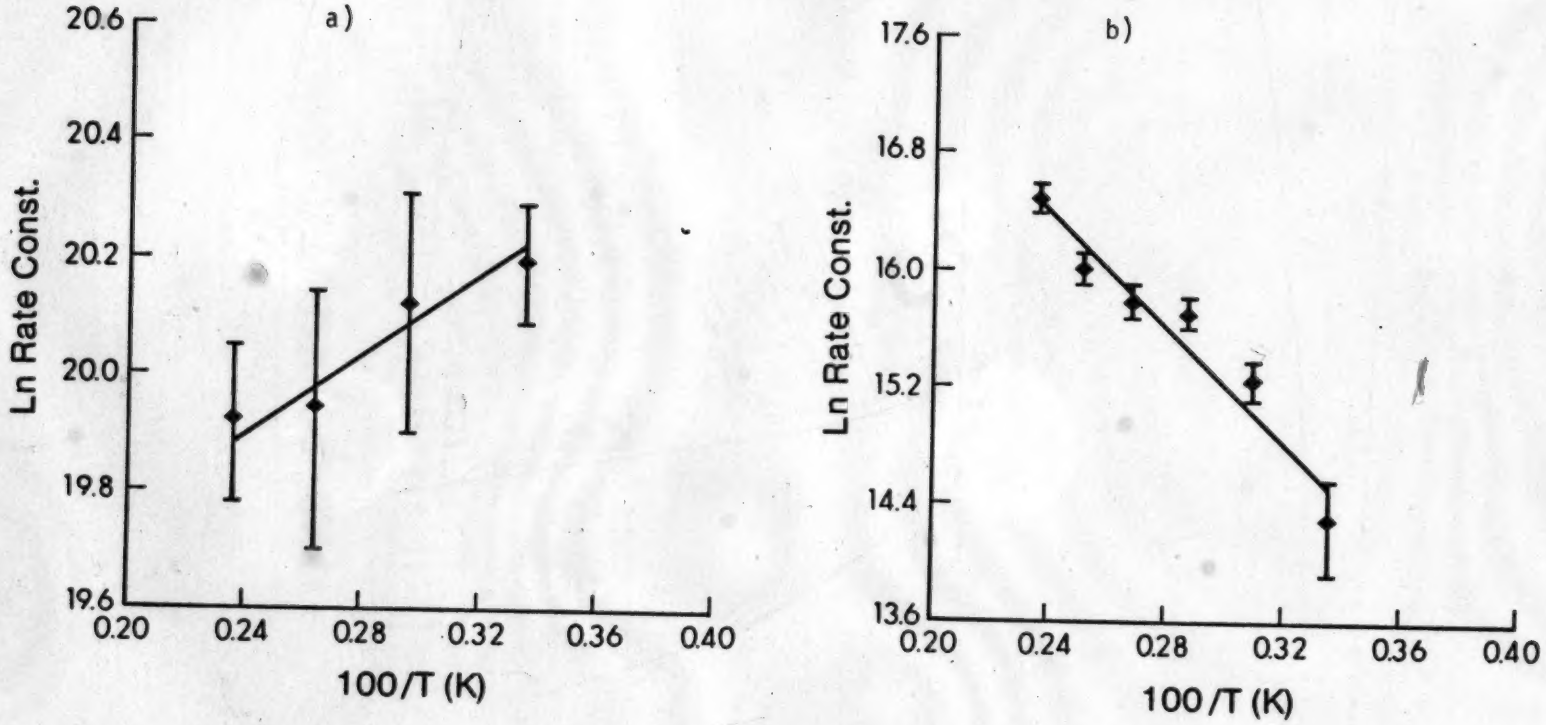

Fig.III-21. Arrhenius plots for Reaction of CBr with a) Ethylene and b) Isobutene.

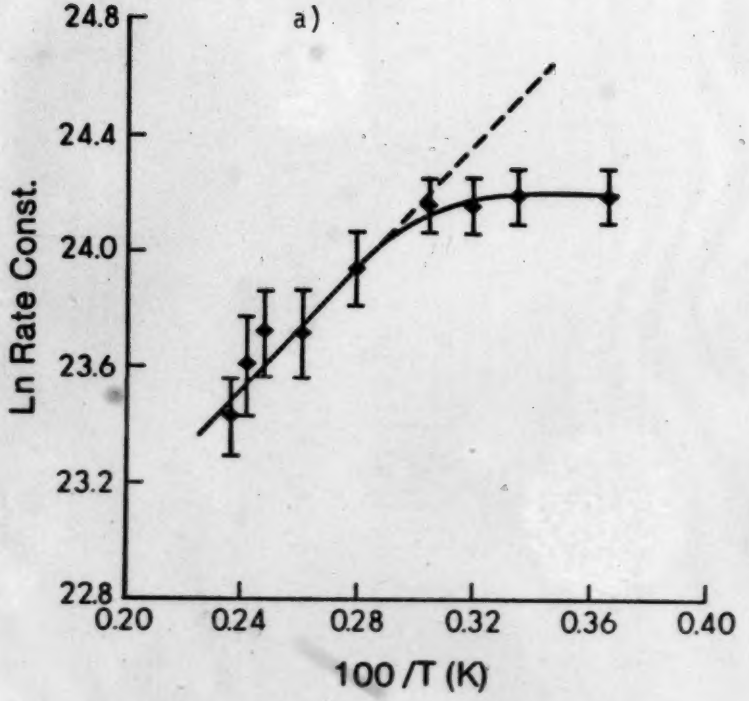

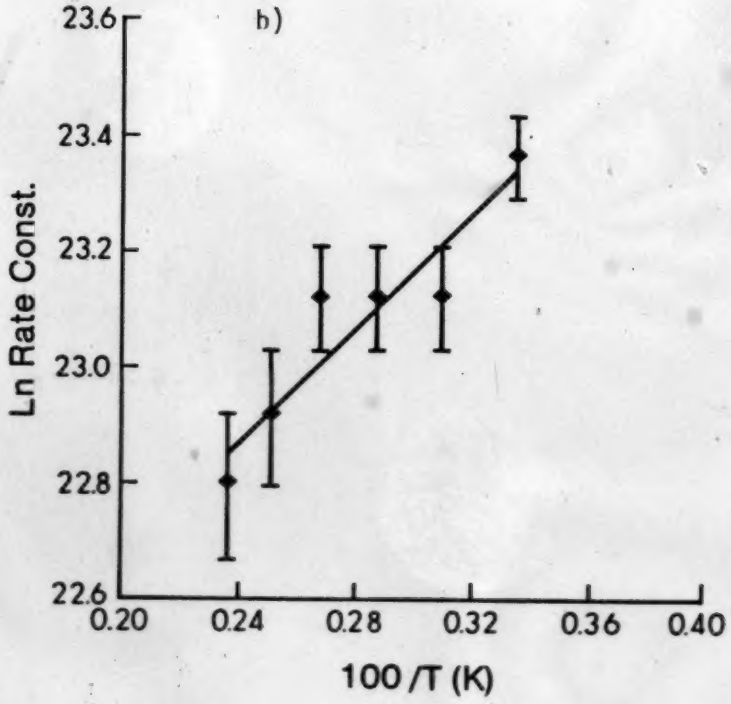

Fig.III-22. Arrhenius Plots for Reaction of CBr with a) 2,3-dimethyl-2-butene and b) t-2-butene.

Table III-11. Arrhenius Parameters for the Reactions of CBr

Substrate	E_a(kcal mole^{-1})	A(10^{-9} M^{-1}sec^{-1})
Ethylene	-0.6 ± 0.3	0.2 ± 0.1
t-2-Butene	-0.9 ± 0.3	2.7 ± 1
2,3-dimethyl-2-butene*	-1.9 ± 0.3	1.7 ± 2
2-methylpropane	3.9 ± 0.5	2 ± 1

* Determined from straight line part of Arrhenius plot at high temperatures (see Fig.III-22a). The parameters determined by a standard least squares analysis on all the data are:

E_a = -1.2 ± 0.3 kcal mole^{-1} and A =(4.5 ± 2)x10^9 M^{-1}sec^{-1}

H) Halosilylidyne Sources

The halogenated silanes $SiBr_4$ and Si_2Cl_6 were used as sources of the halosilylidynes, SiBr and SiCl respectively, since it was reported that the flash photolysis of these compounds produced the absorption spectra of the halosilylidynes (156,157). The ultraviolet absorption spectra of these halogenated silanes are shown in Fig. III-23 along with that of hexamethyldisilane.

I) Transient Absorption Spectra from Photolysis of Si_2Cl_6

The absorption spectra shown in Fig. III-24 and III-25 result from the flash photolysis of 0.20 torr Si_2Cl_6 with 50 torr Argon in a quartz system. One exposure with a flash energy of 2900 J at 40 microsecond delay were the conditions used to obtain the spectra.

The absorption spectrum shown in Fig. III-24 occurs in the region 274-297 nm and is due to two transitions of the SiCl radical; $B^2\Sigma^+ - X^2\Pi_r$ and $B'^2\Delta - X^2\Pi_r$. There are a series of vibrational bands associated with the first transition. The wavelengths of the absorption bands were determined by calibration with an iron arc spectrum and are listed in Table III-12. The assignments were made by comparison with the reported spectra (152).

The absorption spectrum shown in Fig. III-25 occurs in the region 302-340 nm and is assigned to the $^1B_1 - {}^1A_1$ transition of the $SiCl_2$ radical. The spectrum consists of a series of vibrational bands whose wavelengths were determined by calibration with an iron arc spectrum and are listed in Table III-13. The spectrum features a vibrational progression with an average interval of 148 cm^{-1}.

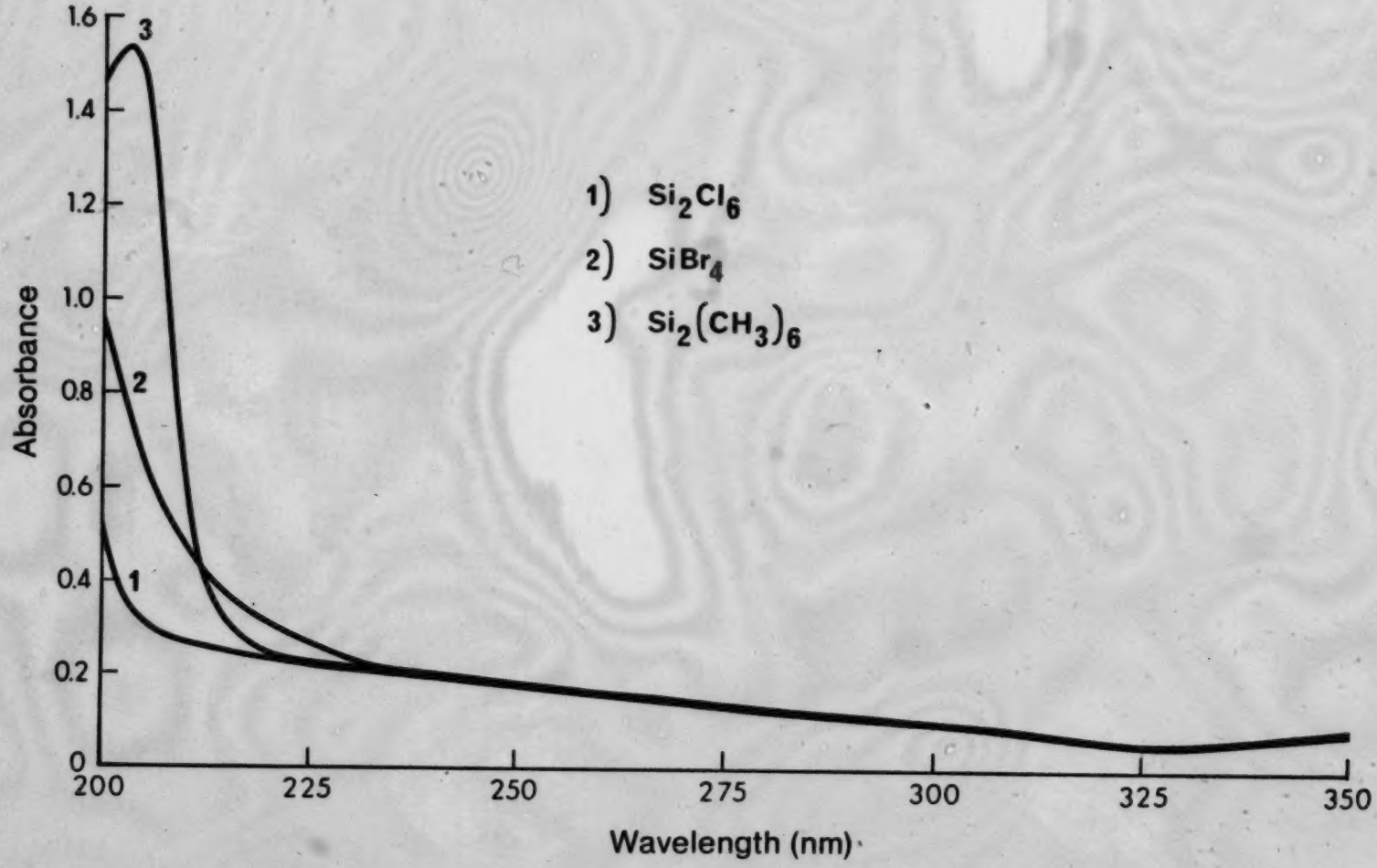

Fig.III-23. UV Absorption Spectra of Silanes.

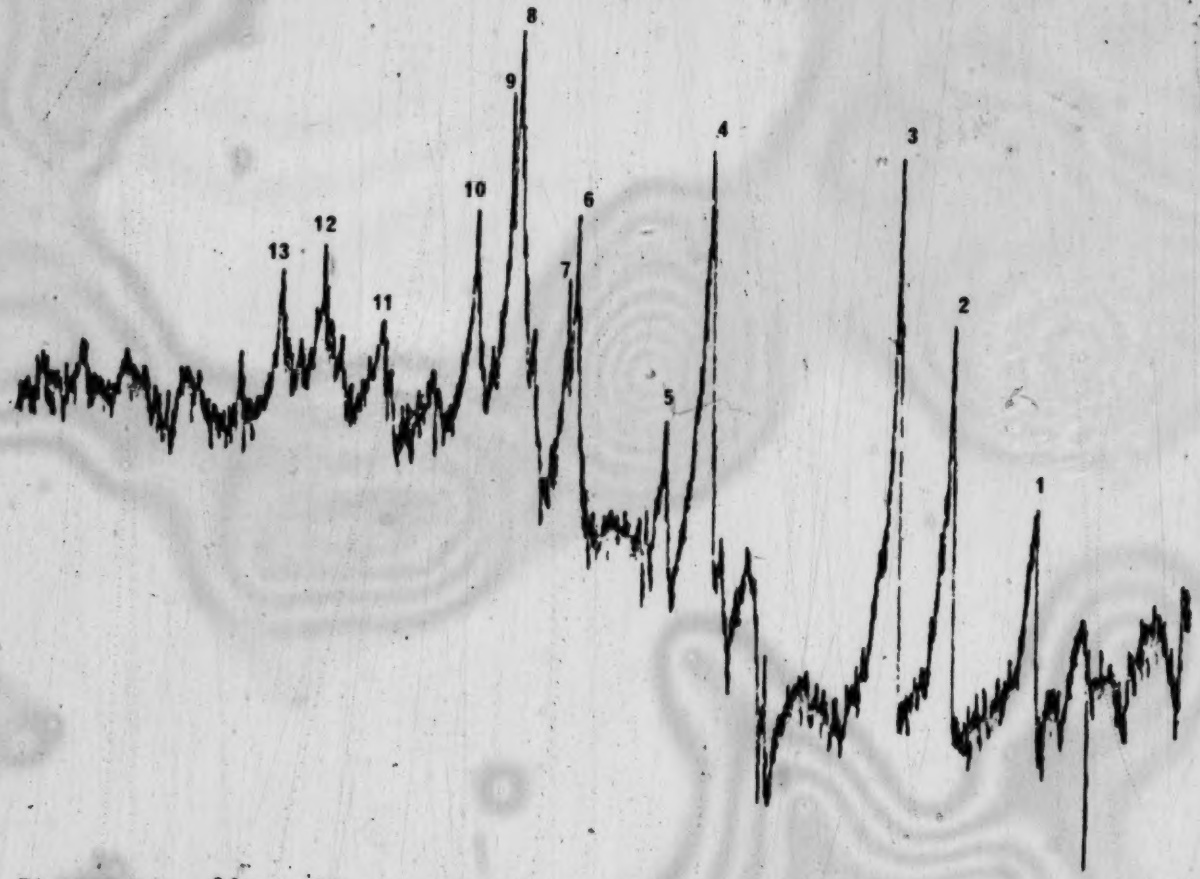

Fig.III-24. **Absorption spectrum of SiCl**

Table III-12 Assignment of the SiCl Spectrum

Peak No.	Assigned Wavelength (nm)	Transition[a]	Ref. (152)
1	296.93	$A(0\text{-}1)Q_1$	297.00
2	294.21	$A(0\text{-}0)\ {}^{o}P_{12}$	294.21
	294.13	$A(0\text{-}0)\ P_2$	294.16
3	292.40	$A(0\text{-}0)\ P_1$	292.43
	292.32	$A(0\text{-}0)\ Q_1$	292.38
4	286.54	$A(1\text{-}0)\ P_1$	286.58
	286.49	$A(1\text{-}0)\ Q_1$	286.52
5	285.17	$A(2\text{-}1)\ Q_1$	285.22
6	282.62	$A(2\text{-}0)\ {}^{o}P_{12}$	282.66
	282.58	$A(2\text{-}0)\ P_2$	282.60
7	282.32	$B(0\text{-}0)P_2$	282.35
8	280.99	$A(2\text{-}0)\ P_1$	281.02
	280.93	$A(2\text{-}0)\ Q_1$	280.96
9	280.68	$B(0\text{-}0)Q_1$	280.71
10	279.77	$A(3\text{-}1)Q_1$	279.77
11	277.26	$A(3\text{-}0)P_2$	277.30
12	275.68	$A(3\text{-}0)\ P_1$	275.72
	275.63	$A(3\text{-}0)\ Q_1$	275.67
13	274.54	$A(4\text{-}1)Q_1$	274.58

a) There are two electronic transitions

$$A - B^2\Sigma^+ - X^2\Pi_r$$

$$B - B'^2\Delta - X^2\Pi_r$$

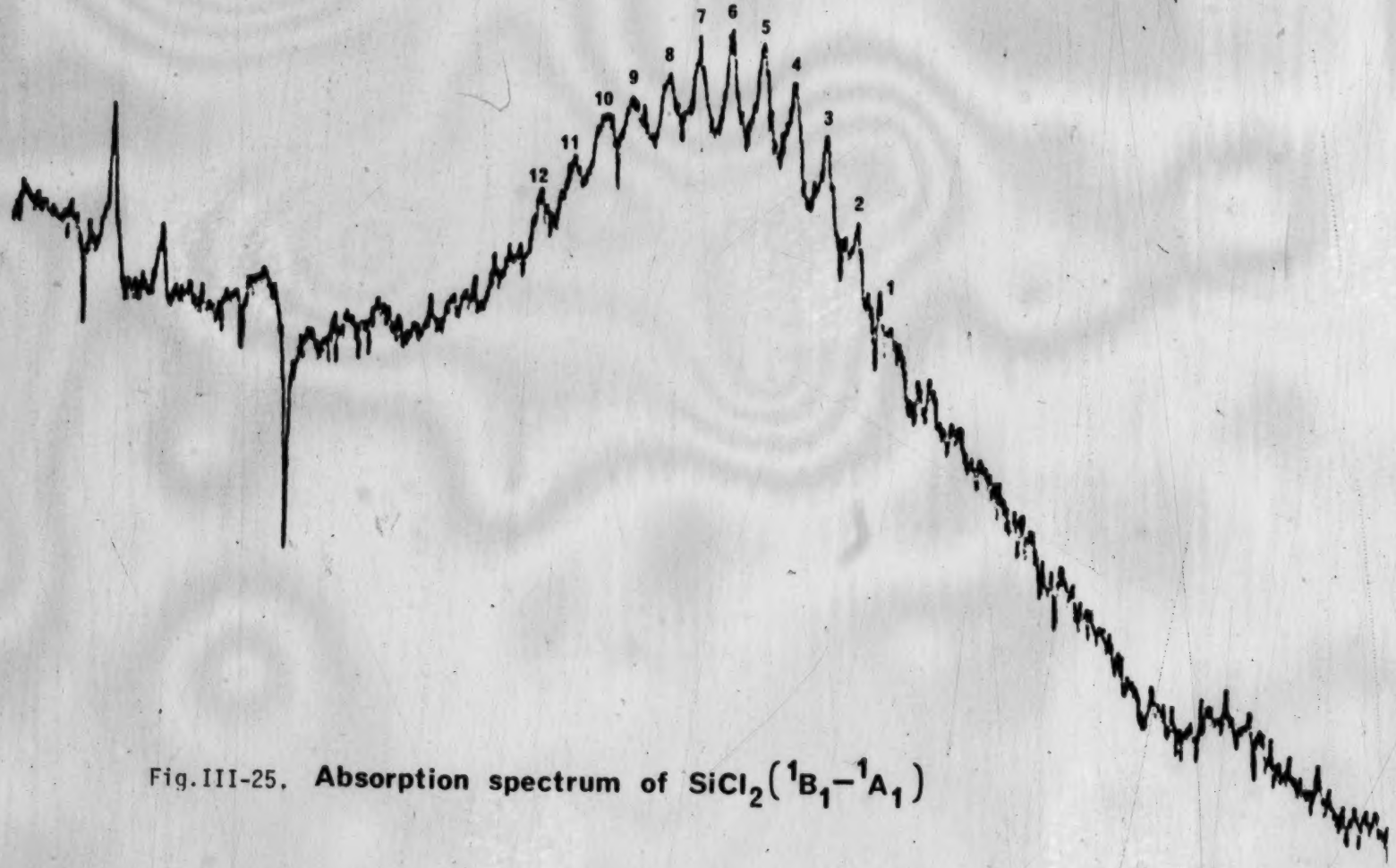

Fig.III-25. **Absorption spectrum of $SiCl_2(^1B_1-^1A_1)$**

Table III-13 Assignment of $SiCl_2$ Spectrum

Peak No.	λ (nm)	ν (cm^{-1})
1.	325.07	30763 (154)
2	323.45	30917 (139)
3	322.00	31056 (151)
4	320.44	31207 (157)
5	318.84	31364 (141)
6	317.41	31505 (137)
7	316.04	31642 (146)
8	314.58	31788 (152)
9	313.09	31940 (138)
10	311.74	32078 (159)
11	310.20	32257 (157)
12	308.70	32394

J) Transient Absorption Spectra from the Photolysis of $SiBr_4$

The absorption spectrum shown in Fig. III-26 results from the photolysis of 0.10 torr $SiBr_4$ with 50 torr Argon in a Suprasil reaction vessel. One exposure with a flash energy of 2900 J at 40 microsecond delay were the conditions used to obtain the spectrum.

The absorption spectrum observed is due to the $B^2\Sigma$-$X^2\Pi$ transition of SiBr and consists of a series of vibrational bands. The wavelengths of these absorption bands were determined by calibration with an iron arc spectrum and are listed in Table III-14. Some of the absorption bands consist of overlapping transitions from the two subsystems, $^2\Sigma$-$^2\Pi_{1/2}$ and $^2\Sigma$-$^2\Pi_{3/2}$, since the magnitude of the spin orbit coupling splitting of the ground electronic state in SiBr is nearly identical to the interval between the vibrational levels in this state. The vibrational assignments were made on the basis of the assignments reported in reference 151. Absorption bands 1-9 and 11 (see Fig. III-26) were assigned while absorption bands 10 and 12-21 had not been reported. The vibrational assignments for the unreported bands were checked by comparing the calibrated wavelengths with those calculated from the following formula given in reference 150.

1. for subsystem $^2\Sigma$-$^2\Pi_{1/2}$ where $u = v + 1/2$

$$\nu_{head}\ (cm^{-1}) = 33571.0 + (571.2\ u'-2.4\ u'^2) - (425.3\ u''-1.5\ u''^2)$$

2. for subsystem $^2\Sigma$-$^2\Pi_{3/2}$ where $u = v + 1/2$

$$\nu_{head}\ (cm^{-1}) = 33153.0 + (571.2\ u'-2.4\ u'^2) - (425.3\ u''-1.5\ u''^2)$$

No other transitions of SiBr were investigated in this study.

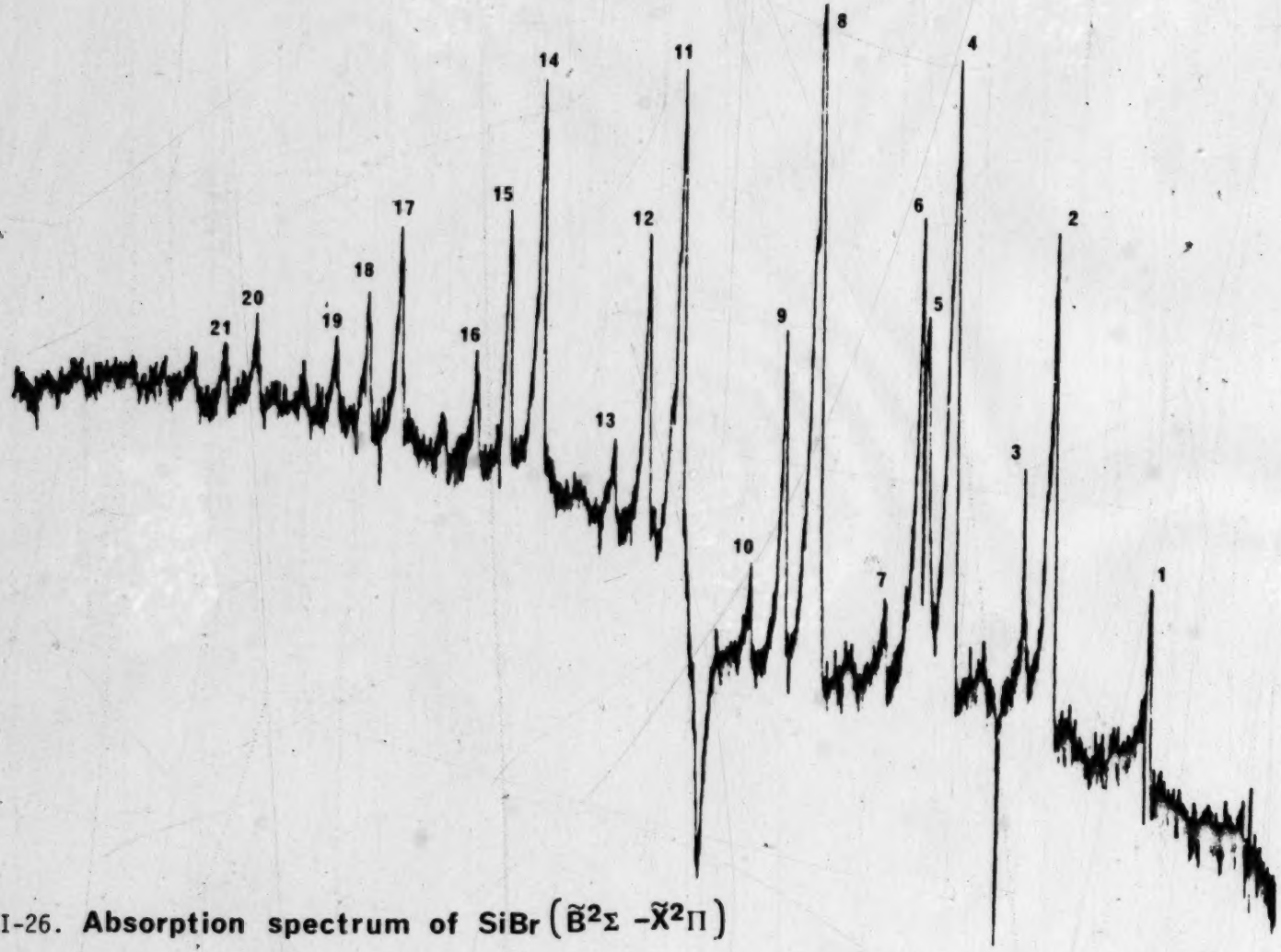

Fig.III-26. **Absorption spectrum of SiBr** $(\tilde{B}^2\Sigma - \tilde{X}^2\Pi)$

Table III-14 Wavelength Calibration of the Absorption Spectrum of SiBr ($B^2\Sigma$-$X^2\Pi$)

Absorption Band	Wavelength (nm)	Vibrational Assignment (v'-v")	
		$^2\Sigma$-$^2\Pi_{1/2}$	$^2\Sigma$-$^2\Pi_{3/2}$
1	304.80*	0-2	0-1
2	300.96*	0-1	0-0
3	299.81	1-2	1-1
4	297.18*	0-0	
5	296.08*	1-1	
6	295.90*		1-0
7	294.66	2-2	2-1
8	292.30*	1-0	
9	291.08*	2-1	2-0
10	289.94	3-2	3-1
11	287.53*	2-0	
12	286.4	3-1	3-0
13	285.34	4-2	4-1
14	283.01*	3-0	
15	281.98*	4-1	4-0
16	280.97	5-2	5-1
17	278.66*	4-0	
18	277.63	5-1	5-0
19	276.75	6-2	6-1
20	274.45	5-0	
21	273.35	6-1	6-0

*indicates the bands observed in quartz photolysis system.

The absorption spectrum shown in Fig. III-27 results from the flash photolysis of 1.0 torr $SiBr_4$ with 30 torr Argon in a quartz system. One exposure with a flash energy of 2900 J and 50 microsecond delay were the conditions used to obtain the spectrum. The absorption occurs in the region 342 - 400 nm with a maximum at 362 nm and is assigned from this study to the $^1B_1$-$^1A_1$ transition of $SiBr_2$ (see Discussion).

K) Analysis of the SiBr Spectrum and Decay

Three absorption bands of SiBr were analysed for kinetic measurements, peaks 4,8 and 11 (see Fig. III-26) which correspond to the vibrational bands 0-0, 1-0 and 2-0 respectively of the $B^2\Sigma$-$^2\Pi_{1/2}$ electronic transition. Therefore all three transitions are due to the ground vibrational and electronic state of SiBr. All three absorption peaks were found to obey Beer's absorption law (see Section III-C). The decay of the spectra followed first order kinetics with all three peaks having the same background decay, $k' = 27 \pm 1$ msec^{-1} (see section III-D). When ethylene was added to the mixture, the intensity of the peaks was strongly diminished and the decay rate became very inconsistent. The results are shown in Table III-15.

L) Analysis of the SiCl and $SiCl_2$ Spectral Decay

The SiCl spectrum was weak and decayed too rapidly to allow reliable kinetic measurements. However, the $SiCl_2$ spectrum decay was slow enough for analysis. The background decay followed first order reaction kinetics, $k' = 18 \pm 1$ msec^{-1}. Table III-16 shows the results of adding ethylene to the reaction mixture. An upper limit for reaction rate constant of $SiCl_2$ + ethylene can be calculated to be $k_2 < 1.5 \times 10^7$ $M^{-1}sec^{-1}$.

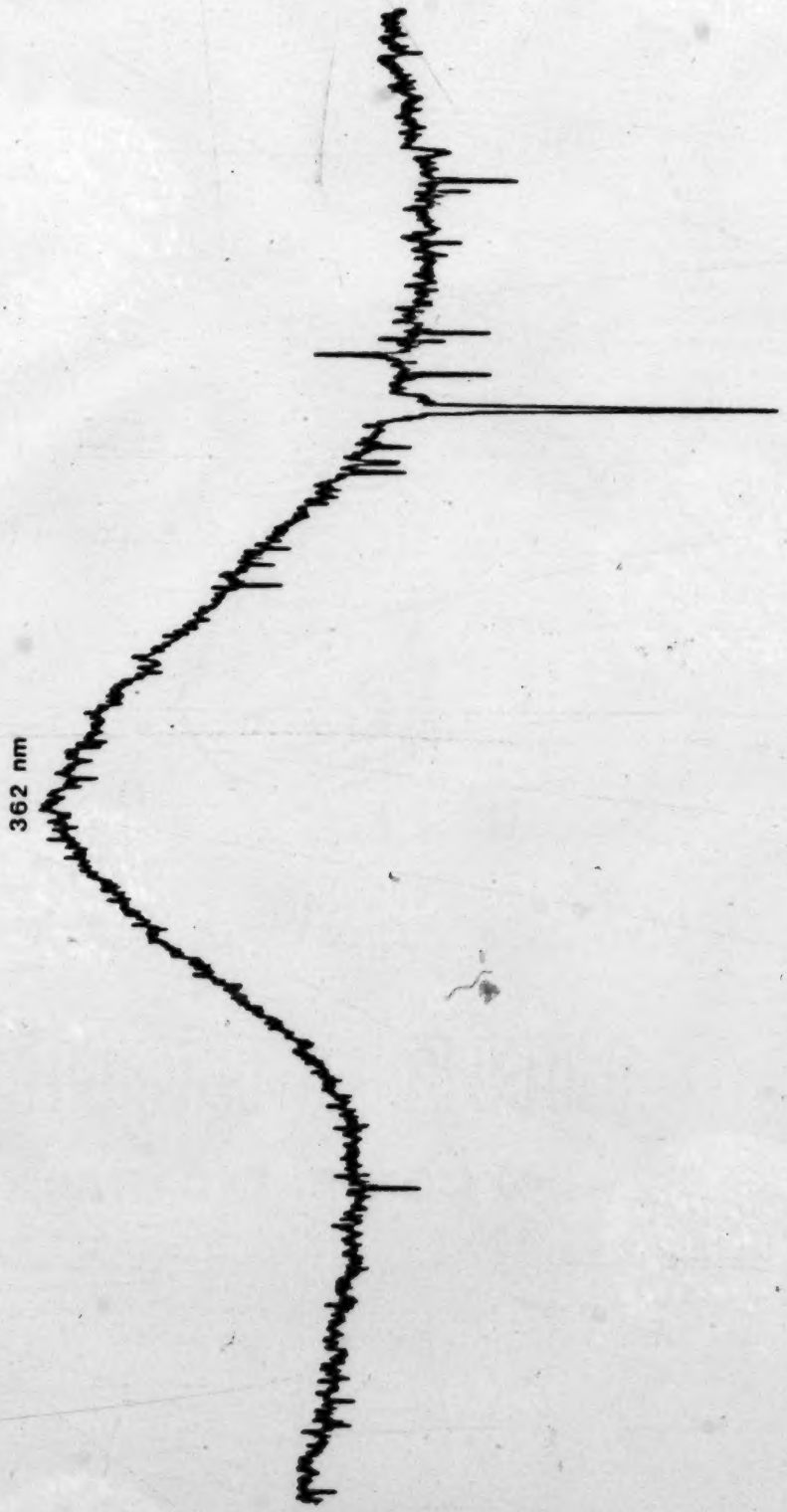

Fig.III-27. **Absorption spectrum of $SiBr_2$ ($^1B_1 - {}^1A_1$)**

Table III-15. Decay of SiBr bands in presence of Ethylene

Conc. (micromolar)	k"($msec^{-1}$)		
	(0-0)	(1-0)	(2-0)
0.0	26.4 ± 1.1	25.4 ± 0.8	28.5 ± 0.8
5.34	24.9 ± 2.4	25.0 ± 1.0	27.0 ± 2.3
10.69	30.8 ± 3.1	24.6 ± 1.8	23.7 ± 2.7

Table III-16. Decay of $SiCl_2$ Absorption in presence of Ethylene.

Conc. (micromolar)	k"($msec^{-1}$)
0.0	17.9 ± 0.5
5.34	16.0 ± 0.6
10.69	18.2 ± 0.6
16.03	18.8 ± 0.8

IV. DISCUSSION

A) Photochemistry of Halogenated Methanes

The absorption spectra of halogenated methanes are due to a $n\sigma^*$ electronic transition, n being the lone pair orbital on the halogen and σ^* the antibonding orbital for the carbon-halogen bond. The σ^* orbital is formed from out of phase combination of the carbon sp^3 orbital and halogen p orbital and therefore possesses a large amount of p character. Since $p \leftrightarrow p$ transitions are forbidden by the Laporte selection rule, the intensity of the $n \rightarrow \sigma^*$ transition is weak resulting in low molar absorption coefficients (154).

This ultraviolet ($n\sigma^*$) photolysis of halogenated methanes results in dissociation of the weakest carbon-halogen bond (60,154). The dissociation energy of the carbon-bromine bond in brominated methanes is 60-70 kcal $mole^{-1}$ (60,158). From the absorption spectrum of the brominated methanes shown in Fig. III-1, one can calculate the amount of energy absorbed at the peak maximum and how much excess energy is available after bond dissociation using an average D_o(Br-CHXBr) of approximately 65 kcal $mole^{-1}$.

		Excess Energy (kcal $mole^{-1}$)
$CHFBr_2$	$\longrightarrow$ $CHFBr + Br$	64
$CHClBr_2$	$\longrightarrow$ $CHClBr + Br$	73
$CHBr_3$	$\longrightarrow$ $CHBr_2 + Br$	64

Now the question arises as to the distribution of the excess energy. CH_3I and CH_2I_2 have been investigated with regard to the energy distribution after photolysis (159,160). The methyl radical from the

photolysis of CH_3I contained 12% of the excess energy while the CH_2I fragment from the photolysis of CH_2I_2 contained 80-90% of the available energy. This difference in energy partitioning is explained in terms of the impulsive model (60),

$$\frac{E_{int}^{BC}}{E_{avl}} = 1 - \frac{\mu_{A-B}}{\mu_{A-BC}}$$

where E_{int}^{BC} is the internal energy of the fragment BC, E_{avl} is the available energy, μ_{A-B} is the reduced mass of A and B and μ_{A-BC} is the reduced mass of A and BC. From the equation, the internal energies of the halomethyl radicals can be estimated. The results show that ~80% of the excess energy goes into the internal energy of the halomethyl radicals (78% for CHFBr, 79% for CHClBr and 81% for $CHBr_2$).

Now in order to evaluate Simons and Yarwood's mechanism of halomethylidyne arising from the decomposition of vibrationally excited halomethyl radicals (50,51), the reaction enthalpies of these reactions must be calculated. The enthalpy of formation of the halomethylidynes and hydrogen halides are reported, but ΔH_f° values for two of the halomethyl radicals have to be estimated (60,113,158). The reaction enthalpies are calculated and shown below along with 80% of the excess energy available at the absorption maximum.

	ΔH(kcal mole^{-1})	Excess Energy(kcal mole^{-1})
CHFBr → CF + HBr	53	51
→ CBr + HF	59	51
CHClBr → CCl + HBr	70	58
→ CBr + HCl	60	58
$CHBr_2$ → CBr + HBr	61	51

It is clear that in all cases, there is not enough energy available to cause the unimolecular decomposition. This does not rule out this mechanism because the difference between required and available energy is not large and can be accounted for by uncertainties in the calculation of the reaction enthalpies and the distribution of the excess energy. If the bromomethyl radicals receive all of the excess energy available at the absorption maximum or 80% of the excess energy available at the short wavelength limit of absorption (200 nm) then there is enough to satisfy the reaction enthalpies of the unimolecular decompositions.

The fact that the halomethylidyne absorption intensity is quenched by increasing pressure strongly indicates formation from an excited precursor. There is also the possibility that secondary photolysis of the halomethyl radical produces halomethylidyne. Laser photolysis of chlorinated methanes has shown that $CCl(A^2\Delta)$ is formed by absorption of 2-3 193 nm photons although the mechanism of photolysis is uncertain (59).

Therefore the mechanism of formation of the halomethylidyne suggested by Simons and Yarwood should be complemented with the possibility of secondary photolysis.

$$CHXBr_2 \xrightarrow{h\nu} CHXBr + Br$$

$$CHXBr^{\dagger} \longrightarrow CX + HBr$$

$$\longrightarrow CBr + HX$$

$$\xrightarrow{M} CHXBr$$

$$CHXBr \xrightarrow{h\nu} CX + HBr$$

$$\xrightarrow{h\nu} CBr + HX$$

B) Background Reactions and Decay of the Halomethylidynes

The background rate decay of the halomethylidynes is best described by a first order decay:

$$-\frac{d[CX]}{dt} = k'[CX]$$

Since the halomethylidynes must be reacting with other species, the background rate decay is pseudo first order

$$-\frac{d[CX]}{dt} = k_b[R][CX]$$

where $k_b[R] = k'$ and [R] is effectively constant during the decay of CX. The problem now is to establish what R is and what reactions are removing CX.

Photolysis of $CHXBr_2$ by the accepted mechanism results in a variety of photolytic products:

$$CHXBr_2 \longrightarrow \begin{cases} CHXBr + Br \\ CX + HBR + Br \\ CBr + HX + Br \end{cases}$$

Therefore the possible reactions of CX are the following:

$$:\dot{C}X + CHXBr_2 \xrightarrow{1}$$

$$:\dot{C}X + \cdot CHXBr \xrightarrow{2}$$

$$:\dot{C}X + \cdot Br \xrightarrow{3}$$

$$:\dot{C}X + :\dot{C}X\ (:\dot{C}Br) \xrightarrow{4'}$$

$$:\dot{C}X + HBR\ (HX) \xrightarrow{5}$$

Because the yield of CX, CBr, HX, HBr is thought to be low (154), reactions 4 and 5 are negligible. The background rate constant can be calculated if two assumptions are made:

- assume that either reaction 1 or reactions 2 and 3 are mainly responsible for removal of CX
- assume that a certain percentage of the halogenated methane is photolysed. Two cases will be used, 50% and 5% decomposition.

First the reaction with the parent compound, 1 , will be examined. The average values of k' and the initial pressures of $CHXBr_2$, which are used in the calculations, are listed along with the calculated values of k_b.

Reaction	k' ($msec^{-1}$)	P ($CHXBr_2$) torr	$k_b \times 10^{-9} M^{-1} sec^{-1}$ 50%	5%
$CF + CHFBr_2$	10	0.15	2.5	1.3
$CCl + CHClBr_2$	19	0.30	2.5	1.3
$CBr + CHBr_3$	28	0.10	10	5.3

These calculated background rate constants are very high. Comparison with reported rate constants for reaction of CCl with halogenated methanes (see Table I-6) shows that these calculated rate constants are at least 1 - 2 orders of magnitude higher and consequently this reaction sequence for removal of CX is considered negligible.

Now the background rate constant will be calculated in the same manner assuming reactions 2 and 3 are mainly responsible for removing CX.

Reaction	k'(msec^{-1})	P($CHXBr_2$) torr	$k_b \times 10^{-9}$ $M^{-1}sec^{-1}$	
			50%	5%
CF + CHFBr and Br	10	0.15	1.2	12
CCl + CHClBr and Br	19	0.30	1.2	12
CBr + $CHBr_2$ and Br	28	0.10	5.0	50

These calculated rate constants agree very well with measured radical - radical recombination rate constants which are in the range 10^9 - 10^{10} $M^{-1}sec^{-1}$ (162). For example;

$$\cdot CCl_3 + \cdot CCl_3 \rightarrow C_2Cl_6 \qquad k = 3 \times 10^{10}\ M^{-1}sec^{-1} \quad (163)$$

$$\cdot CF_2Cl + \cdot CF_2Cl \rightarrow C_2F_4Cl_2 \qquad k = 1 \times 10^{10}\ M^{-1}sec^{-1} \quad (164)$$

$$\cdot CF_3 + \cdot CF_3 \rightarrow C_2F_6 \qquad k = 3 \times 10^{9}\ M^{-1}sec^{-1} \quad (165)$$

These results imply that radical-radical reactions are removing the halomethylidyne. There is other evidence to support this. Choi et al (54) found that the pseudo first order rate constant, k', increased with increasing flash energy. The increase in flash energy means a greater degree of photolysis and greater concentration of the radicals, ·CHXBr and ·Br, making the value of $k_b[R]$ larger.

In this study it was found that k' for CBr was unaffected by temperature variation (see Table III-2). This is characteristic of radical-radical reactions due to zero activation energy.

These results suggest that removal of CX after photolysis of $CHXBr_2$ is mainly due to the following reactions:

$$:\dot{C}X + \cdot CHXBr \rightarrow C_2HX_2Br$$

$$:\dot{C}X + \cdot Br \rightarrow :CXBr$$

However this interpretation also seems to present some problems. For the rate expression to be pseudo first order the concentrations of

the reacting radicals, [R], must be essentially constant during the decay of the halomethylidyne. Radical termination reactions such as:

$$\cdot CHXBr + \cdot CHXBr \rightarrow C_2H_2X_2Br_2$$

$$\cdot CHXBr + \cdot Br \rightarrow CHXBr_2$$

should be quite fast as shown previously and would be expected to change the radical concentration. Now the decay of carbynes has been reported to be pseudo first order by a variety of techniques such as: flash photolysis - kinetic absorption spectroscopy(73,53-55); pulse radiolysis - kinetic absorption spectroscopy (83) and laser photolysis - fluorescence spectroscopy (79,93,96,121) and all of these techniques generate other radicals and are faced with the same problem. The solution seems to be that radical propagation reactions are the dominant reactions during the decay of the halomethylidyne and not the radical termination reactions mentioned above.

In summary, the mechanisms for the generation and decay of halomethylidynes have been shown to have many uncertain factors caused by the formation of other radicals and lack of experimental detail. As a suggestion to further research in carbynes, perhaps the photolysis of difluoroacetylene would generate fluoromethylidyne cleanly, which would facilitate conventional mechanistic studies.

C. Reaction of CBr with Isobutane

The rate constant for the reaction of CBr with 2-methylpropane (isobutane) at 298°K is 1.6×10^6 $M^{-1}sec^{-1}$. Since CCl and CBr do not display any measurable reactivity with primary and secondary carbon - hydrogen bonds (note the variation of rate constants in Table I-6

for CCl reactions with alkanes), this measured rate constant must be for reaction with the weaker tertiary C-H bond. This value is one order of magnitude smaller than the reported rate constant for this reaction (see Table I-8). Since CCl and CBr are expected to have similar reactivity, the rate constant measured here for CBr reaction is supported by the reported values for CCl reaction with isobutane, k_2 = (4.5 and < 2) x 10^6 $M^{-1}sec^{-1}$ (see Table I-6). In contrast, CH reacts with primary, secondary and tertiary C-H bonds indiscriminately at rates close to the collision frequencies (see Table I-4).

The reaction of carbynes with C-H bonds is believed to be a concerted insertion reaction. Carbethoxymethylidyne is reported to insert into C-H bonds, but unlike CH which reacts indiscriminately, CCO_2Et is reported to discriminate between allylic and other C-H bonds (95). CCl and CBr, in their reactions with primary, secondary and tertiary C-H bonds, display greater discrimination.

The explanation for this is the effect of substituents on the reactivity of carbynes, in the same way as carbenes are affected. Singlet methylene, $CH_2(^1A_1)$, inserts very rapidly into C-H bonds (see Table I-4). However CCl_2 and CBr_2 discriminate greatly between C-H bonds preferring to react with tertiary and allylic C-H bonds (2). To explain this increased reactivity of weaker C-H bonds a polarized transition state was proposed in which there is partial positive charge on the carbon of the reacting C-H bond(2) :

$$:CX_2 + \equiv C\text{-}H \rightarrow \equiv C^{\delta+}\cdots H\cdots C^{\delta-}X_2 \rightarrow \equiv C\text{-}CX_2H$$

where CX_2 represents a halogenated singlet carbene. Analogously for carbyne reactions, the same polarized transition state could explain the preference of CCl and CBr for tertiary C-H bonds.

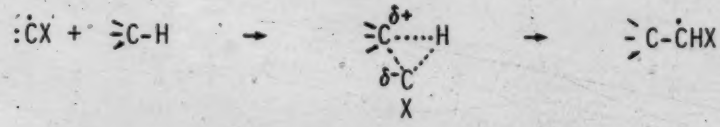

For the reaction of CCl with silanes, it was found that the reactivity of the Si-H bond is in the order tertiary > secondary > primary which was explained by the above insertion reaction mechanisms (54).

The rate constant equation determined for the reaction of CBr with isobutane is $k_2 = 2 \times 10^9 \exp(-3.9/RT)$. The Arrhenius plot (fig III-21b) did not indicate that the reaction with the primary C-H bonds became important at higher temperature. Therefore the activation energy for reaction with the primary C-H bond should be at least 2-3 kcal $mole^{-1}$ higher.

This is the only insertion reaction of a carbyne for which activation parameters have been determined to date. Activation parameters and rate constants are not available for insertion reactions of the more widely investigated carbenes with the exception of methylene.

D. Reaction of Halomethylidynes with Alkenes

The experimentally determined rate constants for the reaction of CF, CCl and CBr with alkenes are listed in the Table IV-1. The reactivity of all three halomethylidynes follows an electrophilic trend, that is, the rate constants increase with increasing alkyl substitution on the

Table IV-1. Rate Constants for Reactions of Methylidyne and Halomethylidynes with Alkenes.

Substrate	$k_2 \times 10^{-9}$ $M^{-1}sec^{-1}$			
	CH	CF[c]	CCl[c]	CBr[c]
Ethylene	69 ± 6[a] 130 ± 50[b]	0.04 ± 0.01	0.16 ± 0.01	0.52 ± 0.02
Propylene		0.3 ± 0.1	1.0 ± 0.1	3.0 ± 0.2
1-Butene		0.4 ± 0.1	1.7 ± 0.2	3.5 ± 0.3
t-2-Butene		1.1 ± 0.2	2.6 ± 0.2	7.4 ± 0.8
2-methyl-2-propene		1.1 ± 0.3	3.5 ± 0.3	8 ± 1
2-methyl-2-butene			8 ± 1	17 ± 2
2,3-dimethyl-2-butene			14 ± 3	23 ± 6
cyclohexene			3.1 ± 0.2[d]	
1,3-cyclohexadiene			1.4 ± 0.2[d]	
1,4-cyclohexadiene			3.7 ± 0.2[d]	

a - ref. 83

b - ref. 79

c - this work

d - ref. 54b

olefinic double bond. Since the rate constants for the reactions of CCl and CBr with alkanes are very low (Table I-6, Table III-10), one can conclude that the reactions of halomethylidynes with C-H bonds are not responsible for the high rate constants observed and therefore the reactivity trend is due to the interaction of the halomethylidyne with the olefinic double bond. The measured rate constants for the reactions of CCl can be compared to previously reported values (see Table I-6). The rate constant for ethylene is in good agreement with Wampler's value while Tyerman's value is 2 times higher. Tyerman's values are two times higher for propylene and three to four times higher for trans-2-butene and iso-butene. The rate constants for CBr may also be compared to previous results (see Table I-8). The rate constants are in good agreement with the values for ethylene and t-2-butene determined by Strausz et al. while their other values are: propylene, 2 times higher; 1-butene, 3 times higher and 2,3 dimethyl-2-butene, 2 times lower than the values determined here. In this regard it must be pointed that the rate constants for the reaction of CBr with ethylene, t-2-butene and 2,3 dimethyl-2-butene were redetermined in the temperature studies and while there is good agreement for ethylene, the rate constants for the reaction with t-2-butene and 2,3 dimethyl-2-butene are significantly higher (see Tables III-8, III-10). This discrepancy is possibly due to photolysis of the olefin since the wavelength cutoff was different in the two studies (quartz photolysis , $\lambda > 200$ nm, photolysis with ethylene glycol filter, $\lambda > 220$nm).

From Table IV-1 the rate constant for the reaction of CH with ethylene is 200 times faster than that for CBr, 625 times faster than

that for CCl and 2500 times faster than that for CF. This is exactly the trend predicted from the molecular orbital description of carbynes. Donation of the halogen lone pair electons through the delocalized molecular orbital reduces the electrophilic reactivity of the carbyne. Methylidyne, CH, has only one electron in the π orbital resulting in a greater reactivity than the halomethylidynes which have four electrons in the bonding π orbitals. The reactivity trend between halomethylidynes is due to the better overlap between the carbon 2p orbital with the fluorine 2p orbital than with the 3p and 4p orbitals of chlorine and bromine, respectively. This results in greater delocalization of the π orbital following the series CF > CCl > CBr. Therefore the reactivity trend is related to the trend in the bond energies, $D_o(CX)$= 131, 81, 75 kcal $mole^{-1}$ for X = F, Cl, Br, respectively. These observations lead to the conclusion that the main factor influencing the reactivity of carbynes is the electron occupancy and delocalization of the bonding π orbital.

Now the observation that the reactivity of halomethylidynes with alkenes increases with alkyl substitution shows that carbynes are electrophilic reagents and that the reaction proceeds by electron donation of the alkene π electrons to the halomethylidyne.

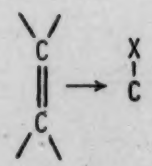

Therefore, it would be expected that as for other electrophilic addition reactions, a correlation exists between log k_2 and ionization potential of the olefin. This linear correlation exists for all three

halomethylidynes as shown in Fig. IV-1,2,3. For CBr, the rate constant for 2,3-dimethyl-2-butene may be considered to deviate from the linear correlation. This deviation may be due to the photolysis of 2,3-dimethyl-2-butene, however the rate constant for reaction between CCl and 2,3-dimethyl-2-butene does not appear to deviate from the linear correlation,so therefore the deviation for CBr may be result of steric factors influencing the reaction and not an experimental artifact. The experimental rate constants for reaction of CBr and CCl with 2,3-dimethyl-2-butene are relatively uncertain due to significant scatter in the data (see Fig III-19d). The reported value for the rate constant for the reaction of CCl with 1,3 cyclohexadiene deviates significantly from the log k_2 vs I.P. correlation. This may be a result of the experimental conditions or the effect of conjugation of the π system. It must be pointed out that these linear free energy correlations must be used with caution and may be valid only for a single structural series since conjugated olefins may not correlate with monolefins. For example for the reaction of $S(^3P)$ with unsaturates, the measured activation energy for reaction with 1,3-butadiene was higher than that expected from the ionization potential (161).

It should be mentioned that electrophilic reactivity has been shown in numerous cases to be caused by variations in the activation energy of the reaction rate constant. Therefore a more meaningful correlation has the form E_a vs I.P. which translates into log k_2 vs I.P. only if the preexponential factors within the series have constant values.

The reactivity trend with alkyl substituted alkenes firmly establishes halomethylidynes as electrophilic reagents and therefore puts

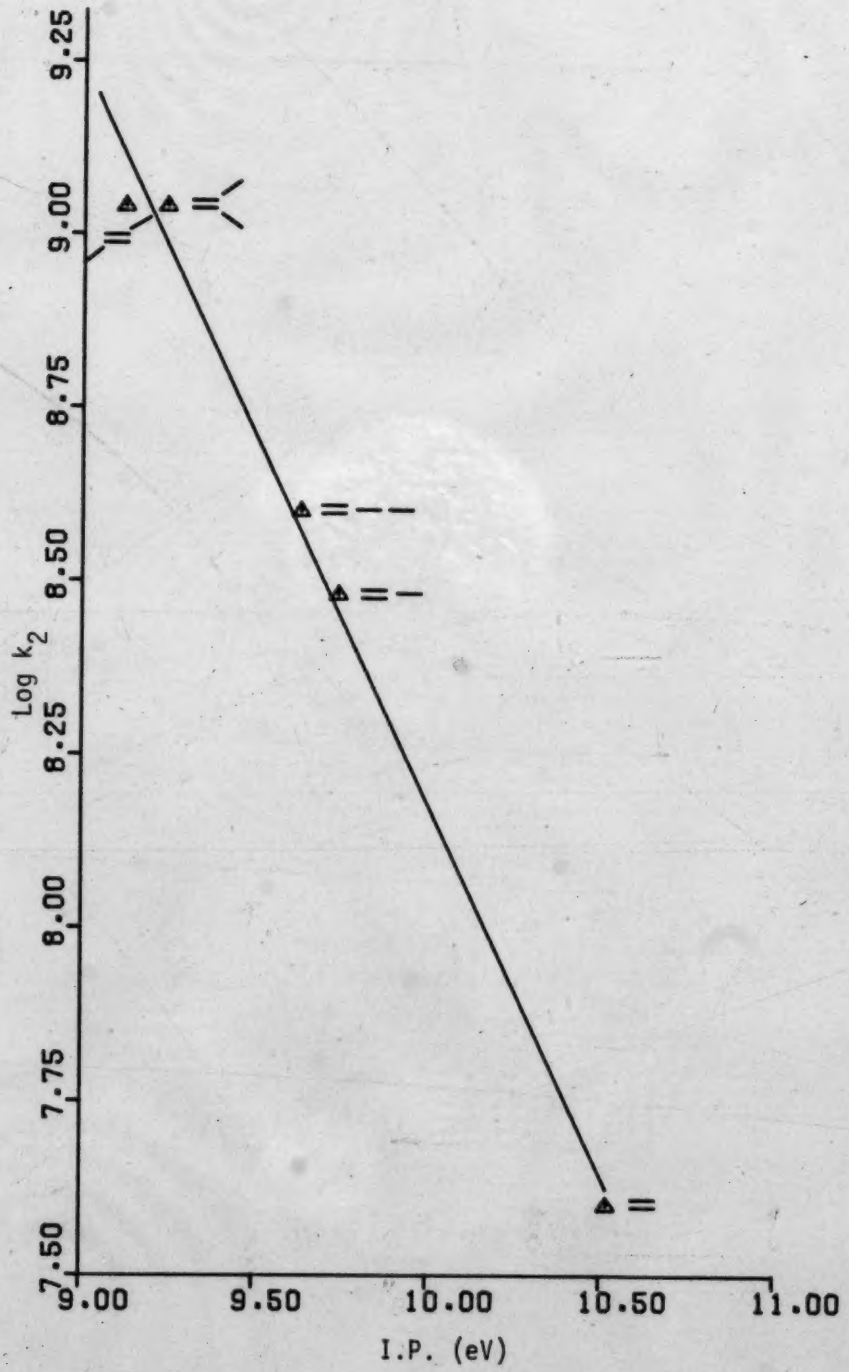

Fig. IV-1. Log k_2 vs Ionization Potential of Alkene for Reaction of CF with Alkenes.

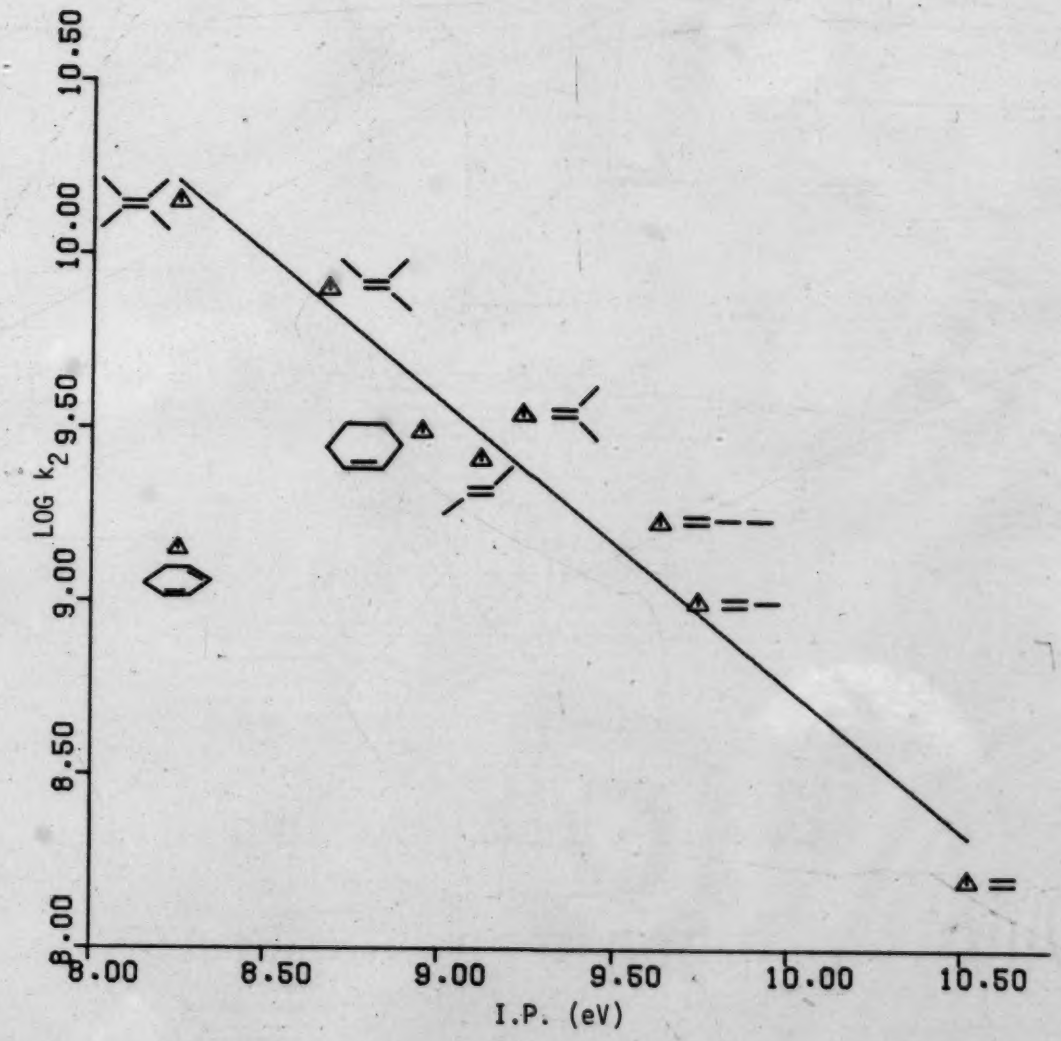

Fig. IV-2. Log k_2 vs Ionization Potential of Alkene for Reaction of CCl with Alkenes.

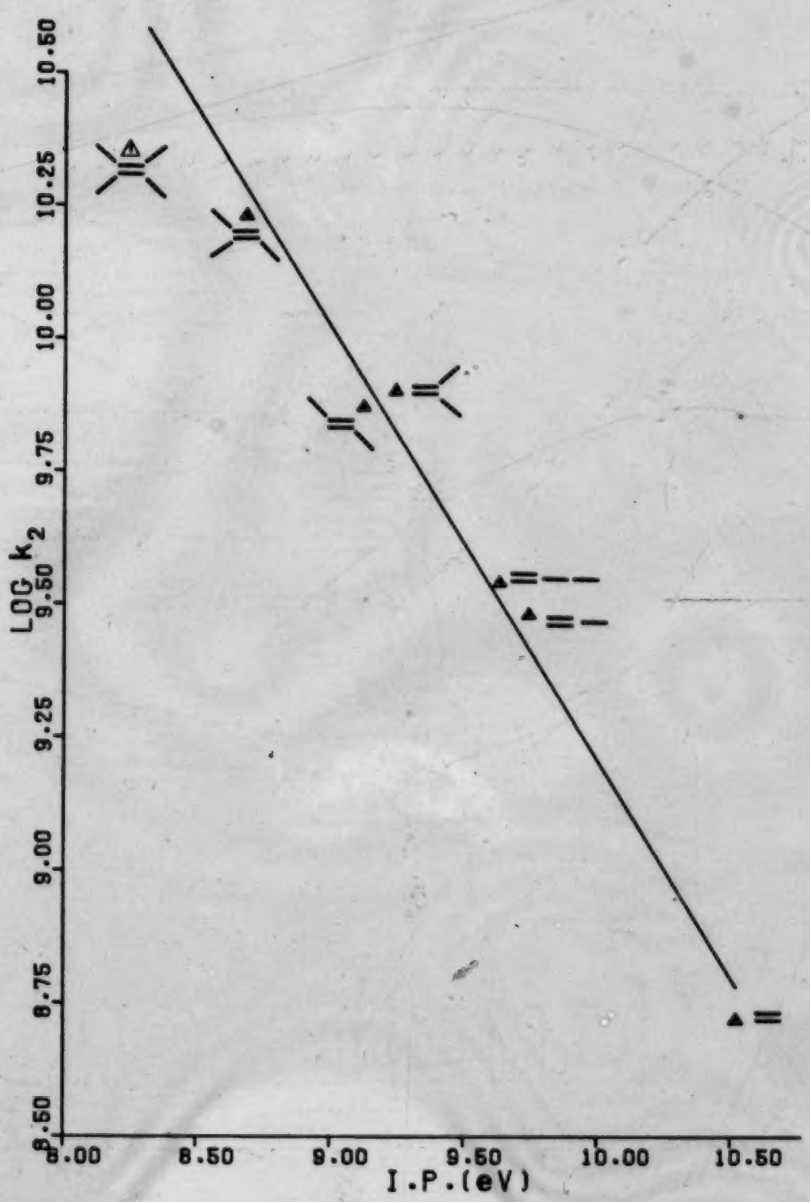

Fig. IV-3. Log k_2 vs Ionization Potential of Alkene for Reaction of CBr with Alkenes.

them in the same category as a number of other reactive species. These include carbenes, Group VI A atoms, halomethyl radicals and various other radicals such as $Br(^2P)$, NF_2, $OH(X^2\Pi)$ and $C_3(^1\Sigma_g^+)$. This group contains two types of radicals, one electron deficient species such as halomethyl radicals, Br, NF_2 and OH and two electron deficient species such as carbenes and Group VI A atoms. It is naturally of interest to determine whether these electrophilic radicals react with alkenes <u>via</u> similar or different mechanisms and how the reaction of three electron deficient halomethylidynes would compare. Therefore it will be instructive to review the currently accepted theories of these reactions to obtain further insight on the halomethylidyne reaction.

Carbene reactions will be summarized first. The characteristic reaction of carbenes with alkenes is addition to yield cyclopropanes. Singlet methylene adds to double bonds in a stereospecific mechanism and triplet methylene addition is non-stereospecific (60). The observation of electrophilic, stereospecific addition of dihalomethylenes to alkenes led to the deduction of singlet ground state for the dihalomethylenes (166). The electrophilicity of their addition to alkenes was represented by the imposition of a positive charge on the alkenic carbons in the intermediate complex or transition state.

(I) 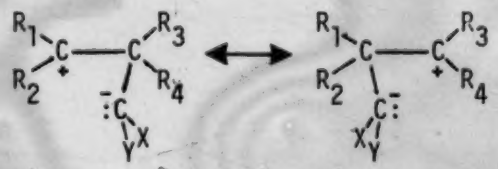 (II)

That neither structure I nor II has overriding importance is recognized by the fact that isobutene has roughly the same reactivity as cis and trans-2-butene. Therefore the generalized transition state for singlet

carbene addition to olefins is represented as a loose charge transfer structure dominated by the interaction of the alkenic π bond with the empty p orbital of the carbene.

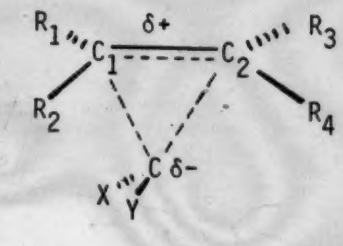

Carbene substituents will affect the alkene addition in two ways. First, stabilization of the carbene by resonance structures shown below

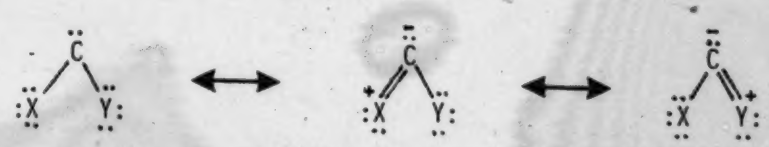

will change the reaction exothermicity. Second, the substituent will affect the energy and position of the transition state along the reaction coordinate. The reaction coordinate is suggested by calculations to consist of a two phase approach (167). The approach to alkenes occurs in an electrophilic fashion (π approach) maximizing overlap between the filled π orbital of the alkene with the vacant p orbital of the carbene. Ab initio calculations indicate that the carbene first approaches the center of the bond and only later veers towards one carbon (167). In all calculated transition states the carbene is off center. At shorter distances, the carbene moves towards one of the ethylene carbons in a so called 'nucleophilic' phase in which the carbene lone pair becomes involved in bonding (σ approach). It is suggested that unselective carbenes have

'early' (π approach) transition states of low energy because the carbene is only slightly stabilized by the substituents while selective carbenes have 'late' (off center σ approach) transition states of higher energy because the carbene is significantly stabilized by the substituents (167).

It is obvious that these features of singlet carbene addition to alkenes are very similar to the measured reactivities of halomethylidynes with alkenes. Therefore it is expected that halomethylidynes add to alkenes in a stereospecific mechanism to yield the cyclopropyl radical as the primary product. The reaction

is expected to be highly exothermic. However, the ΔH_f values of the halocyclopropyl radicals are unknown so the reaction exothermicities cannot be calculated. Nevertheless, the halocyclopropyl radicals formed are expected to be highly excited and may undergo rearrangements and decompositions. This is illustrated below for the reaction of CF with ethylene.

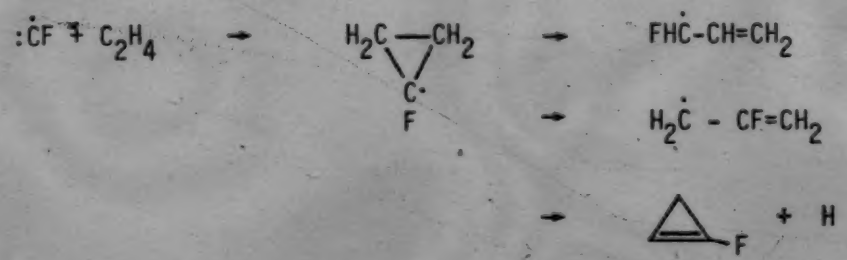

In the photolysis of mercury bisdiazoacetate, the cyclopropyl radicals formed were reported to come from the carbethoxymethylidyne

addition and this addition was stereospecific as is expected for carbyne reactions (95).

In a further analogy to singlet carbenes, the large reaction exothermicity for halomethylidyne addition to alkenes should result in early (π approach) transition states of low energy. Stabilization of the carbyne by the halogen substituent would result in higher activation energies for the reaction suggesting that the measured rate constants decrease in the order CBr > CCl > CF due to increasing activation energy. Therefore, the generalized transition state for the addition of halomethylidynes to alkenes can be drawn as follows.

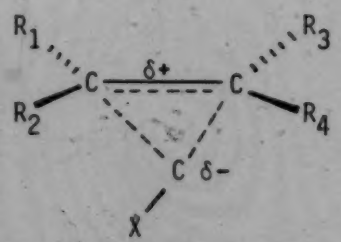

The correlation between log k_2 and alkene ionization potential is evidence for this transition state. This correlation also exists for the reaction of singlet carbenes, triplet oxygen and sulfur, $O(^3P)$ and $S(^3P)$ and hydroxyl radical, $OH(X^2\Pi)$, with alkenes.

Triplet oxygen atoms react with olefins to give the epoxide and its isomeric carbonyl structures, aldehydes and ketones in varying proportions as well as some fragmentation depending on experimental conditions (168). These rearrangements are due to the thermochemistry. Oxygen forms strong single and double bonds resulting in a large exothermicity for the reaction.

Triplet sulfur reactions result in only one product, the episulfide (169). This is due to the weaker bonding properties of sulfur resulting in an exothermic reaction of smaller magnitude.

The addition of triplet sulfur to olefins was found to be completely sterospecific while the stereospecificity of the oxygen reaction was found to be temperature dependent. Determination of the activation parameters showed the change in activation energy was responsible for the electrophilic trend and these activation energies could be correlated with the alkene ionization potential (169,170).

Therefore the reactivities of triplet oxygen and sulfur atoms with alkenes are characterized by the same features as singlet carbene reactions. For oxygen and sulfur additions, the accepted mechanism is that the triplet atom + alkene reactants correlate with the triplet excited state of the product epoxide and episulfide respectively in an exothermic reaction. The transition state can be drawn as below

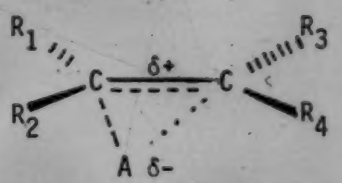

'triplet'

For carbenes, it was suggested that substituent stabilization was the major factor influencing reactivity by variations in the activation energy. For $O(^3P)$ and $S(^3P)$ additions, the experimentally determined activation energies are very close (1.4 kcal $mole^{-1}$ for oxygen and 1.6 kcal $mole^{-1}$ for sulfur addition to ethylene) (170,171). These low values of the activation energies imply 'early' (π approach) transition

states.

The hydroxyl radical, $OH(X^2\Pi)$, reacts with alkenes predominantly *via* addition to form the radical adduct. Absolute rate constants follow an electrophilic trend and the experimentally determined activation parameters indicate the activation energy to be constant, ~ -1.0 kcal mole, for all olefins studied and the preexponential factors increase to account for the electrophilic reactivity (172). These measurements are at variance with the observation that activation energy changes account for electrophilic reactivity.

There are two important features of the electrophilic reactivity of OH. First, the hydroxyl radical reaction rate constant with ethylene is found to be pressure dependent while for $O(^3P)$ no pressure dependence is found (172). The reason for this is due to the thermochemistry of the reaction systems. For $O(^3P)$, the highly energetic addition products can fragment to products other than the initial reactants or be collisionally stabilized whereas for $OH(X^2\Pi)$, fragmentation of the adduct to products other than the initial reactants is thermochemically unfavorable and collisional stabilization of the adduct competes with decomposition back to initial reactants. For $O(^3P)$ reactions the effect of pressure is to alter the product distribution while for $OH(X^2\Pi)$ the effect of pressure is to alter the reaction rate constant. The second feature is that the high pressure limit room temperature rate constants for $OH(X^2\Pi)$ reactions with alkenes are significantly higher than the corresponding $O(^3P)$ reactions (173). The reason for this is the difference in the activation energy. This suggests that the reaction mechanism for OH addition to alkenes differs from that of $O(^3P)$.

The effect of these features on the halomethylidyne reactivity must be assessed. The reaction rate constants were all determined at the same pressure and the effect of pressure was not measured. Perhaps the differences in rate constants between the halomethylidynes are due to different pressure dependencies. This explanation can be discounted for two reasons. First, the measured rate constant for the reaction of CCl with ethylene agrees very closely with the value reported by Wampler et al (127) who observed no pressure dependence between 5 and 100 torr of Argon. Second the relative reactivities of CF, CCl and CBr remain approximately the same for five alkenes. It was found that the OH reaction with propylene and higher alkenes had no pressure dependence (172).

It was suggested that the increase in rate constant between CF, CCl and CBr for the reaction with alkenes was due to the increase in the stability of the halomethylidyne causing the activation energy to decrease. Therefore the investigation of the activation parameters of the reactions of halomethylidynes with alkenes was undertaken.

E. Temperature Dependence of the Reactivity of CBr with Alkenes

The activation parameters have been measured for the reaction of CBr with isobutane, ethylene, trans-2-butene and 2,3 dimethyl-2-butene. The data for the alkene reactions are listed in Table IV-2 along with other rate parameters for similar radical additions to alkenes.

The values of the rate constants for iso-butane suggest that reaction of CBr with the C-H bond in alkenes is unimportant for all temperatures and the activation parameters determined for alkenes are

Table IV-2. Activation Parameters for Radical Addition to Alkenes*

Substrate	$CBr(X^2\Pi)^a$		$O(^3P)^b$		$S(^3P)^c$		$OH(X^2\Pi)^d$		$PhCCl_3^e$	
	E_a	A	E_a	A	E_a	A	E_a	A	E_a	A
Ethylene	-0.6	0.2	1.4	5.3	1.6	7.9	-0.8	1.0		
Propylene			0.33	4.9	0.45	8.3	-1.1	2.5		
1-Hexene									1.1	0.024
t-2-Butene	-1.0	2.7	-0.02	14			-1.1	6.7		
c-2-Butene			-0.27	6.7	-0.2	2.8	-0.97	6.3		
t-2-Pentene									1.0	0.054
2-Methyl 2-butene							-0.90	11.4	-0.77	0.044
2,3-Dimethyl 2-butene	-1.9	1.7	-1.1	8.1	-1.3	4.9			-1.7	0.019

* E_a (kcal $mole^{-1}$) A (x 10^{-9} $M^{-1}sec^{-1}$)

a - this work

b - ref. 171

c - ref. 170

d - ref. 172

e - ref. 174 (activation parameters determined in solution)

for the reaction with the π bond. The main features for this reaction are a negative activation energy for all three alkenes and curvature in the Arrhenius plot for 2,3-dimethyl-2-butene (see Fig III-22a)

Negative activation energies for a gas phase bimolecular reaction were first determined for the reaction of $Te(^3P)$ with 2,3 dimethyl-2-butene (175). Activation parameters determined for the reaction of $O(^3P)$ and $S(^3P)$ with alkenes show that the activation energies become negative when the ionization potential of the alkene becomes low enough (170). For the reaction of $OH(X^2\Pi)$ with alkenes, all activation energies determined are negative (172). There have been various explanations given for this phenomenon of negative activation energy.

The explanation for the negative temperature dependence of the reactions of Group VI A atoms with some alkenes was considered in terms of crossing of potential energy surfaces. It was proposed that the atom and olefin initially approach on a potential energy surface with a shallow minimum. The repulsive part of this surface intersects with an attractive potential surface and the rate of the reaction would be determined by the following parameters:

a) the position of the intersection of the two surfaces relative to the zero level of the separated reactants;

b) the number of internal degrees of freedom in the reaction complex;

c) the temperature dependent probability of crossing of the system between the two surfaces.

The positive temperature dependence of the ethylene reaction can be explained by a crossing occurring at an energy above that of the

the separated reactants and the negative temperature dependence of the 2,3-dimethyl-2-butene reaction, by a crossing at an energy below that of the seperated reactants. This is qualitatively illustrated in Fig.IV-4.

Another possible interpretation of the phenomenon has been offered based upon transition state theory (172). The radical addition to alkenes is viewed as a bimolecular process with zero or near zero activation energy. In this case, the temperature dependence of the rate constant is determined by the temperature dependence of the preexponential factor which is given from transition state theory by,

$$A = \tau \left(\frac{\kappa T}{h}\right) \frac{Q^{\ddagger}_{R\text{-alkene}}}{Q_{alkene}\, Q_R}$$

where τ is the transmission coefficient

$\frac{\kappa T}{h}$ is the frequency factor

Q is the partition function

R is the radical

For the reaction of the hydroxyl radical with alkenes, the preexponential factor becomes,

$$A \alpha \left(\frac{Q^{\ddagger}_{OH\text{-alkene}}}{Q_{alkene}}\right) T^{-3/2}$$

because for the OH radical the vibrational partition function will be approximately unity over the temperature range studied and the translational and rotational partition functions have temperature dependencies of $T^{3/2}$ and T^{1} respectively. Hence, if the ratio of the partition function of the transition state over the partition function of the alkene, $(Q^{*}_{OH\text{-alkene}}/Q_{alkene})$, is temperature independent, then A varies as

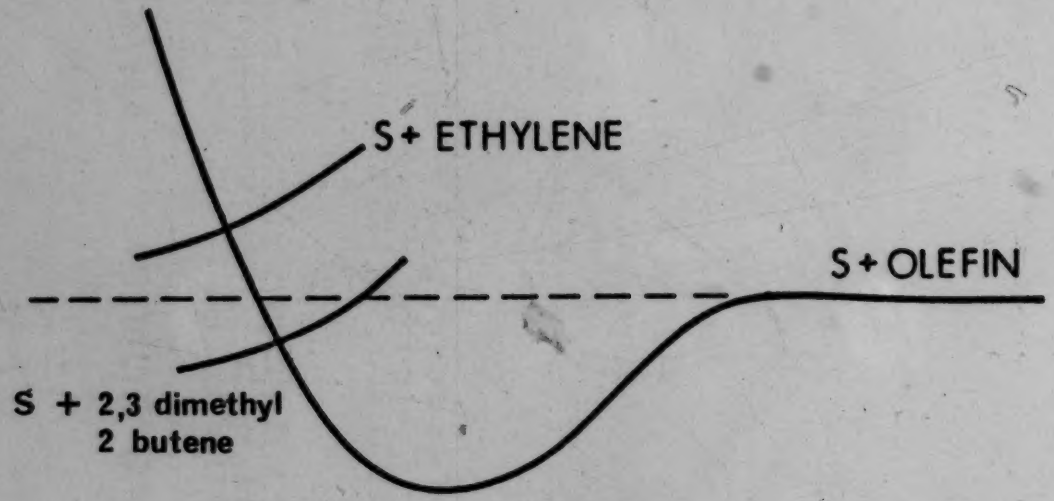

Fig. IV-4.Qualitative Depiction of Curve Crossing for Positive and Negative Temperature Dependence. (ref. 170)

$T^{-3/2}$. For zero activation energy, the rate constants will also vary as $T^{-3/2}$ as is experimentally determined over a temperarure range of 297-425°K for the reactions of $OH(X^2\Pi)$ with alkenes (172). The assumption of ($Q^{\ddagger}_{OH\text{-alkene}}/Q_{alkene}$) being temperature independent implies a very loose transition state.

However, for the reactions of $O(^3P)$ with alkenes, more thorough and detailed studies based on the same approach did not support the above explanation (176). It was shown that inclusion of two new vibrational frequencies, due to the oxygen-alkene bond, in the partition function of the transition state could account for some, but not all, of the features of the Arrhenius plots. In particular a negative activation energy had to be invoked for the $O(^3P)$ + 2,3-dimethyl-2-butene reaction.

There is now a widely accepted interpretation for the phenomenon of negative temperature dependence for bimolecular reactions, which is, that the reaction under investigation is multistep and involves at least one intermediate that possesses at least two channels for reaction(174, 176,177). The possible mechanism for radical addition to alkenes can be written as follows.

$$R + \text{alkene} \underset{k_{-1}}{\overset{k_1}{\rightleftharpoons}} \text{intermediate} \xrightarrow{k_2} \text{products}$$

If it is assumed that there is an equilibrium between the reactants and the intermediate and that the second step is the rate determining step, then the observed rate is;

$$-\frac{d[R]}{dt} = \frac{k_2 k_1}{k_{-1}} [R] [\text{alkene}]$$

and the observed activation energy is $E_{obs} = E_1 + E_2 - E_{-1}$. If E_1 is considered to be zero, then a negative activation energy arises when $E_2 < E_{-1}$.

This is a simplified kinetic description of the surface crossing mechanism illustrated in Fig. IV-4. The energy barriers can be drawn on these curves to show the relationship as below.

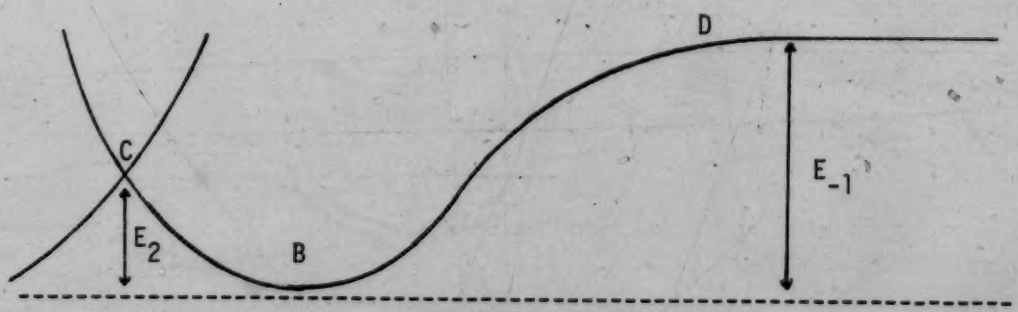

To satisfy the relations, $k_{-1} >> k_2$ and $E_{-1} > E_2$, the relationship between the A factors must be $A_{-1} >> A_2$. The transition state to form the products, point C, must be more constrained than the configuration of reactants at point D. However for the reaction of singlet carbenes, halomethylidynes, Group VIA atoms and the hydroxyl radical with alkenes, the transition state is concluded to be loose resulting in high A factors. Therefore, in order to satisfy the relation $A_{-1} >> A_2$, A_{-1} must be very high, close to the collisional frequency. Also the rate constant to form the intermediate complex, k_1, must be close to the

collision frequency.

This kinetic description can also be used to explain the observed curvature in the Arrhenius plot for the reaction of CBr with 2,3-dimethyl -2-butene which has also been observed for the reaction of phenylchlorocarbene with the same alkene in solution(174). In solution the rate constant k_1 was equated to the diffusion constant which could be calculated. At high temperature in this mechanism, k_2 is the rate determining step and a negative temperature dependence will be observed. However, if the temperature decreases sufficiently, the diffusion rate constant, k_1, will become the rate determining step and since it has a positive temperature dependence, curvature in the Arrhenius plot will result.

The same idea can be applied with some modification to the reaction of CBr with 2,3-dimethyl-2-butene in the gas phase. The rate constant, k_1, can be calculated by assuming a certain fraction of collisions result in the intermediate complex. The equation for k_1 is:

$$k_1 = p \sigma L \left(\frac{8 \kappa T}{\pi \mu} \right)^{1/2}$$

where p = steric factor; L = Avogadro constant

σ = collision cross section; μ = reduced mass of reactants

κ = Boltzmann constant

The value of k_1 will depend upon the value for $p\sigma$, the reactive cross section. By choosing an appropriate value for $p\sigma$, a temperature dependence for k_1 can be calculated which fits the experimental Arrhenius curve at low temperature. In other words the observed rate

constant k_{obsd}, is approximated by k_1 at a sufficiently low temperature as shown in Fig. IV-5. In this figure k_1 was calculated using $p\sigma$ = 0.16 nm^2. From this value p may be obtained since the collision cross section can be calculated by using rough estimates for the molecular diameter of CBr and 2,3-dimethyl-2-butene; R(CBr) = 0.40 nm and $R(C_6H_{12})$ = 0.60 nm (178). From this calculation a steric factor p = 0.05 is calculated.

The nature of the carbyne/alkene intermediate is not revealed by the kinetics however. A structure that is consistent with the proposed reaction mechanism is one in which the π electrons of the alkene interact with the π^* orbital of the carbyne resulting in the formation of a loose charge-transfer complex.

In summary the negative temperature dependence of the reaction of bromomethylidyne with alkenes is postulated to be due to the formation of an intermediate complex which via curve crossing will convert to products. These complexes are very weakly bound and of the charge transfer type. This kinetic model is in agreement with the suggested reaction mechanism for the addition of halomethylidynes to alkenes via loose ('π approach') transition states. Ab initio calculations on the reaction of CH with ethylene suggested asymmetric addition would proceed with zero activation energy (179).

F. Reaction of CBr with Alkynes

The rate constants determined for the reaction of CBr with alkynes are listed in Table IV-3 along with values for CH, CCl, $O(^3P)$, $S(^3P)$ and OH. It is seen from this table that the reagents $CBr(X^2\Pi)$, $CCl(X^2\Pi)$,

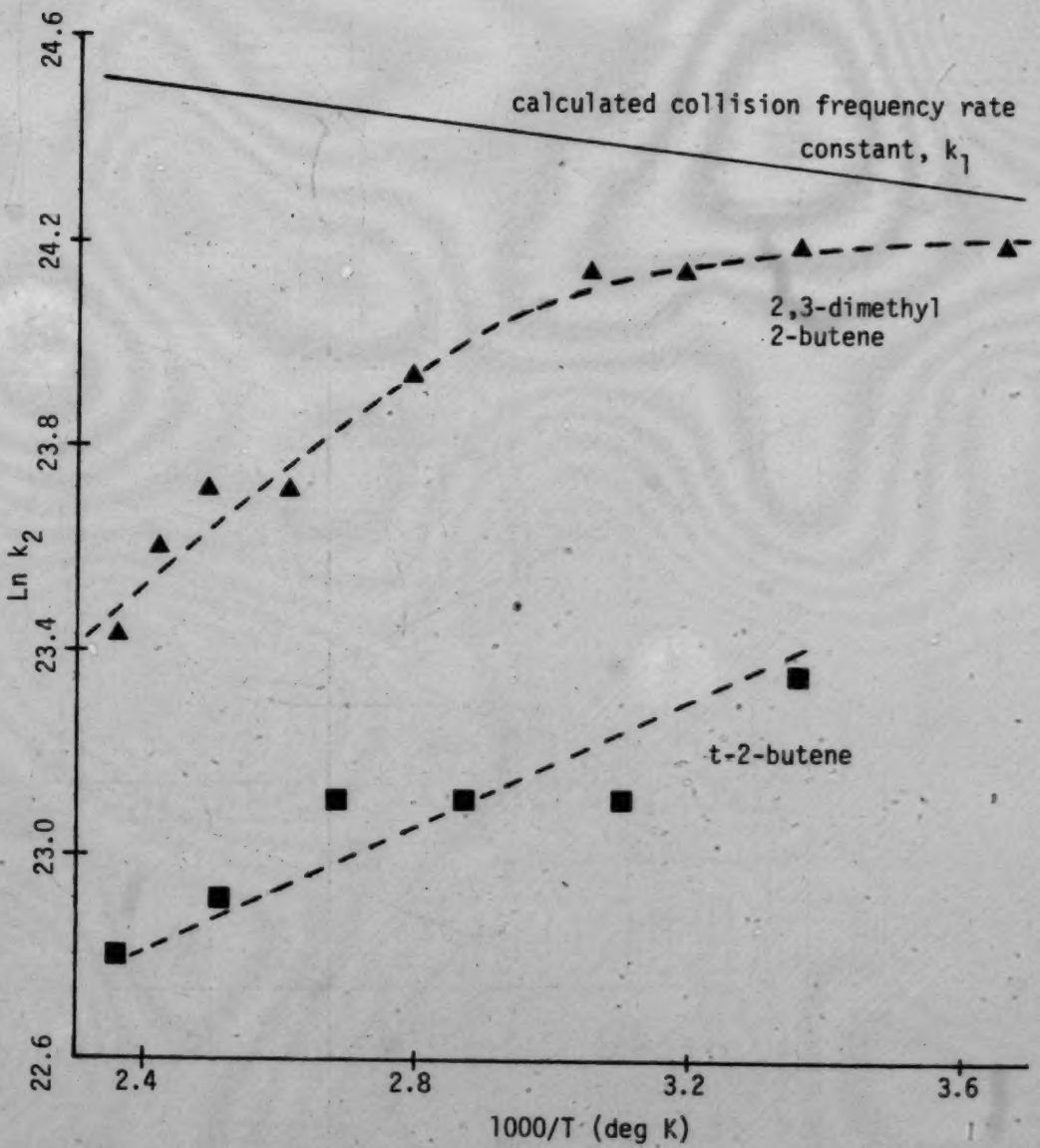

Fig. IV-5. Arrhenius Plots for Reaction of CBr with t-2-butene and 2,3-dimethyl-2-butene.

Table IV-3. Rate Constants for the Reactions of Radicals with Alkynes

Substrate	$k_2 \times 10^{-9}$ $M^{-1}sec^{-1}$					
	$CH(X^2\Pi)$[a]	$CCl(X^2\Pi)$[c]	$CBr(X^2\Pi)$[e]	$O(^3P)$	$S(^3P)$[j]	$OH(X^2\Pi)$[k]
Acetylene	130±20 45±7[b]	0.035±0.004 0.11±0.01[d]	0.081±0.007	0.079[f]	0.23±0.05	0.41
Acetylene-d_2			0.07±0.02	0.094[f]	0.23±0.03	
Propyne	280 90	2.2±0.2 2.4±0.2[d]	4.8±0.6	0.54[g]	4.8±0.2	0.57
1-Butyne		3.7±0.5	6.2±1.1	1.2[h]	3.3±0.2	
2-Butyne		18±3	24±5	2.9[i]	16±2	
1-Pentyne		4.3±0.7	3.6±0.8			
2-Pentyne		25±4	20±3		18±3	
3,3-Dimethyl 1-butyne		2.4±0.3				
2,2,5,5-Tetramethyl 3-hexyne		7.6±0.7	9.7±1.6			
2-Butyne-F_6			0.020±0.002		0.21±0.04	

a - ref. 79
b - ref. 83
c - ref. 53,54b
d - ref. 56
e - this work
f - ref. 180,181
g - ref. 182
h - ref. 183
i - ref. 184,185
j - ref. 186
k - ref. 172

$O(^3P)$ and $S(^3P)$ exhibit a distinct electrophilic character in the sense that their reactivity increases with the number of alkyl substituents and decreases with fluoroalkyl substituents attached to the acetylinic carbon. Comparison of the rate constant for reaction with acetylene for CH, CCl and CBr shows that the CH reaction is 2 to 3 orders of magnitude faster than those of CCl and CBr. This is the expected pattern in reactivity based upon the previous discussion of the electrophilicity of carbynes and parallels the trend observed for the reaction with ethylene. For all alkenes CBr was found to be more reactive than CCl (see Table IV-3). For alkynes this trend seems only to hold for less substituted substrates. The more substituted alkynes do not seem to be able to discriminate between CCl and CBr.

A plot of log k_2 vs ionization potential of the alkynes for CCl and CBr shows a good linear correlation providing additional evidence for the electrophilic nature of these reactions (Figs. IV-6,7). The values for 2,2,5,5 -tetramethyl-3-hexyne clearly deviate from the linear correlation for both CCl and CBr. This effect may be caused by steric hindrance or photolysis of the alkyne as discussed before. However the evidence from the alkene reactions and activation parameters suggests that steric hindrance causes the deviation.

A comparison between the reactivities of CCl and CBr with alkynes and alkenes reveals that, in general, alkynes appear to be somewhat more reactive than alkenes with the exception of acetylene which is 5-6 times less reactive than ethylene towards CCl and CBr. Determination of the activation parameters of the reactions of $O(^3P)$, $S(^3P)$ and $OH(X^2\Pi)$ reactions with alkenes and alkynes shows that both the

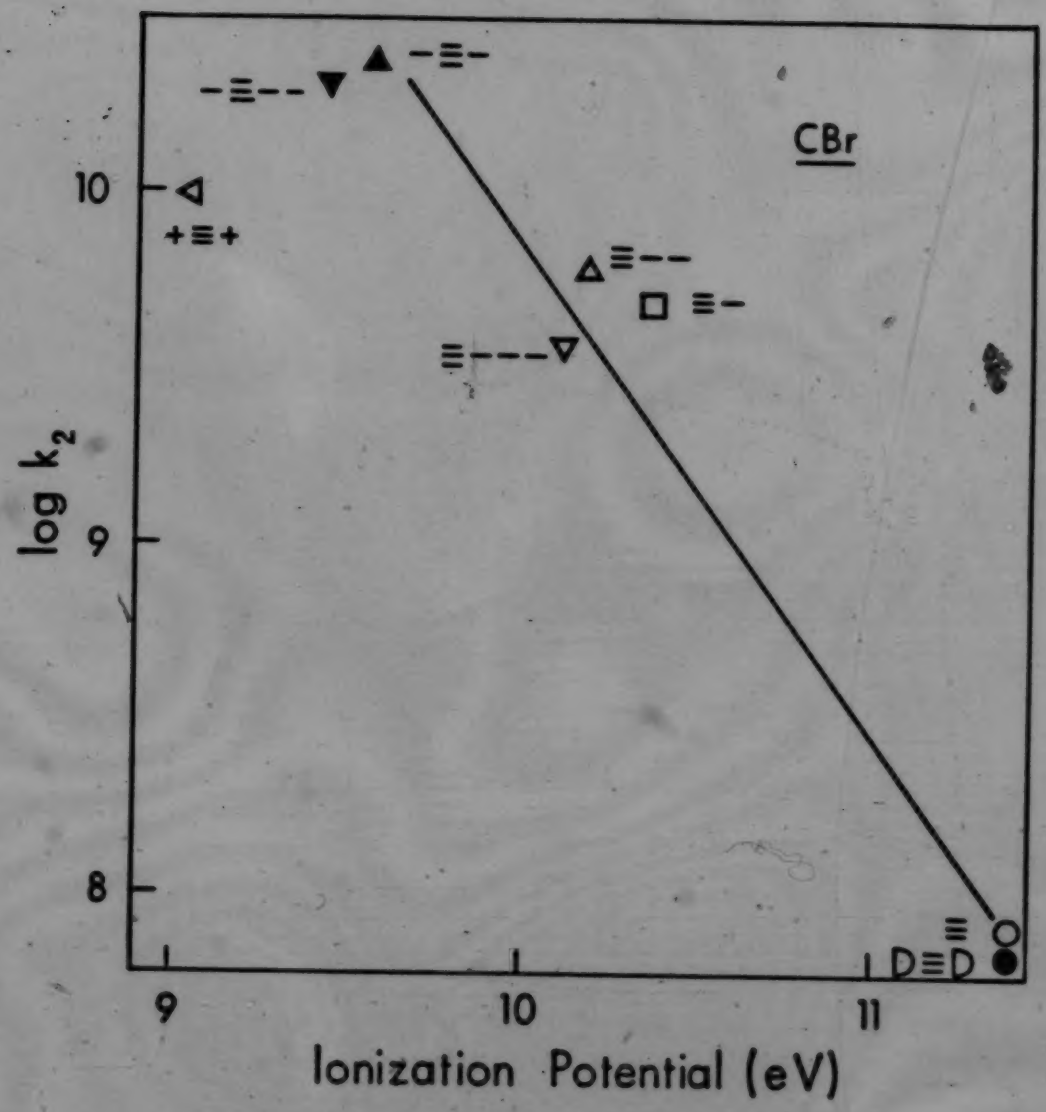

Fig. IV-6. Log k_2 vs Ionization Potential of Alkyne for Reaction of CBr with Alkynes.

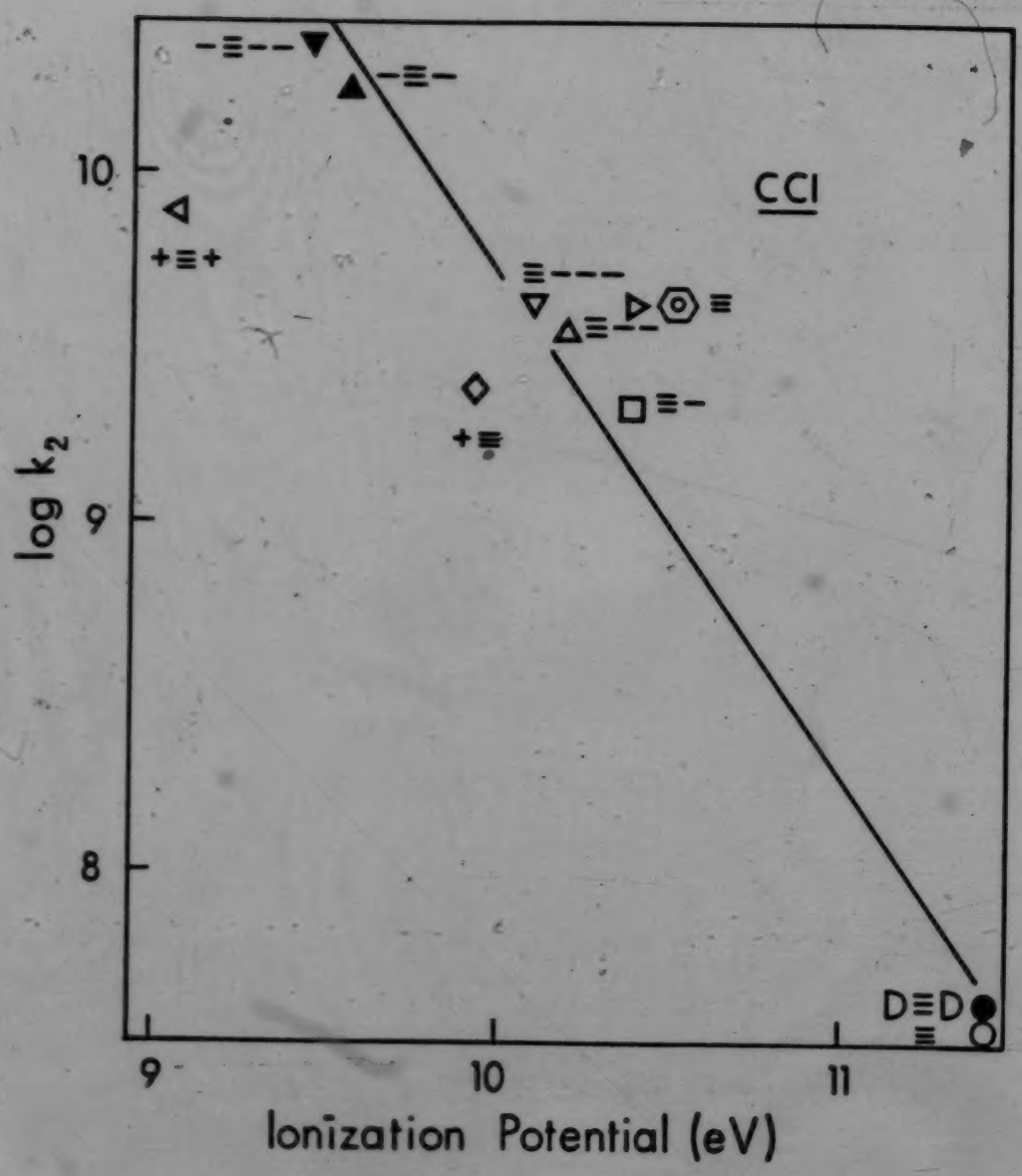

Fig. IV-7. Log k_2 vs Ionization Potential of Alkyne for Reaction of CCl with Alkynes. (ref. 53)

activation energy and A factors increase for alkynes compared to alkenes (186,172). The increase in the activation energy is proposed to be due to the ionization potential differences of the substrates (169). The increase in the A factors was attributed to the gain of entropy in going from a linear acetylenic molecule to a non-linear activated complex (186). Alkynes react more slowly than alkenes with $O(^3P)$, $S(^3P)$ and $OH(X^2\Pi)$, therefore the increase in activation energy is the dominant factor influencing these reactions. By analogy it is proposed that an increase in activation energy is responsible for the lower reactivity of CCl and CBr towards acetylene compared to ethylene whereas an increase in A factors accounts for the greater reactivity of substituted alkynes compared to alkenes.

The reaction products of halomethylidynes with alkynes are expected to be similar to those postulated for the alkene reaction. The reaction should yield the cyclopropenyl radical which may rearrange to the allenyl radical.

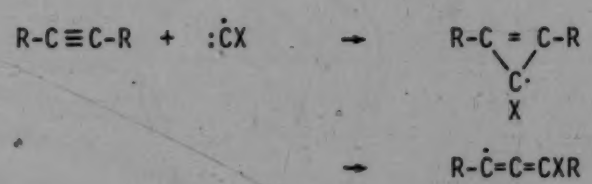

The transition state is proposed to be similar to that of addition to alkenes as shown below.

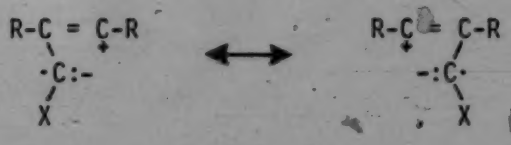

The lower reactivity of acetylene can be explained by noting that this transition state has unfavorable vinyl cation character.

Singlet carbenes undergo electrophilic concerted addition to acetylenes to form the cyclopropenes and relative reactivity studies indicate that cycloaddition to alkenes is favored over the alkyne reaction (2). This observation reinforces the carbene-carbyne relationship. For the reactions with alkynes, $O(^3P)$ and $S(^3P)$ are postulated to have unique reaction mechanisms involving the formation of triplet carbenes as the primary products. For oxygen the reaction

$$O(^3P) + R\text{-}C{\equiv}C\text{-}R \rightarrow R\text{-}\ddot{C}\text{-}\overset{O}{\overset{\|}{C}}\text{-}R \ (T_o)$$

$$S(^3P) + R\text{-}C{\equiv}C\text{-}R \rightarrow R\text{-}\ddot{C}\text{-}\overset{S}{\overset{\|}{C}}\text{-}R \ (T_o)$$

products are CO, alkenes and unsaturated ketones formed in pressure dependent yields as well as polymer (187,188). For sulphur the reaction products are carbon disulphide, benzene and thiophene derivatives as well as polymer (186).

G. Absorption Spectra of $SiCl_2$ and $SiBr_2$

1) Dichlorosilylene , $SiCl_2$

The absorption spectrum shown in Fig III-24 and assigned to $SiCl_2$ is a broad band with vibrational structure and an absorption maximum at 317 nm. Previously observed absorption bands, recorded at high temperature (133) and in a low temperature matrix (134), were structureless with the same absorption maximum. The emission spectrum of $SiCl_2$ was reported to occur from the discharge through $SiCl_4$(125). This emission spectrum was structured and reported to result from

emission from two upper states of $SiCl_2$. The energies of these two upper states were given as 29952 and 28295 cm^{-1} above the ground state, $^1A_1$. The upper state at 29952 cm^{-1} is thought to be $^1B_1$ (123). The vibrational analysis of this transition, $^1B_1 - {}^1A_1$, seen in the emission spectrum, gave the following vibrational frequencies.

$v_1'' = 540\ cm^{-1}$ $\qquad$ $v_1' = 445\ cm^{-1}$

$v_2'' = 248\ cm^{-1}$ $\qquad$ $v_2' = 201\ cm^{-1}$

However these values for the ground state vibrational frequencies do not agree well with infrared spectrum of matrix isolated $SiCl_2$ which gave $v_1'' = 513\ cm^{-1}$ and $v_2'' = 202\ cm^{-1}$ (134,135).

The spectrum of $SiCl_2$ observed in this work is easily analyzed in terms of a single progression with an interval of 148 cm^{-1}. Based on the observation that the absorption spectra of CF_2(31), CBr_2(189), SiF_2(132), GeF_2(190), $GeCl_2$(191) and SnF_2(192) are all dominated by a progression in v_2', the measured interval of 148 cm^{-1} is assigned to the bending frequency, v_2', of the upper state, $^1B_1$. Numerical assignment of each level is not possible without further information. However a tentative assignment of each vibrational transition may be made by analogy. For the above mentioned Group IVA dihalides, the most intense absorption occurs for the transition to $v_2' = 5$ level for CF_2 and SiF_2, to the $v_2' = 9$ level for $GeCl_2$ and GeF_2 and to the $v_2' = 6$ level for SnF_2 Therefore the most intense absorption band observed in this work for $SiCl_2$ ($\lambda = 317.66$ nm) is assigned to the $^1B_1(0,8,0) - {}^1A_1(0,0,0)$ transition with an error of ±1 in the assignment. This

results in an electronic energy of the upper state of $SiCl_2$ ($^1B_1$) of $T_o = 30295 \pm 150\ cm^{-1}$.

2) Dibromosilylene, $SiBr_2$

In the photolysis of $SiBr_4$ an absorption band occurs in the region 340-400 nm. Under adiabatic conditions the intensity is high but the intensity is strongly quenched upon addition of buffer gas. The spectrum does not correspond to the known spectra of SiBr or Br_2. The electronic absorption spectra of $SiBr_3$ and $SiBr_2$ are unknown and it is probable that the absorption is due to one of these species. The absorption spectrum observed in this work is assigned to the $^1B_1 - {}^1A_1$ transition of $SiBr_2$ based upon analogy with the observed spectra of Group IV A difluorides and dichlorides other than carbon (see Table IV-4). The electronic energies of the upper states of Si, Ge, Sn and Pb difluorides have roughly the same value and this relationship occurs for the analogous dichlorides as well. Therefore it is postulated that the electronic energies of the upper $^1B_1$ states of Si, Ge, Sn and Pb dibromides are approximately equal. The observation of an absorption for $SnBr_2$ at 27400 cm^{-1} (193) agrees very well with the value of 27600 cm^{-1} observed in this work for $SiBr_2$.

The only report on the electronic spectrum of $SiBr_2$ in the literature mentions that an emission in 425-595 nm region from a glow discharge in $SiBr_4$ vapor may be due to the $SiBr_2$ spectrum (194). Vibrational analysis of this system gave ground state stretching and bending frequencies of 425 and 120 cm^{-1} which is in reasonable agreement with the assignments from the infrared spectrum of matrix isolated

Table IV-4. Electronic Transitions and Vibrational Frequencies of Group IV A Dihalides. (cm^{-1})

Molecule	$^1B_1$-$^1A_1$	$^3B_1$-$^1A_1$	ν_1"	ν_2"	ν_3"	ν_1'	ν_2'	ν_3'[c]	Ref.
CF_2	36878		1218	668	1110		494		189
CCl_2	17093		726	333	745	626	304		189
CBr_2	14962		595	196	640	468	186	588	189
SiF_2	44109	26310	855	345	872		252		123
$SiCl_2$	30295[a]	22900	512	202	501		148[a]		123
$SiBr_2$	27600[a,b]	20400	402	120	400				135,194
GeF_2	43843			263			164		190
$GeCl_2$	30969	22700		162			95		191
$GeBr_2$			286	110	276				196
SnF_2	40741			180			120		192
$SnCl_2$	31055[b]	22237		120					191
$SnBr_2$	27400[b]		240	83	228				193,197
PbF_2	40560			145			105		192
$PbCl_2$	31000[b]		319	103	296				197
$PbBr_2$			200	64					198

a - assigned from this work

b - energy calculated from band maximum not band origin

c - vibrational frequency of $^1B_1$ state

$SiBr_2$ (195). Moreover emission has been observed from $SiCl_2$, $GeCl_2$ and $SnCl_2$ species which is assigned to a $^3B_1 - {}^1A_1$ transition (171). Therefore it is possible that the reported emission is due to the $^3B_1 - {}^1A_1$ transition of $SiBr_2$.

H. The Photochemistry of Halogenated Silanes

There is a complete analogy between the electronic transitions of silanes and alkanes concerning the originating orbitals as well as the orbitals associated with the excited electron in the lower excited states. Therefore the ultraviolet absorptions of alkyl and fluorine substituted silanes are due to transitions from a bonding σ orbital to intermediate type Rydberg orbitals and there is no evidence for the involvement of 3d orbitals (199). For chlorosilanes, the lone pair electrons of the substituent chlorine have atomic orbital energies sufficiently close to those of the silicon 3d atomic orbitals so that there is partial loss of lone pair character and gain in bonding character of the highest occupied orbital. This is the reason for the increase in bond strength in passing from carbon to the silicon compounds. The UV band of lowest frequency in alkyl chlorides is known to be $n\sigma^*$ where the σ^* orbital is antibonding in the C-Cl bond (199). On the basis of the above argument this band in chlorosilanes $\sigma^* \leftarrow (p\pi)$ is expected to move to higher frequencies. However, this band is not found and most of the bands in these spectra can be attributed as being due to transitions to intermediate Rydberg - valence shell type excited states (199). Therefore the flash photolysis of $SiBr_4$ should

result in excitation to these states which could then dissociate in two ways, bond dissociation and molecular elimination.

			ΔH (kcal mole^{-1})
$SiBr_4$	→	$SiBr_3 + Br$	71
	→	$SiBr_2 + Br_2$	94

Now in the flash photolysis of $SiBr_4$, the spectra of SiBr and $SiBr_2$ are observed. For alkanes photolysis results in Rydberg states which are found to undergo molecular elimination (60). For halogenated methanes, photolysis in the first absorption band is due to a $n\sigma^*$ valence shell transition which results in bond dissociation as discussed previously. Therefore photolysis of $SiBr_4$, which is expected to result in an intermediate Rydberg-valence shell type excited state, should result in both dissociation and molecular elimination. This would be similar to the photolysis of monosilane (124). However, there is also the possibility that $SiBr_2$ is formed by decomposition of $SiBr_3$.

The question also arises, as it did for the halogenated methanes, as to how the monovalent radical, in this case SiBr, is formed. The overall reaction enthalpy is too endothermic,

$$SiBr_4 \rightarrow SiBr + Br_2 + Br \qquad \Delta H = 182 \text{ kcal mole}^{-1}$$

to be caused by photolysis with $\lambda > 165$ nm. Therefore decomposition of a vibrationally excited intermediate is ruled out and secondary photolysis must occur. Either $SiBr_3$ or $SiBr_2$ may be photolyzed

			ΔH(kcal mole^{-1})	Wavelength Requirement
$SiBr_3$	$\xrightarrow{h\nu}$	$SiBr + Br_2$	112	$\lambda < 255$ nm
$SiBr_2$	$\xrightarrow{h\nu}$	$SiBr + Br$	88	$\lambda < 325$ nm

The wavelength cutoff rules out the possibility that the photolysis of $SiBr_2$ in the region 340-400 nm results in dissociation. Therefore SiBr probably arises from secondary vacuum UV photolysis of $SiBr_3$ and/or $SiBr_2$.

The flash photolysis of Si_2Cl_6 results in the absorption spectra of SiCl and $SiCl_2$. The thermal decomposition of Si_2Cl_6 results in $SiCl_4$ and $SiCl_2$ (200). Therefore it is possible that $SiCl_2$ is formed by molecular elimination following photolysis. The absorption band in polysilanes is due to a $\sigma \rightarrow \sigma^*$ transition (201). The photolysis of cyclic and linear permethylated polysilanes results in silylene extrusion (141).

$$(Me_2Si)_6 \xrightarrow{\lambda = 254\ nm} (Me_2Si)_5 + :SiMe_2$$

However, the photolysis of Si_2Me_6 only results in silicon - silicon bond cleavage (202). It is likely then that the photolysis of Si_2Cl_6 results in two primary processes.

$$Si_2Cl_6 \xrightarrow{h\nu} SiCl_4 + SiCl_2$$
$$\xrightarrow{h\nu} 2\ SiCl_3$$

The monovalent silicon radical, SiCl, may arise from secondary photolysis or decomposition of the primary products. The absorption of $SiCl_2$ in the region 300-340 nm will not cause dissociation to form SiCl due to insufficient energy.

$SiCl_2 \rightarrow SiCl + Cl \quad \Delta H = 102\ kcal\ mole^{-1}$ Wavelength Requirement

$\lambda < 280\ nm$

In summary, the photochemistry of halogenated silanes is not well understood due to lack of experimental detail. The flash photolysis of substituted di- and trisilanes appears to offer a method of observing the gas phase absorption spectra of substituted silylenes.

V. SUMMARY AND CONCLUSIONS

This research project investigated the reactivity of halomethylidynes by measuring rate constants for reaction with alkenes and alkynes using the technique of kinetic spectroscopy, and attempted to measure similar rate constants for halosilylidynes. Some new absorption spectra were also observed for dihalosilylene radicals.

The halomethylidynes,CF,CCl and CBr were generated in sufficient concentration for spectroscopic measurements by the flash photolysis of the appropriate halogen substituted dibromomethane, $CHXBr_2$, (X = F, Cl, Br). One carbon - bromine bond is dissociated upon photolysis resulting in a halogenated methyl radical, $^{\cdot}CHXBr$, which undergoes further dissociation resulting in the halomethylidyne radical. This secondary dissociation may be caused by excess vibrational excitation or secondary photolysis and it is unclear to what extent each process contributes to halomethylidyne production.

The concentration of halomethylidyne radicals was monitored by absorption spectroscopy and the decay of the absorption signal was found to be first order in the halomethylidyne.

$$\frac{-d[CX]}{dt} = k'[CX]$$

This observation is in agreement with all other investigations of carbyne reactivity using a variety of techniques. This pseudo-first order decay is believed to be caused by a large excess of radicals relative to the halomethylidyne and their decay is relatively slow compared to that of the halomethylidyne. Introduction of a reactive substrate caused an increase in the pseudo first order decay. Due to

the limitations of the flash photolysis - kinetic spectroscopy technique, only a small increase in the pseudo- first order decay could be measured. From averages of these measurements, the rate constants for halomethylidyne reactions could be determined.

The nature of the reactions of halomethylidynes with alkanes, alkenes and alkynes was deduced on the basis of:

- the variation of the rate constants with substituted alkenes and alkynes;
- the determination of activation parameters for the reactions of CBr with alkenes;
- the reported chemistry of CH and CCO_2Et;
- the prediction that doublet ground state halomethylidynes would display chemical properties analogous to singlet ground state dihalomethylenes.

The halomethylidynes, CF, CCl and CBr, are much less reactive than methylidyne, CH. This is due to the donation of lone pair electrons of the halogen to the carbon through the molecular π orbital. The halomethylidynes are consequently less electrophilic and display selectivity in their reactions with alkanes, alkenes and alkynes.

The reactivity of CCl and CBr with the C-H bond is much less than with the unsaturated C-C bond and this same behaviour is predicted for CF. The reactivity of CCl and CBr with C-H bonds is in the order tertiary > secondary > primary and halomethylidynes are believed to insert into C-H bonds <u>via</u> a polarized transition state.

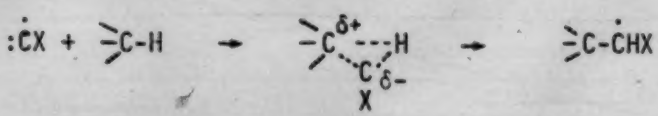

For the reaction of CBr with tertiary C-H bond of 2-methylpropane, the rate constant was determined to be $k_2 = 2 \times 10^9 \exp(-3.9/RT)\ M^{-1}sec^{-1}$.

The rate constants for the reactions of halomethylidynes with alkenes and alkynes range from 10^7 to $10^{10}\ M^{-1}sec^{-1}$. The reactivity series between halomethylidynes for reaction with alkenes is found to be CF < CCl < CBr . This is expected on the basis of the electron donating ability of the halogen and points to the electrophilic nature of halomethylidynes. Further evidence for this is provided by the observation that the rate constant for alkene reaction increases with alkyl substitution for all halomethylidynes and the linear correlation between the logarithm of the rate constant and the ionization potential of the alkene. Based upon these facts and the well established cycloaddition reaction of dihalomethylenes to alkenes, the reaction of halomethylidynes with alkenes is believed to proceed <u>via</u> a polarized, acyclic transition state to yield the cyclopropyl radical in a stereospecific mechanism.

Since these reactions are expected to be very exothermic, the cyclopropyl radical will be excited and may undergo decomposition. It would be very useful to determine the products of halomethylidyne reactions with alkenes using a clean source source of halomethylidyne to confirm this proposed mechanism.

The rate constants for the reaction of CCl and CBr with alkynes are slightly greater than for alkenes, with acetylene displaying a lower reactivity. The reactions are electrophilic in nature

and therefore the reaction of halomethylidynes with alkynes is believed to proceed in the same fashion as with alkenes, that is, via a polarized, acyclic transition state to yield a cyclopropenyl radical.

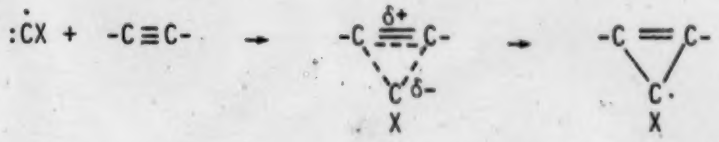

The increase in the rate constant with alkyl substitution for the reaction of halomethylidynes with double and triple bonds is believed to be caused by a decrease in the activation energy for addition, as has been demonstrated for other electrophilic radicals. The activation parameters for the reaction of CBr with ethylene, trans-2-butene and 2,3-dimethyl-2-butene were determined and it was found that the activation energies did in fact decrease resulting in larger rate constants. However, the activation energies determined were negative and the Arrhenius plot for the reaction of CBr with 2,3-dimethyl-2-butene was found to be curved. These features are best explained by a reaction sequence in which the halomethylidyne and alkene form an intermediate, best described as a loose π complex, which forms the product via a curve crossing at an energy level lower than that of the seperated reactants.

The halosilylidynes, SiCl and SiBr, were observed by absorption spectroscopy following the flash photolysis of Si_2Cl_6 and $SiBr_4$, respectively, as expected. No rate constants for reaction with ethylene could be determined. The absorption spectra of $SiCl_2$ and $SiBr_2$ were also observed in the flash photolysis of the same compounds. The transition for $SiCl_2$ was concluded to be $^1B_1$-$^1A_1$

and the vibrational bands were analyzed to give a bending frequency in the upper state, $\nu_2' = 148\ cm^{-1}$, by analogy to other absorption spectra of Group IV A dihalides. The electronic energy of the upper state, $^1B_1$, was estimated to be 30295 cm^{-1}. The previously unreported electronic absorption spectrum of $SiBr_2$ is assigned to the $^1B_1$-$^1A_1$ transition by analogy to other Group IV A dihalide absorption spectra. The absorption band is continuous with a maximum at 362 nm (27600 cm^{-1}). The photolysis of appropriately substituted disilanes should provide an opportunity to observe silylene electronic absorption spectra.

Bibliography

1. W. Pryor, "Free Radicals", McGraw-Hill, New York (1966)
2. a) "Carbenes", M. Jones Jr. and R.A. Moss, Ed., Vol. I & II, John Wiley and Sons, New York (1973,1975); b) W. Kirmse, "Carbene Chemistry", 2nd ed., Academic Press, New York (1971)
3. a) C. Mackay in "Carbenes", M. Jones Jr. and R.A. Moss,Ed., Vol. II, John Wiley and Sons, New York (1975) pp. 1-22 ; b) W. Braun, A.M. Bass, D.D. Davis and J.D. Simmons, Proc. Roy. Soc. (Lond.), A312 (1969) 417; c) D. Husain and L.J. Kirsch, Chem. Phys. Lett., 8 (1971) 543; d) D. Husain and L.J. Kirsch, Trans. Farad. Soc., 67 (1971) 2025
4. R.A. Moss, Acc. Chem. Res., 13 (1980) 58
5. G. Herzberg, "Spectra of Diatomic Molecules", 2nd ed., Van Nostrand, New York (1950)
6. a) P. Swings and O. Struve, Phys. Rev., 39 (1932) 142 ; b) W.S. Adam, Astrophys. J., 93 (1941) 11 ; c) P. Swings, C.T. Elvey and H.W. Babcock, Astrophys. J., 94 (1941) 320
7. a) K.H. Geib and V.M. Vaidya, Proc. Roy. Soc. (Lond.), A178 (1941) 351 ; b) A.G. Gaydon and H.G. Wolfhand, Proc. Roy. Soc. (Lond.), A194 (1948) 169
8. E. Fagerholm, Ark. Mat. Astron. Fysik, 27A (1940) 19
9. H.W. Harkins, Trans. Farad. Soc., 30 (1934) 221
10. R.G.W. Norrish, G. Porter and B.A. Thrush, Proc. Roy. Soc. (Lond.) A216 (1953) 165
11. R.A. Anderson, J. Peacher and D.M. Wilcox, J. Chem. Phys., 63 (1975) 5287
12. E.H. Fink and K.H. Welge, J. Chem. Phys., 46 (1967) 4315

13. J.E. Hesser and B.L. Lutz, Astrophys. J., 159 (1970) 703

14. a) J. Hinze, G.C. Lie and B. Liu, Astrophys. J., 196 (1975) 621 ; b) K.H. Becker, H.H. Brenig and T. Tatarczyk, Chem. Phys. Lett., 71 (1980) 242

15. G. Herzberg and J.W.C. Johns, Astrophys. J., 158 (1969) 399

16. D. Feldman, Z. Naturforsch., 25 (1970) 621

17. A. Kasdan, E. Herbst and W.C. Lineberger, Chem. Phys. Lett., 31 (1975) 78

18. H. Sun and K.F. Freed, Chem. Phys. Lett., 78 (1981) 531

19. R.H. Barnes, C.E. Moeller, J.F. Kircher and C.M. Verber, Appl. Opt., 12 (1973) 2531

20. I. Messing, C.M. Sadowski and S.V. Filseth, Chem. Phys. Lett., 66 (1979) 95

21. J.E. Butler, L.P. Goss, M.C. Lin and J.W. Hudgens, Chem. Phys. Lett., 63 (1979) 104

22. C. Fotakis, M. Martin, K.P. Lawley and R.J. Donovan, Chem. Phys. Lett., 67 (1979) 1

23. W.M. Jackson, J.B. Halpern and C.S. Lin, Chem. Phys. Lett., 55 (1978) 254

24. E.B. Andrews and R.F. Barrow, Proc. Phys. Soc. (Lond.), A64 (1951) 481

25. J.E. Hesser and K. Dressler, J. Chem. Phys., 45 (1966) 3149

26. Y.Y. Kuzyakov and V.T. Tatevskii, Opt. Spect., 5 (1958) 699

27. T.L. Porter, D.E. Mann and N. Acquista, J. Mol. Spect., 16 (1965) 228

28. P.K. Carroll and T.P. Grennan, J. Phys. B, 3 (1970) 865

29. D.E. Mann, H.P. Broida and B.E. Squires, J. Chem. Phys., 22 (1954) 348

30. J.P. Simons and A.J. Yarwood, Proc. Chem. Soc., (1962) 62

31. B.A. Thrush and J.J. Zwolenik, Trans. Farad. Soc., 59 (1963) 582

32. M.E. Jacox and D.E. Miligan, J. Chem. Phys.,50 (1969) 3252

33. F.B. Wampler, J.J. Tiee, W.W. Rice and R.C. Oldenburg, J. Chem. Phys., 71 (1979) 3926

34. J.J. Tiee, F.B. Wampler andW.W. Rice, Chem. Phys. Lett., 68 (1979) 403

35. F.C. van den Heuvel, W.L. Meerts and A. Dymanus, Chem. Phys. Lett. 88 (1982) 59

36. K. Kawaguchi, C. Yamada, Y. Hamada and E. Hirota, J. Mol. Spect., 86 (1981) 136

37. A. Carrington and B. Howard, Mol. Phys., 18 (1970) 225

38. D.S. Hsu, M.E. Umstead and M.C. Lin, ACS Symp. Ser., 66 (1978) 128

39. D.L. Hildenbrand, Chem. Phys. Lett., 32 (1975) 523

40. T.H. Dunning, W.P. White P.M. Pitzer and C.W. Mathews, J. Mol. Spect., 75 (1979) 297

41. R.K. Asundi and S.M. Karim, Proc. Ind. Acad. Sci., 6A (1937) 328

42. T. Horie, Phys. Math. Soc. Jap., 21 (1939) 143

43. P. Venkateswarlu, Phys. Rev., 77 (1950) 79

44. Y.Y. Kuzyakov and V.M. Tatevskii, Opt. Spect., 7 (1959) 301

45. G. Pannetier and P. Lafitte, Compt. Rend., 226 (148) 72

46. R.D. Verma and R.S. Mulliken, J. Mol. Spect., 6 (1961) 419

47. R.D. Gordon and G.W.King, Can. J. Phys., 39 (1961) 252

48. I.E. Ovcharenko, Y.Y. Kuzyakov and V.M. Tatevskii, Opt. Spect., 19 (1965) 294

49. A.J. Merer, D.N. Travis and J.K.G. Watson, Can.J. Phys., 44 (1966) 447

50. J.P. Simons and A.J. Yarwood, Trans. Farad. Soc., 57 (1961) 2167

51. J.P. Simons and A. J. Yarwood, Trans. Farad. Soc., 59 (1963) 90

52. D. Husain, Nature, 195 (1962) 796

53. F.C. James, H.K.J. Choi, O.P. Strausz and T.N. Bell, Chem. Phys. Lett., 53 (1978) 206

54. a) H.K.J. Choi, F.C. James, O.P. Strausz and T.N. Bell, Chem. Phys. Lett., 68 (1979) 131 ; b) H.K.J. Choi, Ph.D. Thesis, University of Alberta, 1981

55. W.J.R. Tyerman, Trans. Farad. Soc., 65 (1969) 2948

56. W.J.R. Tyerman, J. Chem Soc. A, (1969) 2483

57. W.J.R. Tyerman, Spect. Acta., 26A (1970) 1215

58. C. Yamada K. Nagai and E. Hirota, J. Mol. Spect., 85 (1981) 416

59. J.J. Tiee, F.B. Wampler and W.W. Rice, J. Chem. Phys., 72 (1980) 2925

60. H. Okabe, "Photochemistry of Small Molecules ", Wiley Interscience, New York (1978)

61. H. Kupfer and G. Herzberg, "Constants of Diatomic Molecules", Vol. IV, Van Nostrand, New York (1979)

62. M. Bialski and F. Grein, J. Mol. Spect., 61 (1976) 321

63. E.H. Coleman and A.G. Gaydon, Farad. Soc. Disc., 2 (1947) 166

64. G. Pannetier and P. Lafitte, Compt. Rend., 226 (1948) 72

65. R.A. Durie and T. Iredale, Trans. Farad. Soc., 44 (1948) 806

66. P. Venkateswarlu, Proc. Ind. Acad. Sci. 25A (1947) 138

67. R.D. Verma, Proc. Ind. Acad. Sci., 47A (1958) 196

68. R.N. Dixon and H.W. Kroto, Trans. Farad. Soc.,59 (1963) 1484

69. "Tables of Interatomic Distances", Chem. Soc. Lond. (1958)

70. A.J. Merer and D.N. Travis, Can.J. Phys., 43 (1965) 1795

71. R.E. Rebbert and P.A. Ausloos, J. Photochem., 1 (1972/73) 171

72. W. Braun, A.M. Bass and M. Pilling, J. Chem. Phys., 52 (1970) 5131

73. W. Braun, J.R. McNesby and A.M. Bass, J. Chem. Phys., 46 (1967) 2071

74. A.H. Laufer and H. Okabe, J. Am. Chem. Soc., 93 (1971) 4137

75. A.H. Laufer and H.Okabe, J. Phys. Chem., 76 (1972) 3504

76. M.C. Lin, Int. J. Chem. Kinet., 6 (1974) 1

77. M.C. Lin, J. Phys. Chem., 77 (1973) 2726

78. M.C. Lin, J. Chem. Phys., 61 (1974) 1835

79. J.E. Butler, L.P. Goss, M.C. Lin and J.W. Hudgens, Chem. Phys., 56 (1981) 355

80. J.R. McDonald, A.P. Baronavski and V.M. Donelly, Chem. Phys., 33 (1978) 161

81. S.E. Bialkowski and W.A. Guillory, J. Chem. Phys., 68 (1978) 3339

82. J. Calloman and D.A. Ramsay, Can. J. Phys., 35 (1957) 129

83. M.W. Bosnali and D. Perner, Z. Naturforsch., 26A (1971) 625

84. G.M. Reaburn and D. Perner, Nature, 212 (1966) 1042

85. T. Rose, C. Mackay and R. Wolfgang, J. Am. Chem. Soc., 88 (1966) 1065

86. C. Mackay, J. Nicholas and R. Wolfgang, J. Am. Chem. Soc., 89 (1967) 5758

87. P.N. Clough, S.E. Schwartz and B.A. Thrush, Proc. Roy. Soc. (Lond.) A317(1970) 575

88. R.E. Rebbert and P.A. Ausloos, J. Photochem., 8 (1978) 17

89. R.E. Rebbert and P.A. Ausloos, J. Photochem., 4 (1975) 419

90. R.E. Rebbert and P.A. Ausloos, J. Photochem., 6 (1976/77) 265

91. J.J. Tiee, F.B. Wampler and W.W. Rice, Chem. Phys. Lett., 65 (1979) 425

92. M.E. Jacox and D.E. Milligan, J. Chem. Phys., 53 (1970) 2688

93. R.S. McDaniel, R. Dickson, F.C. James, O.P. Strausz and T.N. Bell, Chem. Phys. Lett., 43 (1976) 130

94. A.J. Merer and D.N. Travis, Can. J. Phys., 44 (1966) 525

95. O.P. Strausz, G. Kennepohl, F. Garneau, T. Dominh, B. Kim, S. Valenty and P.S. Skell, J. Am. Chem. Soc., 96 (1974) 5723

96. I. Messing, C. Sadowski, T.Carrington and S. Filseth, J. Chem. Phys., 74 (1981) 3874

97. A. Fontijn, Prog. React. Kinet., 6 (1971) 75

98. M. MacGregor and R.S. Berry, J. Phys. B, 6 (1973) 181

99. C. Vinckier, J. Phys. Chem., 83 (1979) 1234

100. N. Basco and R.G.W. Norrish, Can. J. Chem., 38 (1960) 1769

101. B.R. Brooks and H.F. Scaefer, J. Chem. Phys., 67 (1977) 5146

102. P.P. Porter, A.H. Clark, W.E. Kashan and W.G. Braun, 11th Symp. (Int.) on Combustion, The Combustion Institute (1967) p 907

103. A.H. Laufer, Revs. Chem. Int., 4 (1981) 225

104. D. Husain, S.K. Mitra, and A.N. Young, J. Chem. Soc. Farad. II, 70 (1974) 1721

105. R. Gordon and P.A.Ausloos, J. Chem. Phys., 46 (1967) 4823

106. W. Braun, K.H. Welge and J.R. McNesby, J. Chem. Phys., 45 (1966) 2650

107. A.P. Wolf, Adv. Phys. Org. Chem., 2 (1964) 20

108. D. Hsu and M.C. Lin, Int. J. Chem. Kinet., 10 (1978) 839

109. A.P. Modica, J. Chem. Phys., 44 (1966) 1585

110. T.L. Burks and M.C. Lin, J. Chem. Phys., 64 (1976) 4235

111. R.E. Rebbert, J. Photochem., 8 (1978) 363

112. G.S. Hammond, J.Am. Chem. Soc., 77 (1955) 334

113 S.W. Benson , 'Thermochemical Kinetics', J. Wiley and Sons, New York (1976)

114. P.S. Skell and M.S. Cholod, J. Am. Chem. Soc., 91 (1969) 7131

115. D.D. Davis, J.F. Schmidt, C.M. Neely and R.J. Hanrahan, J. Phys. Chem., 79 (1975) 11

116. S.J. Valenty and P.S. Skell, J.Org. Chem., 38 (1973) 3937

117. S.J. Valenty and P.S. Skell, J. Am. Chem. Soc. , 95 (1973) 5042

118. G. Schatz and M. Kaufman, J. Phys. Chem., 76 (1972) 3586

119. D. Hsu, M.E Umstead and M.C. Lin, ACS Symp. Ser., 66 (1978) 128

120. R.A. Mitsch and A.S. Rodgers, Int. J. Chem. Kinet., 1 (1969) 439

121. J.J. Tiee, F.B. Wampler and W.W. Rice, Chem. Phys. Lett., 73 (1980) 519

122. A.J. Merer and D.N. Travis, Can. J. Phys., 44 (1966) 1541

123. H. Burger and R. Eujen, Top. Curr. Chem., 50 (1974) 7

124. P.P. Gaspar,' Silylenes', chapters in Reactive Intermediates, M. Jones Jr. and R.A. Moss, Editors, Vol. I and II, Wiley Interscience, New York (1977,1981)

125. R.K. Asundi, M. Karim and R. Samuel, Proc. Phys. Soc., 50 (1938) 581

126. O.M. Nefedov, S.P. Kolesnikov and A.I. Ioffe, J. Organomet. Chem. Lib., 5 (1977) 181

127, W.H. Atwell and D.R. Weyenberg, Angew. Chem. Int. Ed., 8 (1969) 469

128. A.J. Souval, Solar Phys., 10 (1969) 319

129. a) T.J. Millar, Astrophys. Space Sci., 72 (1980) 509
b) J.L. Turner and A. Dalgrano, Astrophys. J., 213 (1977) 386

130. A.Mairidis and J.F. Harrison, J. Phys. Chem., 86 (1982) 1979

131. J.F. Harrison, R.C. Liedtke and J.F. Liebman, J. Am. Chem. Soc., 101 (1979) 7162

132. V.M. Khanna, G. Besenbruch and J.L. Margrave, J. Chem. Phys., 46 (1967) 2310

133. K. Wieland and M. Heise, Angew. Chem., 63 (1951) 438

134. D.E. Milligan and M.E. Jacox, J. Chem. Phys., 49 (1968) 1938

135. G. Maas, R. Hauge and J.L. Margrave, Z. Anorg. Allgem. Chem., 392 (1972) 295

136. L.A. Kuznetsova and Y.Y. Kuzyakov, J. Appl. Spect., 10 (1969) 278

137. E.A. Chernyshev,N.G. Komalenkova and S.A. Baskerova , Uspekhi. Khim.,45 (1976) 1782

138. M.A. Ring, ' Homoatomic Rings,Chains and Macromolecules of Main Group Elements', A.L. Rheingold, Ed., Elsevier, Amsterdam (1977) p. 261-275

139. I.M.T. Davidson and M.E. Delf, J. Chem. Soc. Farad. Trans. I, 72 (1976) 1912

140. M. A. Ring, Inorg. Chem.,12 (1973) 2968

141. M. Ishikawa and M. Kumada, Revs. Si, Ge, Sn, Pb Cpds., 4 (1979) 7

142. R. West, M. Fink and J. Michl, Science, 214 (1981) 1343

143. E. Chernyshev, T. Krasnova, V. Stepanov and M. Labartova, Zh. Obsch. Khim., 48 (1978) 2798

144. J.L. Margrave and P.W. Wilson, Acc. Chem. Res., 4 (1971) 145

145. J.L. Margrave and D.L. Perry, Inorg. Chem., 16 (1977) 1820

146. D. Seyferth and D.P. Duncan, J. Am. Chem. Soc., 100 (1978) 7734

147. J.C. Thompson, A.P.G. Wright and W.F. Reynolds, J. Am. Chem. Soc., 101 (1979) 2236

148. H. Strobel, "Chemical Instumentation", 2nd ed., Addison Wesley New York (1973)

149. L.C. Jones Jr. and L.W. Taylor, Anal. Chem., 27 (1955) 228

150. W. Jevons and L.A. Bashford, Proc. Phys. Soc., 49 (1937) 554

151. L.A. Kuznetsova, N.E. Kuzmenko and Y.Y. Kuzyakov, Moscow Uni. Chem. Bull., 23 (1968) 18

152. a) I. Ovcharenko and Y.Y. Kuzyakov, Opt. Spect., 13 (1962) 362
b) I. Ovcharenko, Y.Y. Kuzyakov and V. Tatevskii, Opt. Spect. Suppl., 2 (1963) 6

153. G. Porter in "Techniques of Organic Chemistry", 8 , Wiley, New York (1963) p. 1055

154. J.R. Majer and J.P. Simons, Adv. Photochem., 2 (1963) 137

155. K. Kimura and S. Nagakura, Sect. Act., 17 (1961) 166

156. G.A. Oldershaw and K. Robinson, Trans. Farad. Soc., 67 (1971)1870

157. G.A. Oldershaw and K. Robinson, J. Mol. Spect., 38 (1971) 306

158. "Handbook of Chemistry and Physics", 55th ed., R. Weast, Ed. CRC Press, Cleveland (1975)

159. P.M. Kroger, P.C. Demou and S.J. Riley, J. Chem. Phys., 65 (1976) 1823

160. S.J. Riley and K.R. Wilson, Farad. Disc. Chem. Soc., 53 (1972) 132

161. O.P. Strausz, W.B. O'Callaghan, E.M. Lown and H.E. Gunning, J. Am. Chem. Soc., 93 (1971) 559

162. L. Bertrand, G. R. DeMare, G. Huybrechts, J. Olbregts and M. Toth Chem. Phys. Lett., 5 (1970) 183

163. J.M. Tedder and J.C. Walton, Chem. Comm., (1966) 140

164. J.R. Majer, C. Olavsen and J.C. Robb, Trans. Farad. Soc., 65 (1969) 2988

165. N. Basco and F.G. Hathorn, Chem. Phys. Lett., 8 (1971) 291

166. P.S. Skell and A.Y. Garner, J. Am. Chem. Soc., 78 (1956) 5430

167. N.G. Rondan, K.N. Houk and R.A. Moss, J.Am. Chem. Soc., 102 (1980) 1770

168. R. Cvetanovic, Adv. Photochem., 1 (1963) 115

169. O.P. Strausz, Pure Appl. Chem., 4 (1972) 165

170. A. van Roodeselaar, Ph.D. Thesis, University of Alberta, 1976

171. R. Atkinson and J.N. Pitts Jr., J. Chem. Phys., 67 (1977) 38

172. J.N. Pitts Jr., R. Atkinson, K. Darnell, A. Winer and A. Klojld, Adv. Photochem., 12 (1979) 375

173. J.S. Gaffney and S.Z. Levine, Int. J. Chem. Kinet., 11 (1979) 1197

174. N.J. Turro, G. Lehr, J. Butcher, W. Guo and R.A. Moss, J. Am. Chem. Soc., 104 (1982) 1754

175. J. Connor, A. van Roodeselaar, R.W. Fair and O.P. Strausz, J. Am. Chem. Soc., 93 (1971) 560

176. D.L. Singleton and R. Cvetanovic, J. Am. Chem. Soc., 98 (1976) 6812

177. U. Maharaj and M.A. Winnik, J. Am. Chem. Soc., 103 (1981) 2328

178. J.O. Hirschfelder, C.F. Curtiss and R.B. Bird, "Molecular Theory of Gases and Liquids", John Wiley and Sons, New York (1954)

179. R.K. Gosavi, O.P. Strausz and H.E. Gunning, Chem. Phys. Lett., 76 (1980) 159

180. J.T. Herron and R.E. Huie, J. Phys. Chem. Ref. Data, 2 (1973) 467

181. F. Stuhl and H. Niki, J. Chem. Phys., 55 (1971) 3954

182. C. A. Arrington and D.J. Cox, J. Phys. Chem., 79 (1975) 2584

183. J.M. Brown and B.A. Thrush, Trans. Farad. Soc., 63 (1967) 630

184. P. Herbrechtsmeier and H.G. Wagner, Ber. Bunsenges. Phys. Chem., 79 (1975) 461

185. P. Herbrechtsmeier and H.G. Wagner, Ber. Bunsenges. Phys. Chem., 79 (1975) 673

186. A. van Roodeselaar, I. Safarik, O.P. Strausz and H.E.Gunning, J. Am. Chem. Soc., 100 (1978) 4068

187. J. Fenwick, G. Frater, K. Ogi and O.P. Strausz, J. Am. Chem. Soc., 95 (1973) 124

188. H.E. Avery and S.J. Heath, Trans. Farad. Soc., 68 (1972) 512

189. V.E. Bondybey and J.H. English, J. Mol. Spect., 79 (1980) 416

190. R. Hauge, V.M. Khanna and J.L. Margrave, J, Mol. Spect., 27 (1968) 143

191. J.W. Hastie, R. Hauge and J.L. Margrave, J. Mol. Spect., 29 (1969) 152

192. R. Hauge, J.W. Hastie and J.L. Margrave, J. Phys. Chem., 72 (1968) 3510

193. S.S. Batsanov, S.S. Derbeneva and N.A. Shestakova, Izv. Akad. Nauk. S.S.S.R., Neorg. Mater., 2 (1966) 2259

194. L.A. Kuznetsova and Y.Y. Kuzyakov, J. Appl. Spect., 10 (1969) 278

196. R. Isabel, G. Smith,R. McGraw and W. Guillory, J. Chem. Phys., 58 (1973) 818

197. H. Huber, G.A. Ozin and A. vander Voet, Nature(Lond.) Phys. Sci., 232 (1971) 166

198. I.R. Beattie and R.D. Perry, J. Chem. Soc. A, (1970) 2429

199. R. Roberge, C Sandorfy and O.P. Strausz, Theor. Chim. Acta (Berl), 52 (1979) 171

200. A.M. Doncaster and R. Walsh, J. Chem. Soc. Farad. Trans. I, (1980) 272

201. B.G. Ramsey, "Electronic Transitions in Organometalloids", Academic Press, New York (1969)

202. P. Boudjouk and R.D. Koob, J. Am. Chem. Soc., 97 (1975) 6595

203. A.J. Merer and R.S. Mulliken, Chem. Revs., 69 (1969) 639

APPENDIX

The negative deviation from Beer's absorption law is due to the narrow,sharp,Q_1 absorption bands of CF,CCl and CBr and the inability of the microdensitometer to adequately resolve them. Since the empirical Beer correction factors are solely dependent on the operational parameters of the microdensitometer, it is important to detail them.

The two critical factors for measuring optical density are the spectral band width and the scanning speed.

For the Joyce loebl Microdensitometer, the effective slit width is the width of the final physical aperture divided by the total optical magnification. The total optical magnification is that due to the objective plus a projection factor of 2.2. The objective lens is a Vickers N7221 with a 10/0.25 (x40) magnification. The width of the final physical aperture was always 0.40 mm. The effective slit width was therefore;

$$\text{Effective slit width} = \frac{\text{Final Physical Aperture Width}}{\text{Magnification (Objective x Projection Factor)}}$$

$$= \frac{0.40 \text{ mm}}{40 \times 2.2}$$

$$= 0.0045 \text{ mm}$$

This effective slit width can be combined with the dispersion of the spectrograph in any wavelength region to yield the spectral band width.

The scanning speed is controlled by the speed of the recording chart table divided by the setting of the ratio arm which links the scanning table to the recording chart table. The recording chart table speed was usually 2.0 mm/sec. For the CCl and CBr Q_1 absorption bands

the ratio arm setting was 20 giving a scanning speed of 0.1 mm/sec. For the CF absorption bands, the ratio arm setting was 10 giving a scanning speed of 0.2 mm/sec.